UNIVERSITAT DE BARCELONA

Tesi Doctoral

Effects of mechanical stimuli of vibration and stretch on airway epithelial cells

Memòria presentada per

Ferranda Puig i Cotado

per optar al grau de Doctor

Treball dirigit pel Dr. Ramon Farré i Ventura
a la Unitat de Biofísica i Bioenginyeria
del departament de Ciències Fisiològiques I,
Facultat de Medicina, Universitat de Barcelona.

Als meus pares i a la meva germana,
amb molta estima

El secret de la saviesa, del poder i del coneixement
és la humilitat.

Ernest Hemingway (1896-1961)
Escriptor

Agraïments

Vull agrair l'ajuda i el recolzament rebut durant aquests quatre anys de doctorat a totes aquelles persones que tant en l'àmbit personal com científic m'han fet costat, m'han escoltat i en definitiva, m'han donat tot el seu suport i confiança.

En especial, vull agrair al Dr. Ramon Farré, director d'aquesta tesi, l'oportunitat d'introduir-me en el món científic, un món que m'apassiona, així com la dedicació i la confiança que des del primer dia ha dipositat en mi. Moltes gràcies.

Als altres professors de la Unitat, el Dr. Daniel Navajas, la Dra. Mar Rotger i el Dr. Domènec Ros, els hi vull agrair els coneixements, els bons consells i l'ajuda rebuda durant aquests anys.

Al Jordi Alcaraz, perquè tot i estar a l'altra punta de món, sempre està disponible per atendre els meus dubtes científics i les meves neures personals. Gràcies per escoltar-les!!!. I moltes gràcies per fer-me sentir com a casa quan vaig estar a Berkeley. Sempre recordaré la meva estada a Califòrnia.

A la Lara i a la Mireia els hi vull agrair que m'iniciessin en aquest món tant fascinant de la biologia cel·lular. Moltes gràcies, noies, sempre us tinc en ment i més del que us podeu imaginar.

Vull agrair als companys de laboratori l'ajuda i la contribució a la feina. En especial, al Miguel Ángel, per estar sempre receptiu i ajudar a muntar qualsevol artefacte que faci mal a les cèl·lules. A l'Isaac, per portar al laboratori la "grassia" andalussa i compartir algunes confidències. Al Pere, per retornar-me el somriure i fer-me riure entre experiment i experiment explicant les seves anècdotes. Al Xavi Trepat per proporcionar-me el dispositiu amb el qual he pogut realitzar moltes mesures durant aquests quatre anys. Finalment, vull donar les gràcies a tots els companys que en un moment o altre han passat per la Unitat durant la realització de la meva tesi. Amb ells he intercanviat alegries, decepcions, riures còmplices, fracassos i algun que altre cotilleo. Moltes gràcies, Núria, Irene, Raimon, Carles, Maria Elena, Aitor, Gemma, Alba, David Ramonet, Laura Chimenti.

En l'àmbit personal, vull agrair amb molt de carinyo al Xavi, per tot i per res, per recolzar-me en tot moment, per entendre'm o intentar-ho, per criticar-me, per fer-me veure la vida des d'un altre punt de vista, per estar al meu costat, per estimar-me. Gràcies pel teu suport.

A la Neus, que m'aguanta des de fa 13 anys, però que sé que puc comptar amb ella en qualsevol moment i compartir els moments més importants de la meva vida, com aquest. A la Mònica, la Susanna, l'Àngels, l'Aran, la Sònia, la Natàlia, la Susana, l'Ana Belén. Algun dia ho aconseguirem!!! En definitiva, a totes aquelles persones que han deixat la seva

petjada en la meva persona i que han fet que sigui com sóc i per tant també han contribuït indirectament en la realització d'aquesta tesi.

Finalment, vull agrair el suport incondicional de la meva família, dels meus pares i de la meva germana, de la iaia abuelita i de la iaia Isabel, que les dues en la seva manera van descobrir que la vida no era com havien somniat de petites.

Contents

Chapter I

Introduction

I.1 Mechanical stimuli in Airway cells

Cells can sense, process and respond to a variety of stimuli from surrounding cells and from their biochemical and biophysical environment. Most studies in cell biology have mainly reported how cells respond to biochemical stimuli. However, very little is known about how cells sense and respond to mechanical stimuli as well as about the cellular structures responsible for cell mechanical behavior, although recent nanomanipulation devices have provided information on cells mechanics (Zhu et al., 2000). Cell mechanics can provide information about how cells sense and respond to mechanical forces as well as how they use these forces to control their shape and behavior. Although mechanical forces and deformations are essential in specialized cellular functions including proliferation, differentiation, apoptosis, motility, signal transduction, gene expression, cellular shape, to name a few (Chicurel et al., 1998;Zhu et al., 2000) the knowledge of the mechanics of living cells is far to be complete due to the complexity of the cellular behavior after an external force is applied. Cells belong to the category of very soft matter, requiring very low forces to be deformed (in the nanonewton or piconewton regime). In fact, after a low and brief external perturbation, the cell can store mechanical energy allowing it to recover its shape. But this cellular reply is not immediate. Cells can also dissipate energy due to internal friction, so that this viscous resistance can delay the cellular response induced by external forces. This behavior is similar to viscoelastics materials. In other words, cells have some elastic or solid-like characteristics, which confer the cell with the ability to rapidly recover its shape in response to external deformation, but they have also some dissipative or liquid-like characteristics, which enable the cell to alter its shape and flow in some cellular processes such as crawling, spreading, division, or contraction (Fabry and Fredberg, 2003).

It is well known that mechanical properties of living cells are determined by their composition and structures as well as the surroundings with which they interact (Zhu et al., 2000), but the main responsible of cell mechanical properties is the cytoskeleton (CSK), which exhibits properties of both solid-like and liquid-like depending of the circumstances.

The determination of cell response to mechanical stimuli is of particular relevance in lung cells, which are continuously subjected to permanent and cyclic mechanical perturbations due to breathing, airflow and blood flow (Table I.1). However, very little is known about the cell mechanical behavior in response to these kind of dynamic mechanical perturbations (Stamenovic and Wang, 2000). The lung is a unique organ subjected to several complex physical forces throughout life. From clinical observations and physiological studies, it has been recognized that physical forces play an important role in regulating the structure, function, and metabolism of the lung (Liu et al., 1999). As an example, physical forces contribute to the branching of the airways during lung development and also influence lung growth after birth and cell proliferation and differentiation during adulthood. These mechanical forces applied to lung cells can be

Origin	**Mechanical stimuli**	**Affected pulmonary components**	**Affected cells**
Breathing	Cyclic strain with frequencies around breathing (0.3 Hz)	The whole lung	All lung cells, although strain is more prominent in cells of the alveolar wall and epithelium.
Airflow	Shear stress and cyclic strain due to shear stress	Airways and blood vessels	Epithelial cells and vascular endothelium
Bloodflow	Shear stress, hydrostatic pressure and strain	Pulmonary and bronchial arteries	Vascular wall: endothelial cells, fibroblasts and smooth muscle cells.
Surface tension	Shear stress	Air-liquid interface and small airways	Vascular endothelium, pleural fluid on pleural mesothelial cells, fluid hypophase on airway and alveolar epithelial cells
Water flowing across a cell membrane	Osmotic forces	Cells that transport ions and water	Pulmonary endothelial end epithelial cells
Preexisting lung tension	Prestress	The whole lung	All cells

Table I.1: Physical forces that affect lung cells. Adapted from Alcaraz, 2001

classified in specific physical terms such as stress (force per unit area), strain (the change in length in relation to the initial length), and shear stress (force per unit surface area in the direction of flow exerted at the fluid: surface interface). Therefore, other terms such as stretch and deformation have also been used by many investigators as a synonymous of strain. (Liu et al., 1999). Most lung cells are subjected to some degree of strain due to breathing movements. But while strain is more prominent in cells of the alveolar wall and epithelium, shear forces act mainly in the vascular bed, although these forces also play a role in cells other than vascular endothelium, such as pleural mesothelial cells. Vascular endothelium is also subjected to strain during vessel distention and hydrostatic (blood) pressure, as well as cells of the media (smooth muscle cells) and fibroblasts (Wirtz and Dobbs, 2000). Osmotic forces should also be taken into consideration, which can result to be important in cells that transport ions and water, such as pulmonary endothelial and epithelial cells. By contrast, the force induced by gravity on a cell has been estimated to be less than 1 pN/cell. Tensile forces generated within the cytoskeleton and exerted on adhesion structures may be 50–10 000 times greater than this value (Wirtz and Dobbs, 2000).

Inappropriate physical forces exerted on lung cells and tissues contribute to many pathophysiological situations. The narrowing of airway tone during hyperesponsiveness is associated with an increase in cell stiffness and cell contraction. High alveolar pressures and/or volumes that cause direct strain or increased tissue shear stress are presumed causes of mechanical ventilation-induced lung injury (Wirtz and Dobbs, 2000). An alteration of physical forces is an important factor in inflammatory diseases in the lung such as asthma, which is characterized by leukocyte infiltration, epithelial sloughing, basement membrane thickening, edema and hyperplasia of mucus-secreting glands, and hypertrophy of bronchial smooth muscle (Amin et al., 2000). Moreover, chronic airway obstruction contributes to airway smooth muscle hyperplasia and hypertrophy. Furthermore, patients with obstructive sleep apnea (OSA) exhibit inflammation and injury in the upper airway tissues due to the mechanical perturbation induced by eccentric muscle contractions and tissue vibration, which can lead to changes in the anchorage between the epithelium and the subepithelial connective tissue (Paulsen et al., 2002;Boyd et al., 2004). Thus, a better understanding of how physical forces act on lung cells may help us to design strategies in the treatment and prevention of physical force-related disorders such as pulmonary hypoplasia, barotrauma, pulmonary hypertension, obstructive sleep apnea/hypopnea

syndrome, fibrosis, asthma, acute lung injury, and chronic obstructive pulmonary diseases (Liu et al., 1999). Two strategies can be used to study the contribution of physical factors in lung diseases. The first one is based on the collection of cells from animal models of these diseases or from human patients and then to study their responsiveness to mechanical stimulation in vitro. The second one, if the properties of inappropriate physical factors are well defined, focuses on the simulation of these conditions with the various devices currently available.

Using the second strategy, we have focused on studying the effects of two mechanical forces such as vibration and stretch on airway epithelial cells, which are related with two airway disorders: obstructive sleep apnea and acute lung injury, respectively.

I.2 VIBRATORY STIMULUS ON AIRWAY EPITHELIAL CELLS. OBSTRUCTIVE SLEEP APNEA.

I.2.1 Obstructive Sleep Apnea

Obstructive sleep apnea (OSA) is a prevalent disorder affecting up to 2% in women and 4% in men over the age of 35 (Paulsen et al., 2002) and the prevalence of this syndrome in a general population is high and increase with age in both sexes (Duran et al., 2001). Obstructive sleep apnea syndrome also affects to children (between 1 to 10%) (Ferreira et al., 2000;Chan et al., 2004). People with OSA syndrome literally stop breathing repeatedly during their sleep, often for a minute or longer, due to airway obstruction. Whether the obstruction is incomplete (hypopnea) or total (apnea), the patient makes an effort to breathe and is awaked from sleep. Often, arousals are only partial and are unrecognized by the patient, even if they occur more than 60 times per hour. The most common symptoms from patients suffering this disorder are loud snoring, disrupted sleep and excessive daytime sleepiness. As many persons are not aware of their loud snoring and their arousals, it is very common to interview their bedroom partner to diagnose this syndrome. Obstructive sleep apnea syndrome causes acute adverse effects, including sleep disruption, a compromise in the oxidative balance, fluctuations in blood pressure and cardiovascular complications (Young et al., 2004). This syndrome is usually associated with a reduction in blood oxygen saturation and a decrease in tissue oxygenation (Carpagnano et al., 2003). A

high prevalence of this disorder is found in middle-aged and elderly patients with coronary artery disease (Peker et al., 1999).

I.2.2 Structure of the upper airway

On a normal day, a person inhales approximately 10,000 litres of air. The upper airway is the first conduct for the air and is usually divided into 4 anatomical subsegments (Fig. I.1); the nasopharynx which is linked with the internal nose (10–12 cm of length) via the choanal openings, is situated between the internal nares (choanae) and hard palate; the velopharynx or retropalatal oropharynx located between the hard palate and the soft palate; the oropharynx from the soft palate to the epiglottis and finally the hypopharynx placed between the base of the tongue and the larynx (Ayappa and Rapoport, 2003). One of the functions of the upper airway is to humidify the cold air inhaled through the nose to 98% and warm it to over 30°C. Moreover, it operates as a filter for environmental agents and noxious particles. Another function of the upper airway is to act as a conduct of air

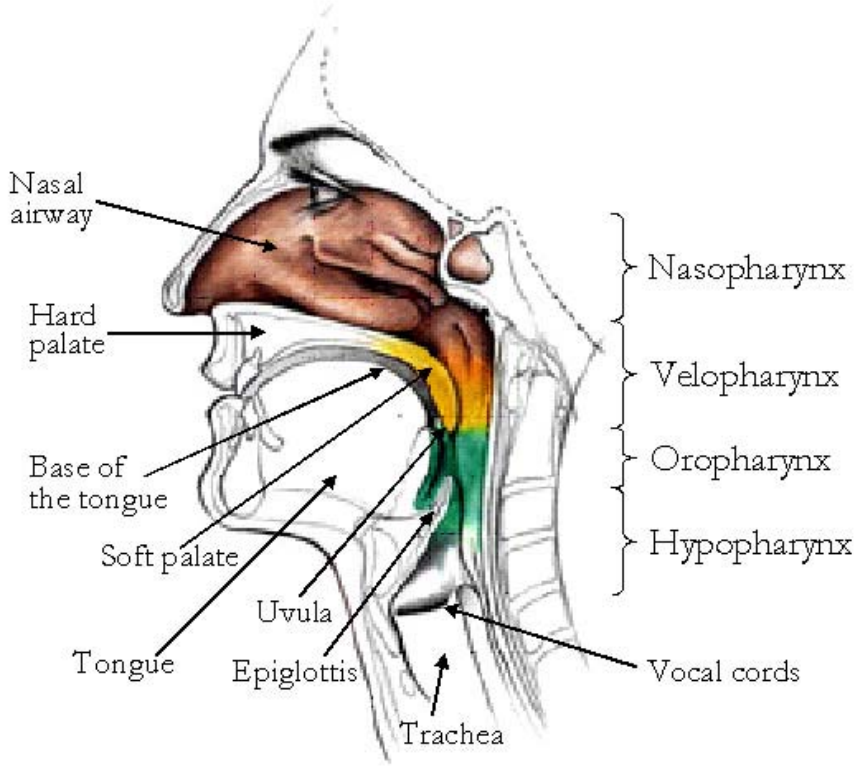

Figure I.1: Anatomy of Human Upper Airway. Adapted from www.med.nyu.edu.

towards the lung and it is also important in speech and smell functions (Fokkens and Scheeren, 2000).

The upper airway is a complex structure composed primarily of muscles and mucosa which covers the muscular wall. There are more than 20 upper airway muscles surrounding the airway that actively constrict and dilate the upper airway. They can be divided into four groups, depending of the upper airway structure: muscles of the soft palate, tongue, hyoid apparatus and the posterolateral pharyngeal walls (Ayappa and Rapoport, 2003). In the uvula, as in the soft palate, there is glandular tissue apart of muscular tissue. This upper airway structure has seromucous glands with the ability to produce large volumes of thin saliva to keep pharynx wet and well lubricated (Back et al., 2004). Mucosa forms the inner lining of the respiratory track and consists of three layers. The first layer is made up of epithelial cells. This single layer is usually covered with mucus, which is composed of a dense network of high molecular weight glycoproteins. These cells are attached to a basement membrane which separates the epithelium from the lamina propria, the second layer. The lamina propria consists of subepithelial connective tissue and lymph nodes. Underneath the lamina propria there is the third layer, a thin layer of smooth muscle. Upper airway mucosa has the same morphology and more or less the same histology than the bronchial mucosa (Fokkens and Scheeren, 2000). As in the mucosal surface is where absorptive and secretive functions occur, the cells present in the mucosa form a protective barrier for microorganisms and toxic agents from the environment

Although 49 cell types have been recognized in the airway, only a small number of these cell types constitute the epithelium (11 epithelial cell types in the tracheabronchial epithelium) (Breeze and Wheeldon, 1977;Thompson et al., 1995). Stratified squamous epithelium (nonciliated) covered with a layer of mucus is present in the nose and the first millimeters of the nasal cavity. But the respiratory tract is known for its pseudo-stratified appearance. Ciliated cells (roughly columnar, approximately 20μm long and 7μm wide with prominent cilia of 0.25μm in width) predominate in the epithelium of the respiratory track (Figure I.2). Together with a small percentage of goblet cells, 5 ciliated for every one goblet cell, and basal cells (flattened, pyramidal-shaped cells with a small cytoplasmic/nuclear ratio) lend, in part, the airway epithelium its pseudo-stratified appearance. Basal cells attach to surrounding ciliated and goblet cells anchoring them to the basement membrane. There is a transitional zone between the stratified squamous epithelium and the ciliated columnar one,

Figure I.2: Scanning electron micrograph of human respiratory epithelium (magnification: X 3250). From Chilvers and O'Callaghan, 2000

which shows gradations ranging from stratified squamous through stratified cuboidal to pseudo-stratified low-columnar type. Therefore, pseudo-stratified columnar ciliated epithelium and/or stratified cuboidal epithelium is mainly present in the surface of the whole respiratory track, including the surfaces of the nasal cavity, paranasal sinuses, Eustachian tube, tympanic cavity, nasopharynx, larynx, trachea, bronchi and smaller airways (Fokkens and Scheeren, 2000). In fact, the bronchial mucous membrane also undergoes a transition from ciliated pseudostratified columnar epithelium through cuboidal epithelium to simple squamous epithelium.

The airway epithelium has several functions, which act to protect the airspaces and preserve normal respiratory function (Table I.2). One of these functions is to defend the respiratory track against inhaled environmental agents such as gases, fumes, droplets, or microorganisms. This defense consists in removing these agents, modulating the inflammatory response due to toxic stimuli, and regulating the cellular activities necessary for responding to injury (Thompson et al., 1995). Ciliated epithelial cells also play an important physiological role in another airway epithelium main function, the mucociliary transport. The co-ordinated movements of the cilia propel micro-organisms, noxious particles and tracheobronchial secretions towards the pharynx where they are elliminated (Fokkens and Scheeren, 2000). Another important feature in the functionality of the epithelium is to contribute to the barrier function. Integration of all these functions is

Functions of the epithelial surface in the upper and lower airway
a) Protection from the external environment b) Mucus secretion c) Mucociliary transport d) Regulation of fluid and ion transport across the airway surface e) Interaction with and/or recruitment of inflammatory cells f) Modulation of repair processes g) Antimicrobial activities h) Interaction with lung parenchymal cells i) Modulation of airway smooth muscle tone j) Protection against oxidant and proteases

Table I.2: Main functions of the human upper and lower airway epithelium. Adapted of Sacco et al., 2004.

required to maintain a healthy epithelium.

I.2.3 Risk factors for obstructive sleep apnea

There are two demographic characteristics in OSA prevalence: age and sex. Age is a factor for developing this syndrome, with a 2- to 3-fold higher prevalence in older people (≥65 years) than those in middle age (30-64 years) (Young et al., 2004). Loss of muscle mass is a common consequence of the aging process. If muscle mass decreases in the airway, it may be replaced with fat, leaving the airway narrow and soft and resulting in frequent episodes of apnea-hypopnea. The other demographic factor is sex. Men have a greater risk for OSA than women due to the fact thatmale hormones can cause structural changes in the upper airway (Young et al., 2004).

It has been observed in some studies that the main risk factor in progression to OSAS is probably weight gain (Friberg, 1999;Young et al., 2004). In fact, obstructive sleep apnea syndrome affects to patients with severe overweight. The accumulation of fat on the sides of pharynx or an increase in the soft palate and tongue causes them to become narrow and predisposed to closure when the muscles relax. Overweighed patients typically have a short and thick neck. A neck circumference greater than 40.6 cm, in a woman, or greater than 43.2 cm, in a man, correlates with an increased risk for the syndrome. Furthermore, increasing neck size is another factor in progression to obstructive sleep apnea (Victor, 1999). However, some subjects with airway obstruction have no weight gain. These patients have anatomic abnormalities of the upper airway such as a diminutive or receding jaw or an enlarged tongue (Victor, 1999) (Figure I.3). Asian patients tend to OSAS due to

their craniofacial and upper airway structure (Young et al., 2004). Nasal congestion at night is also a factor for sleep-disordered breathing (Friberg, 1999). Allergic rhinitis, which can produce nasal obstruction, has been related with some symptoms also found in obstructive sleep apnea syndrome such as snoring or apneas (Larsson et al., 2001;Young et al., 2004). As well as rhinitis, other respiratory diseases affecting mainly the lower respiratory tract, such as chronic bronchitis and asthma, have been associated with symptoms common in obstructive sleep apnea (Larsson et al., 2001). Snoring has also been associated with bronchial inflammation (Chan et al., 1988;Fitzpatrick et al., 1993). On the other hand, sex hormone level changes in women life may play a role in OSA. Only few studies have shown that drastic changes in sex hormone levels such as pregnancy, menarche or menopause can modify the risk of OSA. In a study of a general population, postmenopausal women had more possibilities to develop OSA when compared with premenopausal women, independently of age, obesity and other potential factors (Young et al., 2004). Obstructive sleep apnea syndrome also affect to children. Enlarged tonsils and adenoids are the main factors of this syndrome in childhood. If children with these characteristics did not develop this disorder, large tonsils and adenoids could cause abnormal growth patterns of the lower face and jaw, predisposing to OSA in adult (Young et al., 2004). It has been reported that lifestyle factors also affect patients with OSA. The use of sedative drugs, sleeping pills or drinking alcohol can worsen the patient due to these sedatives relax the pharyngeal musculature (Victor, 1999). Smoking, which can cause inflammation and narrowing of the upper airway can also exacerbate obstructive sleep

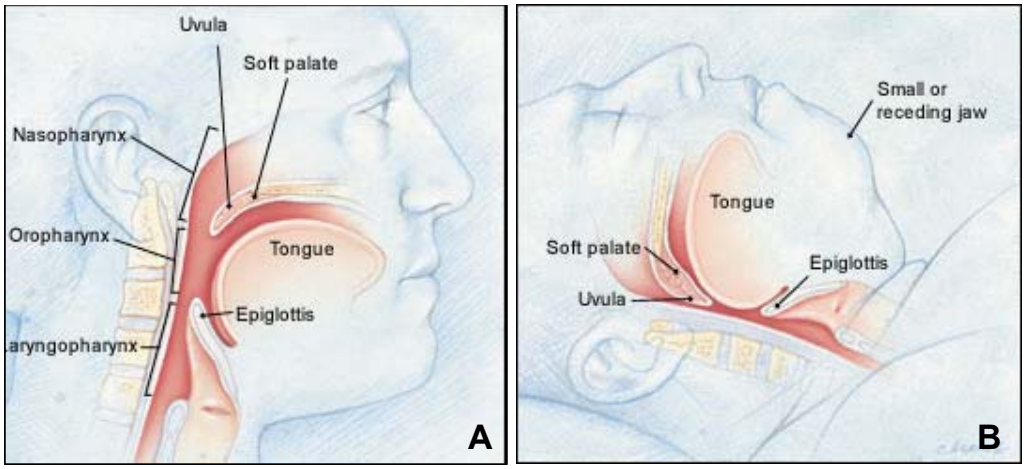

Figure I.3: A: Normal airway. The soft palate, the uvula and the tongue are normal in length and total size The upper airway at the level of the nasopharynx, oropharynx and hypopharynx is normal in size and contour. B: Abnormal airway during sleep. There are various sites of obstruction in the upper airway of patients with obstructive sleep apnea. In this illustration, the patient has a receding jaw, enlarged tongue posteriorly and an elongated and enlarged soft palate impeding air flow during respiration. From Victor, 1999.

apnea. Giving up smoking resolves the prevalence in patients with OSA (Young et al., 2004). In addition to all these factors, the pull of gravity in the supine position during sleep decrease airway size, impeding air flow during respiration (Oksenberg and Silverberg, 1998). There are also some subgroups of people with a high risk to develop this syndrome, such as people with muscular dystrophy, vocal-cord paralysis, post-polio Syndrome, Marfan's Syndrome and Down syndrome (Table I.3).

Risk factors in progression to OSAS
a) Weight gain or overweight b) Short and thick neck c) Anatomic abnormalities as a small or receding jaw or a large tongue d) Use of sedatives, tranquilizers and/or alcohol. e) Smoking f) Menopause g) Nasal obstruction. h) Family history of OSA, although no genetic inheritance pattern has been proven. i) Enlarged tonsils and adenoids, the main factors of OSA in children. j) Craniofacial anomalies, muscular dystrophy, vocal-cord paralysis, post-polio Syndrome, Marfan's Syndrome and Down Syndrome.

Table I.3: Main risk factors for OSA patients in progression of this disorder

I.2.4 Forces acting in the collapse of upper airway during sleep

The lack of obstruction in the upper airway during sleep is determined by the balance between the forces tending to constrict the pharynx through negative intrapharyngeal pressure developed during inspiration and muscular dilating forces in the pharynx generated by pharyngeal muscles (Friberg, 1999). The imbalance between these forces permits the occlusion of the upper airway during sleep. When a person suffering this syndrome falls asleep, the muscles from the base of the tongue and soft tissues as the soft palate relax to a point where the patient starts to snore loudly and the airway collapses and become completely or partially obstructed. When the airway closes, breathing stops, and the patient awakes to open the airway. With each arousal event, the muscles in the airway tissues react alleviating the obstruction and finishing the apneic episode. When normal breathing is restored, the patient falls back to sleep only to repeat the cycle throughout the

night. Apart from inward negative pressure during inspiration, there are more forces tending to obstruct the pharynx, including Bernoulli and gravity effect. Bernoulli effect acts when the pharynx becomes narrow. If the air, which flows through the airway with different diameters, passes through a narrowing as the retropalatal area, the speed of the air will increase, while its pressure will decrease. This effect is correlated with the pharyngeal collapse seen in OSA (Friberg, 1999;Hori et al., 2006). The effect of the gravity in the supine position during sleep decrease airway size, impeding air flow during respiration. The sleep supine posture not only increases the frequency of arousals but also their severity (Oksenberg and Silverberg, 1998).

Under OSA conditions, upper airway is subjected to mechanical stimuli such as vibration and stretch induced by pharyngeal pressure and violent muscle contractions against an occluded airway (Boyd et al., 2004). Snoring, associated to high-frequency oscillations, is a vibratory sound produced during sleep within the upper airway that usually coincides with the inspiratory phase of the respiratory cycle. Using cineradiografies of pharyngeal structures, Liistro G. and coworkers (1991) observed that the behavior of the soft palate was different when the snoring was produced through the nose or through the mouth (Figure I.4). During nasal snoring, the soft palate was situated close to the back of the tongue and only the uvula oscillated at small-amplitude high frequency (around 80 Hz). However, during mouth snoring, the whole soft palate oscillated at ample low-frequency oscillations (around 30 Hz) producing vibration trauma to the pharyngeal tissues (Liistro et al., 1991). These authors also observed a reduction of the pharyngeal lumen preceding the snoring. In addition to vibration stimulus, stretch is also present during snoring and obstructive sleep apnea. This mechanical perturbation may cause pharyngeal nerve and muscle fibers lesions when they are overstretched (Suratt et al., 1983). Pharyngeal nerve injury due to the pharyngeal vibration and stretch has been one cause of the progression to obstructive sleep apnea syndrome (Friberg, 1999).

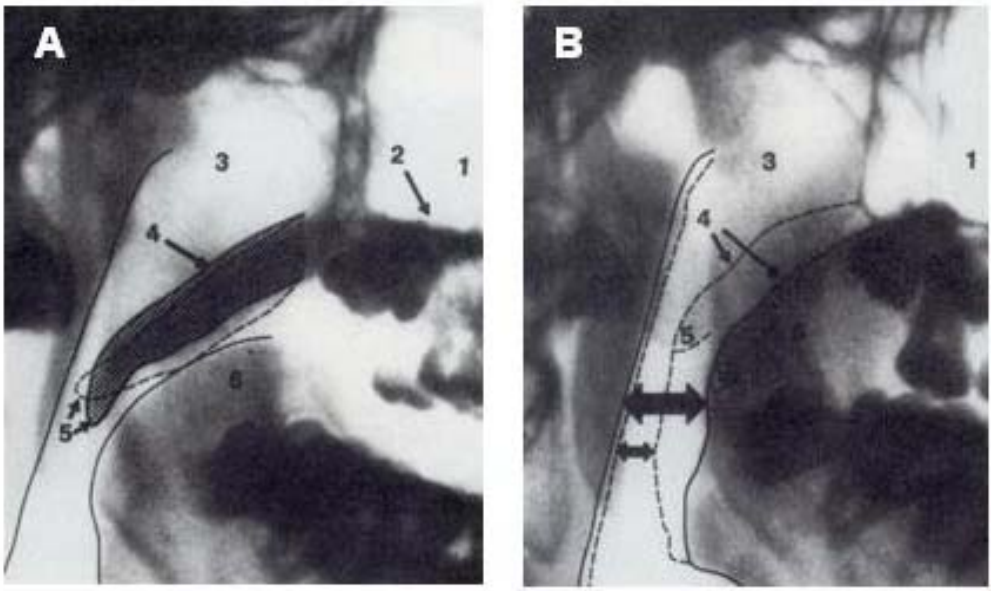

Figure I. 4: Lateral view from cineradiographies of pharyngeal airway and surrounding structures during snoring through the nose (**A**) and the mouth (**B**). **1.** Maxillar sinus. **2.** Hard palate. **3.** nasopharynx. **4.** Soft palate. **5.** Uvula. **6.** Tongue. From Liistro et al., 1991

I.2.5 "The vicious circle of heavy snoring" model

Lugaresi E. developed in 1983 the "heavy snorers disease" theory using clinical observations (Lugaresi et al., 1983). This theory implies that snoring, which usually coincides with the inspiratory phase of the respiratory cycle, would be an early step in the natural evolution of OSA. Friberg in 1999 improved this model using all the mechanisms involved in OSA progression (Figure I.5). As an example and unlike Lugaresi's model, Friberg's theory explains why weight gain is a risk factor for which a person can develop OSA. This model, "The vicious circle of heavy snoring", also contains the forces involved in the collapse of the upper airway mentioned above, including muscular dilating forces, negative pressure during inspiration, the "Bernoulli" effect and the law of gravity. It considers that a non-snorer but vulnerable patient due to some risk factors could start a vicious circle, leading to an increased degree of periodic obstructive breathing causing more morphological abnormalities and pharyngeal nerve and muscle fibers lesions. Finally, a total collapse of the upper airway during inspiration when the patient is sleeping may occur, as happens in severe OSA patients (Friberg, 1999).

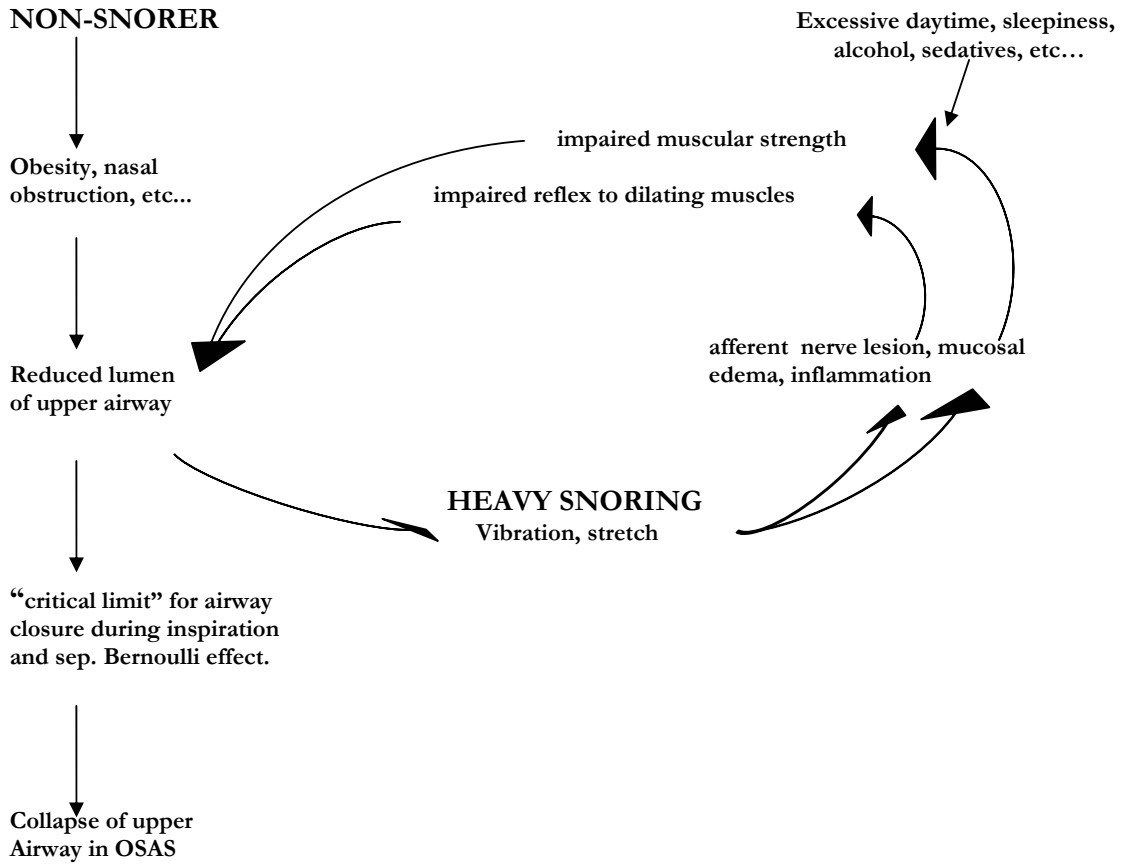

Figure I.5: "The vicious circle of snoring". Friberg's model shows different mechanisms for developing OSAS. Adapted from Friberg D., 1999.

I.2.6 Cell inflammation induced by a vibratory stimulus

The mechanical stimuli such as stretch and vibration have the potential to be the responsible for causing structural damage to nerves and muscle fibers (Friberg, 1999), as well as inflammation within the pharyngeal tissues (Rubinstein, 1995;Sekosan et al., 1996;Boyd et al., 2004). Inflammation is a common phenomena of many respiratory pathologies including obstructive sleep apnea, and in this context, upper airway epithelial cells play a crucial role due to their contribution in the beginning, increase and repair of inflammatory processes. One of this contributions is modulating immune cells activities as polymorphonuclear leukocytes, plasma cells, lymphocytes eosinophils, basophils (Sekosan et al., 1996), T cells (Boyd et al., 2004) and neutrophils (Ohga et al., 2003;Alzoghaibi and Bahammam, 2005), through the release of proinflammatory cytokines (TNF-α and IL-6, IL-8, the granulocyte chemotactic protein-2, GCP-2) (Carpagnano et al., 2002;Ohga et al.,

2003;Ishizaka et al., 2004;Alzoghaibi and Bahammam, 2005) and proteins, such as 8-Isoprostane, a marker of oxidative stress (Carpagnano et al., 2002) C-reactive protein (CRP), an important plasma marker of inflammation regulated by cytokines (Shamsuzzaman et al., 2002), or intercellular adhesion molecule-1 (ICAM-1), a potential mediator responsible for leukocyte attachment to endothelium (Ohga et al., 2003). Among the different markers of inflammation, the most potent chemotactic signaling molecules are chemokines (chemotactic cytokines). IL-8 is a cysteine–X amino acid–cysteine (CXC) chemokine that works as chemotactic agents and activator for neutrophils. These chemokines increase the secretion of enzymes and substances from neutrophils, such as elastase, myeloperoxidase, gelatinase B, and lactoferrin (Luster, 1998). One of the important effects of IL-8 is the ability to increase the number and the expression of adhesion molecules, such as L-selectin and β2 integrins (CD11b/CD18), on neutrophils. Therefore, IL-8 promotes the infiltration of neutrophils from the endothelium to the tissue subjected to the inflammatory challenge. The expression of IL-8 is regulated at both transcriptional and posttranscriptional levels (Kracht and Saklatvala, 2002) and nuclear transcription factor (NF)-κB is the responsible to regulate the synthesis and expression of this cytokine.

From OSA patients exhaled breath condensate (Carpagnano et al., 2002;Carpagnano et al., 2003)), peripheral blood samples (Vgontzas et al., 1997;Ohga et al., 2003;Alzoghaibi and Bahammam, 2005) or nasal lavage fluid (Rubinstein, 1995), simple and completely non-invasive techniques, it is possible to obtain samples with specific markers of inflammation including polymorphonuclear leukocytes and inflammatory mediators such as IL-6, IL-8, TNF- α, 8-isoprostane. But, with these samples it is difficult to know which stimulus has triggered any specific inflammatory marker. There are many potential sources of inflammation derived from upper airway obstruction (increased upper airway resistance, hypoxia, stretch, vibration, obesity, etc.). As an example, IL-8 is upregulated by different stress stimuli. It has been shown that hypoxia induces expression and/or generation of circulating IL-8 because hypoxic stress increases the adherence of neutrophils to endothelial cells, and this increased adherence is mediated by proinflammatory mediators (Ohga et al., 2003). This circulating IL-8 increase indicates that OSA-associated desaturation could lead to upregulatation of IL-8 expression (Ohga et al., 2003). On the other hand, Oudin S. and Pugin J., 2002, showed that human bronchial epithelial BEAS-2B cells submitted to cyclic stretch in vitro produced IL-8, at both the mRNA and protein

levels. These authors used this kind of cells as a representative model of the airway cellular track.

Although the mechanical stimulus of vibration during snoring has been cited as one of the main causes of upper airway damage, the mechanisms involved in vibration-induced cell inflammation are not well understood. However, there is evidence of active mechanotransduction pathways when some types of nonsensory cells are subjected to vibration. Indeed, cells of the musculoskeletal system exhibit a variety of responses when subjected to vibration: modulation of biosynthesis in articular chondrocytes (Liu et al., 2001) and change in the gene expression in osteoblasts (Tjandrawinata et al., 1997;Liu et al., 2001) and in annulus cells (Yamazaki et al., 2002). It has also been reported that vibration induces a variety of effects at tissue level. Indeed, vibratory stimulus results in nerve (Lundborg et al., 1990) and muscle damage (Necking et al., 2004), induces a change in muscle reflex (Bove et al., 2003), or modulates bone growth (Clark et al., 2005). Moreover, it has been shown that mechanical vibration causes damage in arterial endothelial cells (Curry et al., 2002) and in smooth muscle (Curry et al., 2005) and that vibration results in palmar sweating response and central nervous system activity (Ando and Noguchi, 2003). Furthermore, in patients professionally subjected to high-frequency mechanical stimuli, as in the hand-arm vibration syndrome (Stoyneva et al., 2003), there is endothelial dysregulation and damage ((Kennedy et al., 1999). However, to our knowledge, there are no data describing the effects of vibration in airway epithelial cells. One aim of this thesis was to assess whether a vibration stimulus simulating the one experienced by airway tissues in snoring patients induces inflammation in airway epithelial cells (Chapter III).

I.3 STRETCH STIMULUS ON ALVEOLAR EPITHELIAL CELLS. ACUTE LUNG INJURY.

I.3.1 Acute Lung Injury

Acute lung injury (ALI) and its more severe form, the acute respiratory distress syndrome (ARDS), is a cause of acute respiratory failure that develops in patients of all ages from a variety of clinical disorders. The first time this syndrome was described, was in 1967, but it was not until 1994 in the American-European Consensus Conference that this syndrome

was defined and clarified, due to previous definitions lacked specific criteria to identify patients with this syndrome (Ware and Matthay, 2000). The consensus definition has some simple characteristics to recognize patients suffering this disorder, the pulmonary capillary wedge pressure has to be less than 18mmHg and it is necessary the presence of bilateral infiltrates on chest x-ray which usually are consistent with the presence of pulmonary edema. Moreover, this new definition has into consideration the severity of clinical lung injury. Patients with less severe hypoxemia (as defined by a ratio of the partial pressure of arterial oxygen to the fraction of inspired oxygen, P_aO_2/F_iO_2, of 300 or less) are considered to have acute lung injury, and those with more severe hypoxemia (P_aO_2/F_iO_2 of 200 or less) are considered to have the acute respiratory distress syndrome (Ware and Matthay, 2000). Although not strictly part of the definition, there is widespread airway collapse (low lung volumes), surfactant deficiency and reduced lung compliance that results in patients suffering this disorder an increased work of breathing. But although there is now a criteria which permits to recognize patients with acute lung injury, sometimes it is difficult to distinguish ALI/ARDS from other diffuse inflammatory conditions of the lung (Matthay et al., 2003). One difference between ALI/ARDS and other lung diseases such as asthma, chronic obstructive pulmonary disease, and idiopathic pulmonary fibrosis is that these lung diseases occur over a much longer duration, usually years. But the major feature of ALI/ARDS that distinguishes it from most other lung diseases is that ALI/ARDS frequently has systemic components. This systemic process in which ALI/ARDS forms part of, involves microvascular dysfunction of diverse organs including the heart, kidneys, gut, liver, muscle and brain (Matthay et al., 2003;Chow et al., 2003). ALI/ARDS is a major cause of acute respiratory failure with high mortality in critically ill patients (Ware and Matthay, 2000). In fact, ARDS, a devastating clinical syndrome of acute lung injury and defined by consensus physiologic criteria may account for 36,000 deaths per year in a country the size of the U.S. (Matthay et al., 2003).

I.3.2 Structure of the alveoli

After passing the lower airway, air reaches the alveolar space whereby gas exchange occurs. The alveoli are estimated to number about 300 million in both human lungs and are almost completely enveloped in pulmonary capillaries (Figure I.6). There may be nearly 1000 pulmonary capillaries per alveolus. The result is a vast area of contact between alveoli and pulmonary capillaries, probably 50 to 100 m^2 of surface area available for gas exchange by

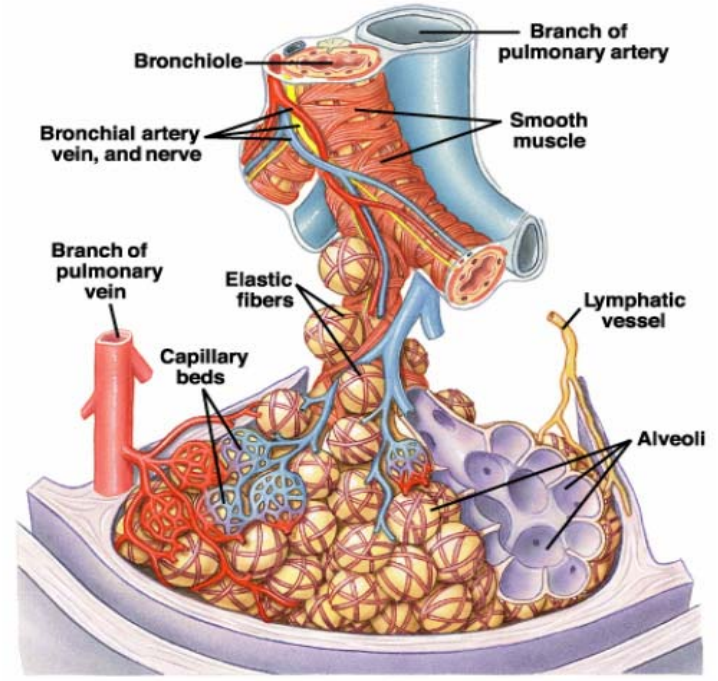

Figure I.6: Structure and main components of a lung lobule. Aadapted from Silverthorn et al., 2001.

passive diffusion (Thompson et al., 1995;Silverthorn, 2001). The alveoli consist of a squamous epithelial layer, the extracellular matrix (ECM) formed by the fusion of the two basement membranes and a closely apposed capillary network (West, 2000). From both anatomical and physiological points of view, the alveolar blood-gas barrier can divide into two parts, the thick side and the thin side. The thin side (0.2-0.3 μm in thickness, ~50% of the alveolar surface) provides an efficient structure for diffusive gas exchange (West, 2000) The thick side (>1 μm in thickness, ~50% of the alveolar surface) is important in the support of the lung (West and Mathieu-Costello, 1999). The extracellular matrix forms part of this thick side. The structure of ECM is of particular interest because of its critical role in determining the strength of the blood-gas barrier. This layer of extracellular matrix (0.1-0.5 μm) is basically formed by four proteins (type IV collagen, laminin, heparan sulfate proteoglycans and entactin/nidogen) (Crouch et al., 1997;West and Mathieu-Costello, 1999;West, 2000). It has been reported that the strength of the of the alveolar blood-gas barrier is attributable to an extremely thin layer of type IV collagen (~ 50 nm thick), which is sandwiched in the middle of the ECM (Crouch et al., 1997). (Figure I.7.).

One of the most important parts of the pulmonary alveoli is the alveolar epithelium. The alveolar epithelium from an adult human is lined by two morphologically distinct epithelial cells: Type I and Type II cells (Crapo et al., 1982) (Figure I.8).

Alveolar epithelial Type I cells (or Type I pneumocytes)

Although Type I pneumocytes have been estimated to occupy about 10% of all lung cellular population, these cells cover about 95% of the alveolar surface. Alveolar epithelial Type I cells are thin, flattened and large squamous cells (diameter of ~ 50 to 100 μm, 0.05-0.2 μm height except for the nuclear region and a volume of ~ 2,000 to 3,000 μm^3), with a very flat surface (Crandall and Matthay, 2001). Although the precise functions of Type I cells remain largely speculative, these cells are thought to be the main responsible for the diffusive gas exchange owing to their extreme thinness.

Alveolar epithelial Type II cells (or Type II pneumocytes)

Type II cells have been estimated to constitute about 60% of alveolar epithelial cells and

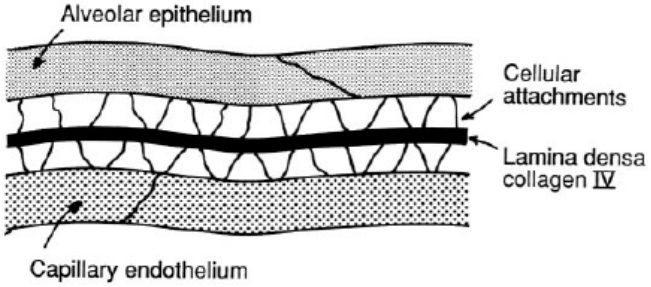

Figure I. 7: A schematic representation of the alveolar blood-gas barrier. From West J.B., 2000

about 15% of all lung parenchymal cells. They cover only about 5% of the alveolar surface, although there are about twice as many Type II cells as there are Type I cells in the human lung. It is because the average Type I cell has a much larger surface area than the average type II cell does. The different contribution to the alveolar surface is due to morphologic differences with Type I cells. Type II pneumocytes are smaller, compact and cuboidal cells (diameter ~ 10 μm, 5-10 μm height and volume of ~ 450 to 900 μm^3) (Crandall and Matthay, 2001). Also, one can distinguish these cells from Type I pneumocytes for the presence of lamellar bodies, and a characteristic apical surface with short microvilli. (Fehrenbach, 2001). The lamellar bodies of alveolar epithelial Type II cells have long been recognised as storage granules from which surfactant is released into the alveolus.

The alveolar epithelial Type II cells are interspersed among Type I cells and can form little protuberances above the largely smooth alveolar epithelial surface. One of the alveolar epithelial Type II cells functions is synthesize, secrete, and recycle all components of the surfactant that regulates alveolar surface tension in the air/liquid interface preventing the alveolus collapse at the end of each expiration. These cells can help to prevent transudation of interstitial fluid into the alveolus (Mackli, 1954) and enhance clearance of inhaled particles. But these cells proliferate, differentiate into alveolar epithelial Type I cells, and remove apoptotic alveolar epithelial Type II cells by phagocytosis, thus contributing to epithelial repair after injury (Evans et al., 1973;Evans et al., 1976). For all these functions, in 1977, Mason R.J. and Williams M.C. developed the concept of the epithelial Type II cells as a "defender of the alveolus" (Mason and Williams, 1977) .

Among the variety of mechanical stimuli experienced by alveolar epithelium, stretch stimulus is believed to be the most determinant from both a biological and a mechanical point of view because epithelial cells undergo considerable stretch during breathing. A

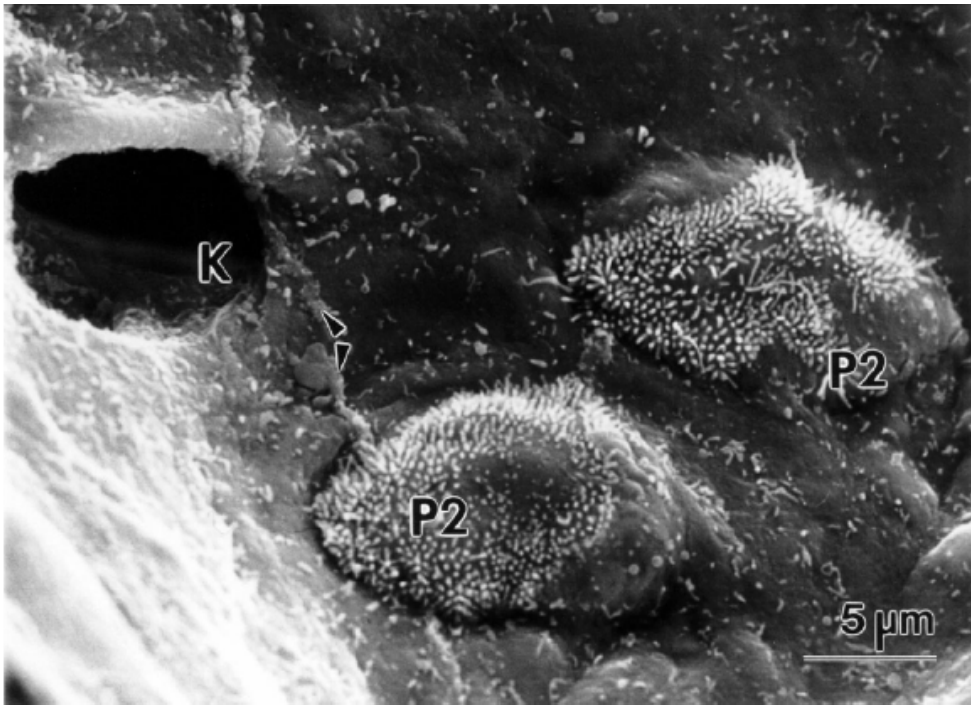

Figure I.8: Human Lung Alveolar Epithelial cells. Scanning electron micrograph of human lung. Two Alveolar Epithelial type II cells (P2) are seen to protrude above the largely smooth alveolar epithelial surface. The cell-cell junction (arrowheads) between two Alveolar Epithelial type I cells is showed. A pore of Kohn (K), an alveolar duct where neighbouring alveolus can communicate, is denoted. From Fehrenbach H., 2001.

number of studies have quantified lung cells deformation from lung tissues. These studies suggest that when the lung inflation increases from 40% to 100% % of total lung capacity (TLC), the alveolar basement membrane surface area increases between 15% (Bachofen et al., 1987) to 35% (Tschumperlin and Margulies, 1999). These studies indicate that alveolar walls carry little stress during normal breathing and that they simply unfold rather than undergoing deformation as the lung inflates. But although the levels of strain experienced by alveolar basement membrane have been characterized, it is not easy to know which is the stretch suffered by epithelial cells in vivo. Some authors have assumed that these cells undergo stretches of 5–10% under physiological breathing conditions, although there are not definitive data (Vlahakis and Hubmayr, 2003).

I.3.3 Risk factors for acute lung injury.

To prevent acute lung injury and acute respiratory distress syndrome it is necessary to identify patients at risk for one of these diseases. The development of ALI/ARDS is associated with several clinical disorders which can be divided into those associated with direct injury to the lung and those that cause indirect lung injury in the setting of a systemic process (Table I.4). Among the direct lung injury risk factors, pneumonia (bacterial, viral, and fungal) and aspiration of gastric and oropharyngeal discontents are the most important and common clinical disorders (Ware and Matthay, 2000;Matthay et al., 2003). Major trauma, sepsis (pulmonary and nonpulmonary), and other disorders such as acute pancreatitis, drug overdose and blood products are included as indirect pulmonary injury risk factors. But the main risk factor in progression to acute lung injury or the acute respiratory distress syndrome is sepsis, approximately 40 percent. Besides, sepsis can complicate ALI/ARDS induced by other causes (Ware and Matthay, 2000;Matthay et al., 2003). There are other secondary factors including chronic alcohol abuse, chronic lung disease, and a low serum pH that can worsen patients with ALI/ARDS. On the other hand, the presence of multiple predisposing disorders substantially increases the risk to develop this syndrome (Ware and Matthay, 2000).

DIRECT LUNG INJURY	INDIRECT LUNG INJURY
Common causes	**Common causes**
Pneumonia	Sepsis
Aspiration of gastric contents	Severe trauma with shock and multiple transfusions
Less common causes	**Less common causes**
Pulmonary contusion	Cardiopulmonary bypass
Fat emboli	Drug overdose
Near- drowning	Acute pancreatitis
Inhalational injury	Transfusions of blood products
Reperfusion pulmonary edema after lung transplantation or pulmonary embolectomy	

Table I.4: Clinical disorders associated with the development of the acute respiratory distress syndrome. From Ware L.B. and Matthay M.A., 2000.

I.3.4 Disruption of the blood-air barrier

Disruption of the alveolar-capillary barrier is a central feature of ALI/ARDS (Ware and Matthay, 2000) resulting in lung edema and infiltration of macromolecules and cells into the pulmonary air spaces. Although lung endothelial cells are the first cells of the lung to be altered in ALI/ARDS triggered by sepsis, trauma, and other systemic conditions, their responses are not completely defined (Matthay et al., 2003). However, it is known that the lung endothelium, in concert with the epithelial barrier, initiates an increase in vascular permeability leading to form pulmonary edema. On the other hand, the different responses of the alveolar epithelium to injury remains incomplete, but the important role of the epithelial integrity in the pathogenesis and resolution of ALI/ARDS has been increasingly appreciated. In normal conditions, the epithelial layer is less permeable to macromolecules and hydrophilic compounds than the endothelial layer (Wiener-Kronish et al., 1991), thus, epithelial injury can contribute to alveolar flooding with protein-rich edema fluid (Ware and Matthay, 2000). Besides, the loss of epithelial integrity and injury to Type II cells can reduce the production of surfactant (Greene et al., 1999), correlating with surfactant deficiency found in patients with ALI/ARDS and can lead to septic shock in patients with bacterial pneumonia. Finally, if injury to the alveolar epithelium is severe, insufficient

epithelial repair may lead to fibrosis (Bitterman, 1992). Like any form of inflammation, ALI and ARDS syndrome represent a complex process in which multiple pathways are involved (Figure I.9). Due to alveolar-capillary barrier disruption, protein rich fluid (plasma proteins such as fibrinogen and inflammatory cells) from capillaries fills the alveolar space. This process is followed by an activation of pulmonary endothelium and macrophages (alveolar and interstitial), an upregulation of adhesion molecules, and a production of different cytokines and chemokines, resulting in a marked accumulation of neutrophils to the injured capillary endothelium (Martin, 2002). These neutrophils transmigrate through the interstitium into the air space, where alveolar macrophages are secreting cytokines including interleukin-1, 6, 8, 10 and TNF-α which act locally to activate neutrophils. Neutrophils release a variety of cytotoxic mediators including proteases, reactive oxygen species (ROS), nitrogen species, leukotrienes, and other proinflammatory molecules, such as platelet-activating factor (PAF) (Ware and Matthay, 2000;Chow et al., 2003). This situation starts a vicious cycle by recruiting more inflammatory cells that in turn produce more cytotoxic mediators, leading to a profound injury to the alveolo-capillary membrane and respiratory failure. The neutrophil activity has been reported to play a critical role in

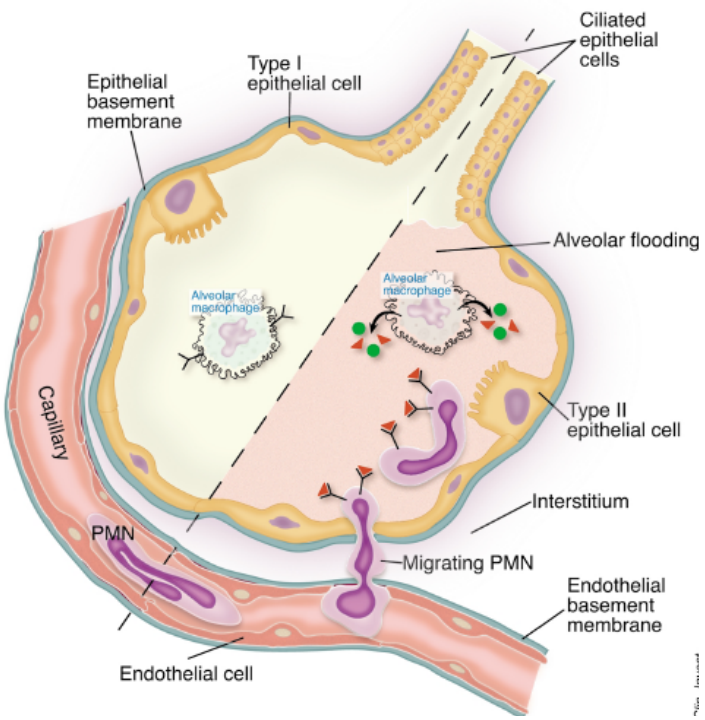

Figure I.9: The normal alveolus (left side) and the injured alveolus in the Acute Phase of Acute Lung Injury and the Acute Respiratory Distress Syndrome (right side).In this drawing, it is shown the two critical barriers, the endothelium and the epithelium. Polymorphonuclear neutrophil (PMN) adhere to the capillary endothelium and migrate into the alveolar space through the interstitium and the epithelium during a murine model of ventilator-induced lung injury. From Martin, 2002.

host defense in this disorder, but their specific function is nowadays not well understood (Martin, 2002).

Thrombin alters the blood-air barrier integrity

It has been shown that when the endothelium is damaged during inflammation, the balance between pro- and anti-coagulant factors is lost and a pro-coagulant state predominates. (Cirino et al., 2000). The serin-protease thrombin, in addition to its role in the coagulation cascade, has been shown to be implicated in the regulation of the permeability of the pulmonary endothelium (Lum and Malik, 1996;Dudek and Garcia, 2001). This protease has been found in bronchoalveolar fluids in a variety of lung inflammatory conditions (Levi et al., 2003), correlating coagulation and inflammation processes. Recent studies have revealed that, thrombin causes a number of proinflammatory and profibrotic effects in the lung through activation of protease-activated receptors (PARs) (Moffatt et al., 2004). Activation of the receptor PAR1 on endothelial cells by thrombin leads to the release of inflammatory mediators such as prostaglandins and nitric oxide (NO), whereas activation of PAR1 on neutrophils leads to migration the neutrophils across the endothelium to the extravascular space (Cirino et al., 2000).

Stretch alters the blood-air barrier integrity

One consequence of ALI/ARDS is a significant decrease in lung compliance that results in an increased effort to breathe, a reason why assisted mechanical ventilation with positive pressure is frequently required and widely used to support most patients (Matthay et al., 2003). Inspiratory airway pressures are often high, suggesting the presence of excessive direct strain on the ventilated lungs. Traditional approaches to mechanical ventilation use tidal volumes of 10 to 15 ml per kilogram of body weigh. It has been shown that mechanical ventilation may be responsible for not only exacerbating pre-existing lung damage and causing multiple organ dysfunctions but also for initiating injury in an otherwise healthy lungs causing increased permeability pulmonary edema (Ricard et al., 2003). This important pathological condition is named ventilator induced lung injury (VILI), historically called "barotrauma", and occurs when the lung is directly damaged by the action of mechanical ventilation. This condition is characterized by the presence of protein-rich alveolar edema, which reflects structural failure of the alveolar epithelial barrier (Pinhu et al., 2003). Some authors have assumed that alveolar epithelial cells undergo stretches of 15–25% in patients with acute respiratory failure who are subjected to

mechanical ventilation (Tschumperlin et al., 2000;Stroetz et al., 2001). Recently, a clinical trial from National Institutes of Health (USA) demonstrated that a lung-protective ventilatory strategy, with low tidal volumes (range, 6 to 8 ml per kilogram of body weigh), considerably reduced the mortality of patients with ARDS when compared to ventilation at high tidal volumes (31.0 percent versus 39.8 percent, respectively) (The- ARDS- network, 2000;Pinhu et al., 2003). This study also reported a decrease in the release of circulating IL-6 cytokine from ALI/ARDS patients treated with lower tidal volumes compared with patients treated with high tidal volumes, indicating a reduction in lung inflammation (The-ARDS- network, 2000).

According to VILI effects, several studies have reported new data about the effects of mechanical stimuli in the range corresponding to high lung tidal volume on alveolar epithelial cells. It has been proposed that cyclic mechanical strain induces proliferation of alveolar epithelial cells (Chess et al., 2000), alveolar cell wounding and plasma membrane repair as a determinant mechanism of VILI (Vlahakis and Hubmayr, 2003). On the other hand, it has been also shown that VILI increases the release of inflammatory mediators such as TNF-α, IL-6 (von Bethmann et al., 1998) and IL-8 (Vlahakis et al., 1999) increasing lung inflammation and causing injury to other organs. Apart from the effects on cellular proliferation and inflammation, alveolar distension also increases surfactant secretion, affecting its metabolism (Wirtz and Dobbs, 1990;Patel et al., 2005).

I.3.5 Model of alveolar epithelial monolayer disruption. Balance of forces.

Acute lung injury and acute respiratory distress syndrome are characterized by disruption of the alveolar-capillary barrier (Ware and Matthay, 2000), and an impairment of cell-cell junctions could be a hallmark of disease progression (Bachofen and Weibel, 1982;Ware and Matthay, 2000). The physical integrity of this semipermeable barrier can be modulated by the dynamic balance between centripetal cell tensional forces arising from cytoskeletal tension and adhesive cell-cell and cell-matrix tethering forces (Dudek and Garcia, 2001). As the alveolar interstitium is continuously subjected to large cyclic stretching during breathing (Tschumperlin and Margulies, 1999), the viscoelastic properties of the cell play a crucial role in regulating this force balance. In fact, under basal conditions, adhesive tethering forces may withstand the cell elastic tension generated during stretching. When alveolar

epithelial cells undergo stretching during mechanical ventilation, the balance of forces in the alveolar epithelium may be compromised (Trepat et al., 2004). It has been observed an increase of 64% in alveolar epithelial cell stiffness, suggesting a partial detachment of cells and a disruption of the epithelial cell layer (Trepat et al., 2004) (Figure I.10). On the other hand, cell mechanics can be altered by inflammatory mediators such as thrombin present in the extracellular medium of injured lungs, potentially compromising the alveolar wall integrity. Thrombin has been shown to be implicated in the regulation of the permeability of the pulmonary endothelium (Lum and Malik, 1996;Dudek and Garcia, 2001). In vitro, thrombin induces gap formation in cultured endothelial monolayers as well as increased intracellular calcium, myosin light chain (MLC) phosphorylation, formation of stress fibers, cytoskeletal remodeling, and modulation of cell-cell and cell-matrix adhesions (Goeckeler and Wysolmerski, 1995;Moy et al., 1996;Murphy et al., 2001). Moreover, stimulation with thrombin increases endothelial cell stiffness and isometric tension of cell monolayers (Moy et al., 1996;Bausch et al., 2001). Recent studies with alveolar epithelial cells suggest that thrombin increases centripetal contractile forces via phosphorylation of the myosin light

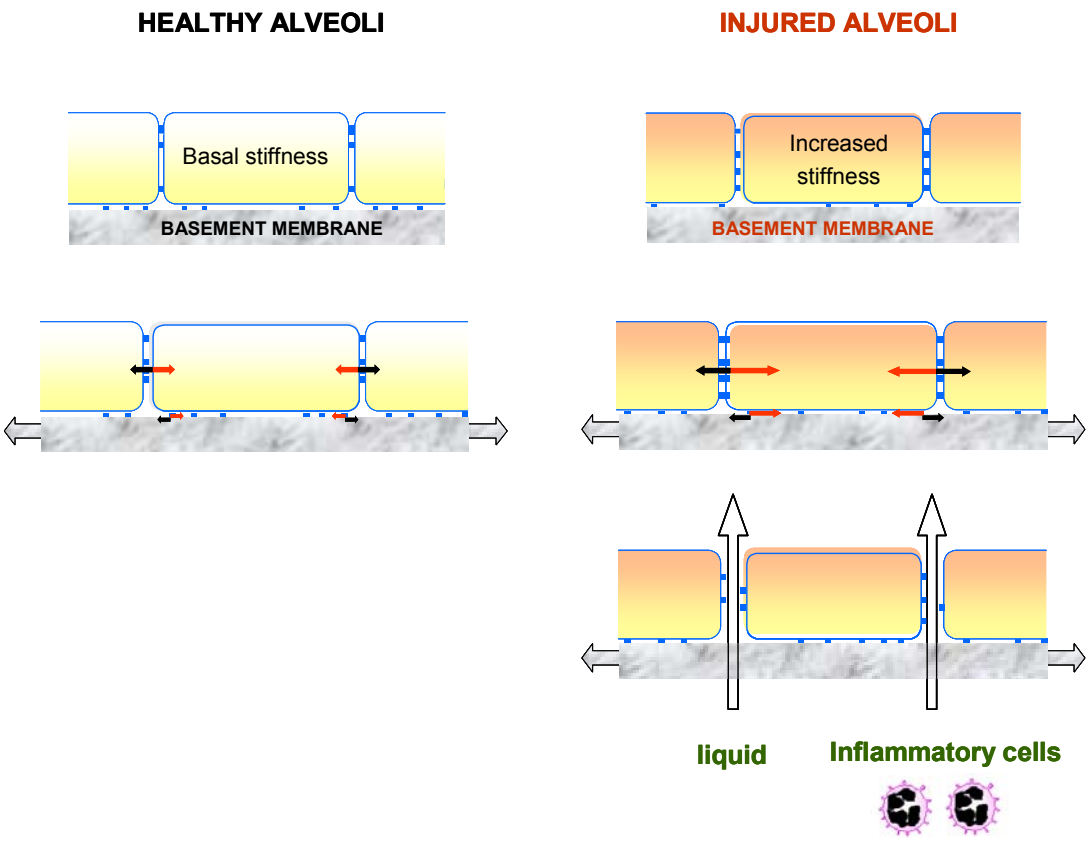

Figure I.10: Model of alveolar epithelial monolayer disruption during stretching because of increased cell stiffness. Basal stiffness (left) and increased stiffness (right). Red arrows: tensional elastic forces generated by cell stretching. Black arrows: adhesive cell-cell and cell-matrix tethering forces (Buscemi, 2004).

chain (MLC) (Kawkitinarong et al., 2004;Gavara et al., 2006). Thrombin has also been reported to increase cell stiffness by threefold (Trepat et al., 2005). This increase in the centripetal forces might not be balanced by the cell-cell and cell matrix tethering forces, leading to paracellular gap formation and increased permeability of the epithelial monolayer. However, a peripheral cytoskeletal remodeling and an increase of the levels of tight junction-associated proteins have been observed in response to thrombin, potentially leading to strengthen the tethering forces, thereby protecting barrier integrity as suggested by increased transepithelial resistance in confluent alveolar epithelial monolayers (Kawkitinarong et al., 2004). However, to our knowledge, there are no data describing the effects of stretch in alveolar epithelial cells when are subjected to some essential features of the extracellular environment of the injured epithelium such as the presence of inflammatory mediators. One of the aims of this thesis is to study the effect of stretch on the structural integrity and micromechanics of human alveolar epithelial cell monolayers exposed to thrombin. (Chapter IV).

Chapter II

Aims of the thesis

GENERAL AIM

The general aim of this thesis was to study the effects of the mechanical stimuli of vibration and stretch on airway epithelial cells in order to better understand the role played by cell mechanics in obstructive sleep apnea and acute lung injury.

SPECIFIC AIMS

To study the effect of a vibratory stimulus on airway epithelial cells

1. To develop a novel cell-vibration stimuli setup to apply high frequency oscillatory perturbations to cultured cells.

2. To study whether a vibration stimulus similar to the one experienced by the upper airway tissues (60 Hz and ± 0.3mm) during snoring have any effect on cell proliferation at three different periods of time (6, 12 and 24h), which are on the order of a night sleep.

3. To assess whether a vibration stimulus at 60 Hz, a frequency between the typical vibration frequencies for mouth and nasal snoring, and at ±0.3mm of amplitude, induce an inflammatory response characterized by an upregulation of interleukin-8 in airway epithelial cells for time periods of 6 hours, 12 hours, and 24 hours.

4. To investigate whether this potential inflammatory response is mediated by three different mitogen-activated protein kinase (MAPK) pathways: ERK, JNK and p38 MAPKs.

To study the effect of stretch on the structural integrity and micromechanics of human alveolar epithelial cell monolayers exposed to thrombin.

5. To develop a new procedure to evaluate loss in adhesion from changes in the distance between the ligand-coated ferrimagnetic beads tightly bound to cell surface via focal adhesions.

6. To measure the effect of stretch on the strain of confluent human alveolar epithelial cells exposed to thrombin

7. To study the effect of stretch on the strain of subconfluent human alveolar epithelial cells exposed to thrombin.

8. To compare the results on the physical integrity between confluent monolayers and subconfluent monolayers.

9. Determine whether there is any difference or similarity on the cell stiffness induced by stretch between confluent and subconfluent human alveolar epithelial cells exposed to vehicle or to thrombin.

Chapter III

Vibration Enhances Interleukin-8 Release in a Cell Model of Snoring-Induced Airway Inflammation

This chapter corresponds to the following publication:

F. Puig, F. Rico, I. Almendros, J. M. Montserrat, D. Navajas and R. Farre. *Vibration Enhances Interleukin-8 Release in a Cell Model of Snoring-Induced Airway Inflammation.* Sleep 28(10):1312-1316, 2005

III.1 ABSTRACT

The inflammation observed in the upper airway and bronchial tissues of patients with obstructive sleep apnea has been attributed in part to the vibratory mechanical stress due to snoring. Although there are wide evidences that epithelial respiratory cells suffer inflammation when are subjected to stretch at low frequencies typical of breathing, there are no data on the potential inflammation induced by high frequency vibration, in part because experimental systems that apply mechanical stimuli are not designed to simulate vibration. The aim of this work was to test a cell model of snoring-induced airway inflammation and to assess whether a vibration stimulus simulating the one experienced by airway tissues in snoring patients induces inflammation in airway epithelial cells. Human bronchial epithelial cells cultures (BEAS-2B cell line) were subjected to vibration (60 Hz, ± 0.3 mm) for time periods of 6 hours, 12 hours, and 24 hours. The vibratory stimulus was applied with and without treatment with inhibitors of the 3 main pathways of mitogen-activated protein kinases (MAPK): p38, MEK1/2, and JNK. The effect of vibration was assessed by comparing cell proliferation and release of interleukin-8 (measured by enzyme-

linked immunosorbent assay) in cells subjected to the vibratory stimulus (both when treated and untreated with MAPK inhibitors) and in controls. Application of vibration up to 24 hours did not significantly modify cell proliferation. By contrast, the concentration of IL-8 in the supernatant was significantly increased after 12 hours and 24 hours of vibration. The inhibition of the p38, MEK1/2, and JNK MAPK pathways significantly reduced the over expression of IL-8 resulting from the vibration stimulus. Our findings indicate that a mechanical vibration simulating snoring triggered an inflammatory cascade, as reflected by the increase in IL-8 release mediated by MAPK pathways. The novel model developed is potentially applicable to studying the effects of the vibration due to snoring in the different cell types (epithelial, endothelial, muscular and neuronal) involved in airway pathophysiology during respiratory sleep disturbances

III.2 INTRODUCTION

Snoring is a vibration of the upper airway, which is very prevalent during sleep in both adults and children (Duran et al., 2001;O'Brien et al., 2003). Snoring occurs when the soft palate and the pharyngeal walls from the upper airway relax and start to vibrate at high-frequency oscillations (Liistro et al., 1991). In addition to its presence in snorers, this breathing event is typically experienced by patients suffering respiratory sleep disturbances such as the obstructive sleep apnea/hypopnea syndrome and the upper airway resistance syndrome (Kimoff et al., 2001;Boyd et al., 2004). At present, there is ample evidence from physiologic, histologic, and molecular studies that the upper airway of patients with respiratory sleep disturbances exhibits different alterations. Sekosan M. and coworkers (1996) demonstrated the presence of inflammation in the uvula mucosa, characterized by plasma cell infiltration and interstitial edema. They concluded that the presence of inflammation in this area contributes to the occlusion of the upper airways seen during sleep in obstructive sleep apnea patients. Paulsen and coworkers (2002) revealed structural changes in the mucosa of the uvula and at the subepithelial-connective tissue boundary of patients with sleep apnea and habitual snorers. Woodson B.T. and coworkers showed that histologic differences occur in snorers and in patients with obstructive sleep apnea compared with non snorers, visible as mucous gland hypertrophy, focal atrophy of muscle fibers, and extensive edema of the lamina propria (Woodson et al., 1991). Moreover, patients with obstructive sleep apnea exhibit muscle and nerve dysfunction (Friberg et al.,

1997;Boyd et al., 2004). In addition to evidence of inflammation in both the muscular and mucosal tissue and denervation, changes within the upper airway of patients with obstructive sleep apnea, loss of sensitivity (Kimoff et al., 2001;Nguyen et al., 2005), sensory neuropathy (Larsson et al., 1992) and structural alteration of the extracellular matrix (Series et al., 2004) have also been found. Moreover, snoring has also been associated with bronchial inflammation. Indeed, the first data describing the relationship between snoring and asthma (Chan et al., 1988) have been confirmed in subsequent studies (Fitzpatrick et al., 1993;Lu et al., 2003). Furthermore, recent data reporting direct measurements of inflammatory markers suggest that, in sleep apnea patients, the inflammation is also present in the bronchi (Salerno et al., 2004;Devouassoux et al., 2004). Although the mechanisms determining airway injury in respiratory sleep disturbances have not been elucidated, it has been suggested that the vibratory mechanical stress associated with snoring could play an important role in damaging the airway tissues (Larsson et al., 1992;Kimoff et al., 2001;Paulsen et al., 2002;Lu et al., 2003;Nguyen et al., 2005) and in the progression of the sleep apnea severity (Pendlebury et al., 1997;Friberg, 1999).

Little is known, however, about the inflammatory effects of a vibratory stimulus on the cells of the airway wall. This lack of information is probably due in part to the fact that the experimental systems that apply mechanical stimuli to airway cells (Liu et al., 1999) are designed to simulate stretch (Oudin and Pugin, 2002;Pugin, 2003), compression (Tschumperlin et al., 2002;Chu et al., 2005) or shear stress (Ni et al., 2004;Cunningham and Gotlieb, 2005) but not vibration. In this work we developed a novel experimental model to test the hypothesis that the application of a vibration stimulus with frequency and amplitude simulating the ones experienced by upper-airway tissues during snoring is capable of inducing an inflammatory response at the cell level. The study was conducted on bronchial epithelial cells and was focused on assessing whether vibration triggers an inflammatory response characterized by an upregulation of interleukin-8 through mitogen-activated protein kinase pathways, as occurs when cells are subjected to substrate deformation (Vlahakis et al., 1999;Oudin and Pugin, 2002).

III.3 MATERIALS AND METHODS

III.3.1 Cell culture.

Human bronchial epithelial cells (BEAS-2B line, CRL- 9609, ATCC, Manassas, Virg) were cultured in a RPMI 1640 medium supplemented with 1% inactivated fetal bovine serum, insulin-transferrin-selenium-G (1.0 g/L, 0.55 g/L, and 0.67 mg/L, respectively) (GIBCO, Gaithersburg, MD), 1 mmol Lglutamine, penicillin-streptomycin (50 U/mL and 50 μg/mL, respectively), 2.5 μg/mL amphotericin B , 10 mmol HEPES, 20 μmol hydrocortisone (Sigma, St Louis, MO), and 10 ng/mL epidermal growth factor (CalBiochem, San Diego, Calif). The day before the experiment, cells ($2 \cdot 10^5$/mL) were plated on Petri dishes (35 mm in diameter) previously collagenated with rat tail collagen type-I (10 μg/mL during 1 hour; Upstate; Lake Placid, NY). At the start of the experiment, the cover of each Petri dish was tightly wrapped by means of Parafilm M (Pechiney Plastic Packaging, Chicago, IL). Two previously drilled holes (1-mm diameter each) in the dish cover allowed gas exchange between the culture medium and the atmosphere. As verified in a preliminary set of measurements, this procedure avoided loss of culture medium (less than 2%) as a result of the vibration applied to the Petri dish.

III.3.2 System to Apply a Vibratory Stimulus to the Cells

A 12" subwoofer loudspeaker (12SP-F, Beyma, Valencia, Spain) driven by a sinusoidal signal at 60 Hz and a power amplifier (LM-12, National Semiconductors, Santa Clara, Calif) was used to subject the cultured cells to vibration. A rigid Plexiglas surface (24 cm in diameter) was glued to the loudspeaker cone, allowing 15 culture dishes to be firmly attached to the horizontal vibrating platform by double adhesive tape (Figure III.1). An accelerometer (ADXL-150, Analog Devices, Norwood, Mass) was coupled to the vibrating platform to continuously measure the acceleration experienced by the cell culture. The amplitude of the power amplifier driving the loudspeaker was set to obtain an amplitude vibration of ±0.3 mm at 60 Hz (corresponding to an acceleration of ±4.3 g (g = 9.8 m/s^2). In a preliminary set of experiments, the accelerometer was moved along the vibrating platform to verify that its displacement at 60 Hz was uniform (within 5% over the whole surface). The loudspeaker-based vibratory system was placed inside a conventional culture

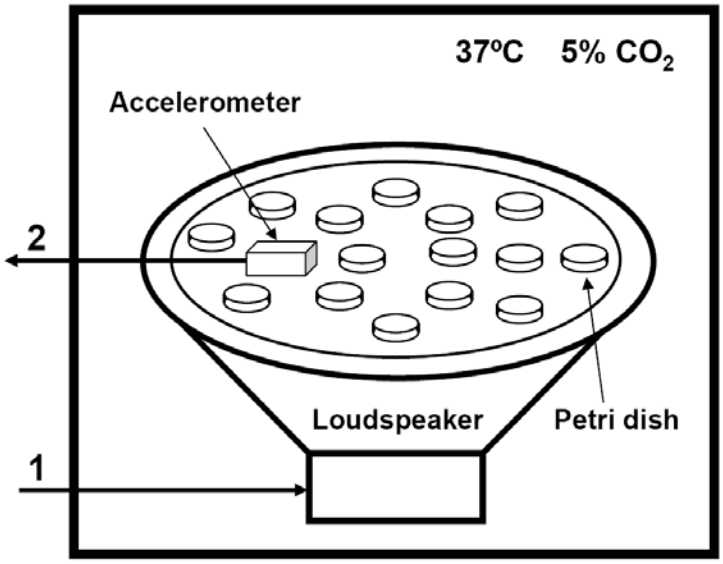

Figure III.1: Diagram of the system to apply a vertical oscillatory stimulus to the cultured cells. The Petri dishes with the cultured cells were firmly attached to a platform glued to the moving loudspeaker cone. An accelerometer allowed us to measure the vibration amplitude. Flexible wires connected the loudspeaker to its power amplifier (1) and the accelerometer to its circuitry (2). The loudspeaker-based vibration system was placed into a conventional culture chamber. From Puig et al., 2005

chamber at 37 ºC and 5% CO_2. Petri dishes used as control (not subjected to vibration) were placed in a similar culture chamber.

III.3.3 Effects of Vibration on Cell Proliferation

Six groups of Petri dishes (n = 15 each) were studied to ascertain whether vibration modified cell proliferation. In 3 of the groups, the vibration stimulus (60 Hz, ±0.3 mm) was applied for 6 hours, 12 hours, and 24 hours, respectively. The other 3 groups were not subjected to vibration and were used as controls at 6 hours, 12 hours, and 24 hours respectively. After the end of each vibration (and control) period, a 100-μm-deep hemocytometer (Brand, Wertheim, Germany) was used to count the number of cells in each dish.

III.3.4 Effects of Vibration on IL-8 Release

Four groups of Petri dishes (n = 18 each) were studied to assess the effect of vibration on

IL-8 production. One group was not subjected to vibration and was used as control. The other 3 groups were subjected to vibration (60 Hz, ±0.3 mm) for 6 hours, 12 hours, and 24 hours, respectively. After the corresponding vibration period, each Petri dish was retired from the vibratory platform and placed in the control culture chamber. Forty hours after the start of the vibration experiment, the cell supernatants were harvested and stored at -20ºC. At the end of this series of experiments, the concentration of human IL-8 in the supernatant of each Petri dish was measured by enzyme-linked immunosorbent assay (ELISA) (Quantikine, R&D Systems, Minneapolis, Minn). (See Appendix 1).

III.3.5 Role of MAPK in the Upregulation of IL-8 Induced by Vibration

To study the effects of MAPK pathways in the increase of IL-8 release induced by vibration, 5 groups of Petri dishes (n = 18 each) were subjected to vibration (60 Hz, ±0.3 mm) for a period of 12 hours. One of these groups was untreated, and each of the other 4 groups was treated with an inhibitor of the MAPK cascade. One of the treatments was a nonspecific tyrosine kinase inhibitor (Genistein, 50 μM; Sigma). The other 3 treatments used to inhibit the main MAPK cascades were (1) a specific p38 MAPK inhibitor (SB 203580, 1 μM; Calbiochem), (2) a specific MEK1/2 inhibitor (PD 98059, 25 μM, upstream of p44/42 MAPK; Calbiochem), and (3) a specific JNK MAPK kinase inhibitor (SP 600125, 1μM; Sigma) (Figure III.2). All the inhibitors were diluted in dimethyl sulfoxide (DMSO) (final concentration: 0.1%) (Sigma). The inhibitor solution (or DMSO vehicle in the control and untreated groups) was applied 30 minutes before the application of the 12-hour vibratory stimulus. A group of nonvibrated nontreated Petri dishes (n = 18) was used as control. The cell supernatants were harvested 40 hours after starting the vibration and stored at -20ºC. At the end of this series of experiments, the concentration of human IL-8 in the supernatant of each Petri dish was measured by ELISA (Quantikine, R&D Systems) as described above.

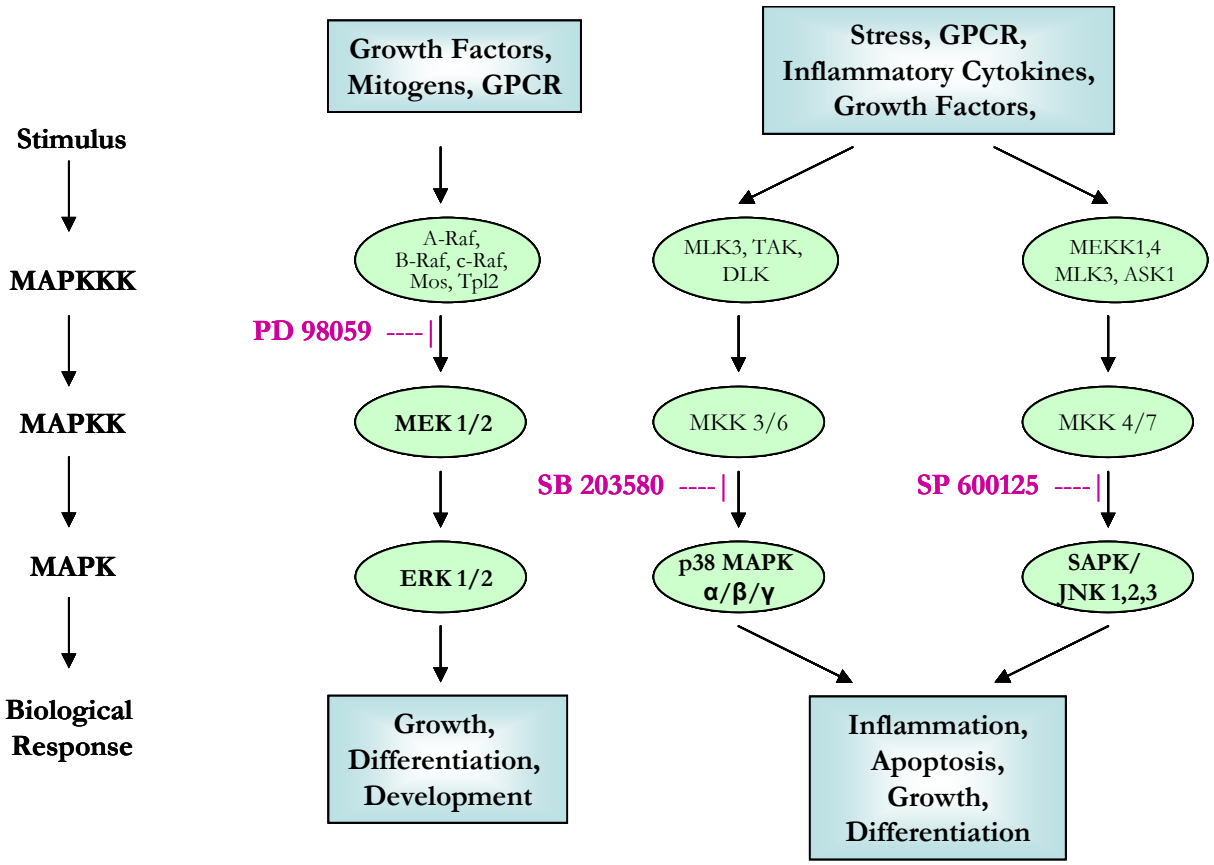

Figure III.2: Activation of different MAPK signaling cascades by different extracellular stimuli. The ERK, JNK and p38 cascades all contain the same series of three kinases. A MEK Kinase (MEKK) or MAPKKK phosphorylates and activates a MAP Kinase Kinase (MEK or MAPKK), then MEK phosphorylates and activates a MAP Kinase (MAPK). Adapted from http://focosi.altervista.org/mapkmap.html.

III.3.6 Statistics

Results were expressed as mean ± SEM. Two-way analysis of variance was used to test whether vibration modified cell proliferation. Comparison between means of IL-8 concentration was carried out with unpaired t tests. The recently recommended (Currant-Everett and Benos, 2004) "false discovery rate procedure" (Currant-Everett, 2000) was employed to determine the critical significance level corresponding to P = 0.05 in multiple comparisons.

III.4 RESULTS

The vibratory stimulus applied did not affect cell proliferation. Figure III.3 shows that application of vibration for periods of 6 hours, 12 hours, and 24 hours resulted in a number of cells slightly lower (3%-6%) than in controls. However, this small difference in proliferation was not statistically significant (P = 0.42).

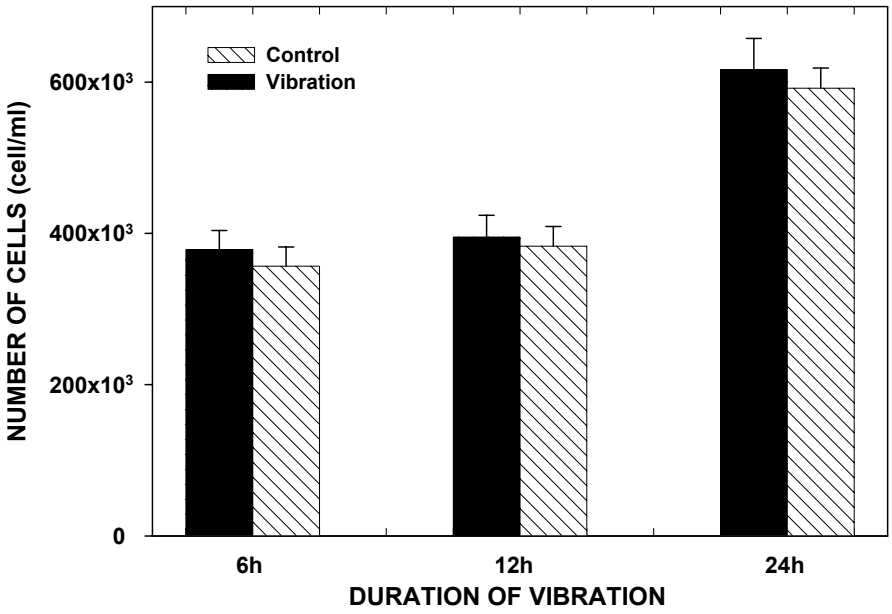

Figure III.3: Cell proliferation in controls and in cells subjected to vibration (60 Hz, ±0.3 mm). Vibration did not induce significant changes in cell proliferation (P=0.42). Data are mean ± SEM. From Puig et al., 2005

The concentration of IL-8 in the supernatant collected 40 hours after the start of vibration was increased with the duration of the oscillatory stimulus (Figure III.4). After 12 hours and 24 hours of vibration, the IL-8 concentration was significantly higher than in control (46% (P = 0.029) and 56% (P = 0.013), respectively).

The MAPK pathways played a role in the increase in IL-8 release resulting from the vibration stimulus. In agreement with the results in Figure III.4, Figure III.5 shows that, in cells subjected to vibration, the concentration of IL-8 was increased with respect to control (P = 0.006). The figure also shows that treatment with the nonspecific tyrosine kinase inhibitor genistein considerably reduced the concentration of IL-8 when compared with the untreated cells subjected to vibration (P < 0.001). Moreover, marked decreases in IL-8 were also observed in the cells treated with the specific p38 MAPK inhibitor (SB 203580) (P = 0.008), the specific MEK1/2 inhibitor (PD 98059) (P = 0.016), or the specific JNK

MAPK kinase inhibitor (SP 600125) (P = 0.022).

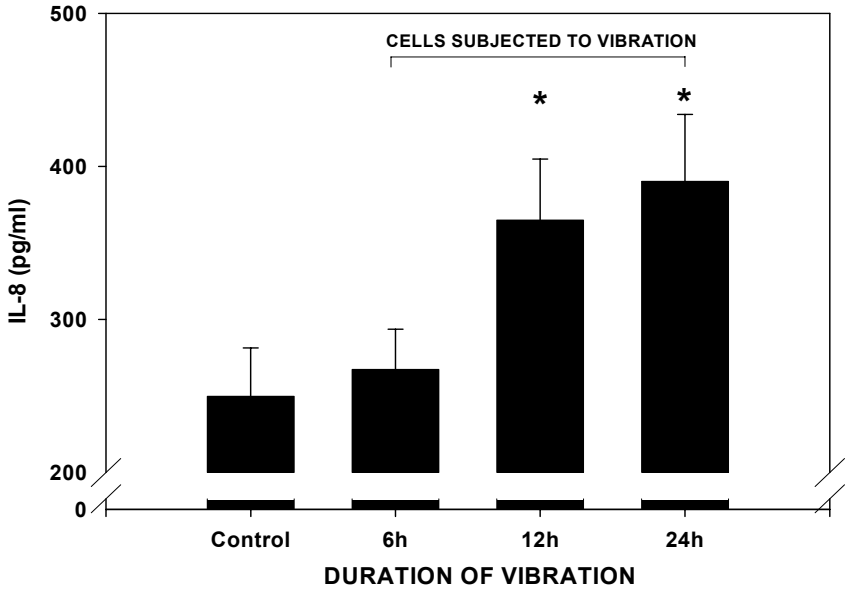

Figure III.4: Concentration of interleukin-8 (IL-8) in the supernatant of control cells and of cells subjected to 6 hours, 12 hours, and 24 hours of vibration (60 Hz, ±0.3 mm). Data are mean ± SEM. The symbol * indicates significant difference from control (P < 0.05). From Puig et al., 2005

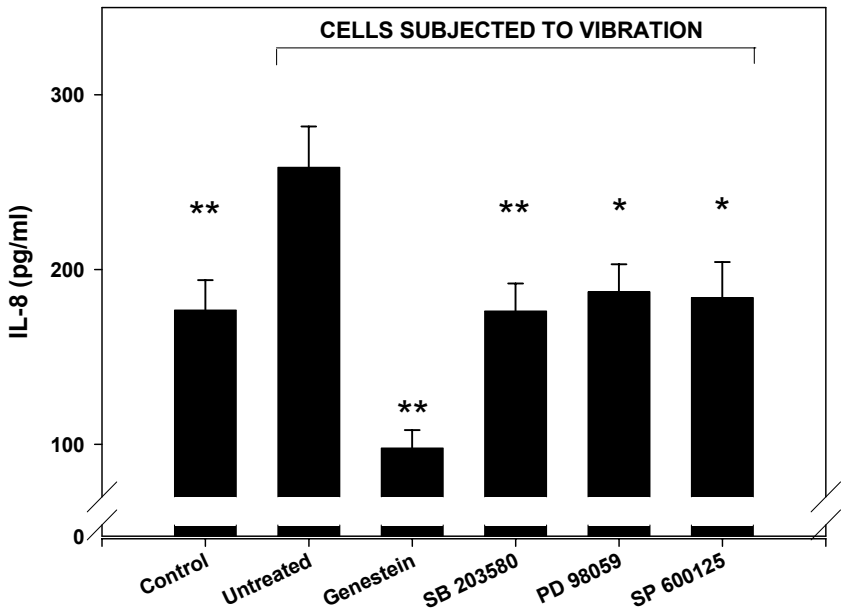

Figure III.5: Effect of treatments with mitogen-activated protein kinases (MAPK) inhibitors (genistein, SB 203580, PD 98059, and SP 600125) in the interleukin-8 (IL-8) supernatant concentration of controls and cells subjected to vibration for 12 hours (60 Hz, ±0.3 mm). Data are mean ± SEM. The symbols * and ** indicate significant difference from the untreated cells subjected to vibration (P < 0.05 and P < 0.01, respectively). All cells were subjected to the same 0.1% dimethyl sulfoxide (DMSO) final concentration. From Puig et al., 2005

III.5 DISCUSSION

The novel experimental setting that we developed allowed us to easily apply vibratory stimuli with well-controlled frequency, amplitude, and duration. Application of vibration simulating snoring to human bronchial epithelial cells, BEAS-2B, resulted in an increased release of the proinflammatory cytokine IL-8, which was reduced by inhibition of MAPK pathways. These results indicate that airway epithelial cell vibration per se could trigger inflammatory signaling.

III.5.1 Cell model

The study was carried out in human bronchial epithelial cells from the cell line BEAS-2B. There are several reasons for which we chose a bronchial cell line instead of upper airway primary culture to carry out this study. Cultures of normal human upper airway epithelial cells, as all primary cultures, offer opportunities to study their responsiveness to mechanical stimulation in vitro. These cultures can be established from several sources of donated airway specimens, including surgeries and autopsies. Of these, one can obtain a great amount of cells. However, obtaining tissues from these sources can be sporadic and difficult. Cell cultures can also be obtained by biopsy (excluding the tonsils, one can obtain normal oropharyngeal tissues) or brushing of airways during bronchoscopy, but the quantity of cells recovered significantly limits the numbers of cultures that can be established. For this reason and because normal human epithelial cellular replication ceases after a limited period of time, many works have been carried out using immortalized human upper airway epithelial cell lines. In 1965, Moorhead P.S. developed a normal human nasal epithelial (NHNE) cell line from squamous cell carcinoma (Moorhead, 1965). But as it is said in the introduction, squamous cells are present in the nose and the first millimeters of the nasal cavity. The cells present in the whole respiratory track are pseudo-stratified columnar ciliated epithelial cells and stratified cuboidal epithelial cells. So, depending of the study, NHNE cell line could not be the most representative cells for describing the airway epithelium. Moreover, the source of this and others cell lines such as cell lines from the pharynx tissue comes from lung carcinomas. As upper airway mucosa has more or less the same histology than the bronchial mucosa (Fokkens and Scheeren, 2000), and the pseudo-stratified columnar ciliated upper airway and bronchial epithelium are constituted by the same type of epithelial cells, in some experiments it is possibly to use

bronchial epithelial cells instead of upper airway epithelial cells and vice versa to study how these cells respond to mechanical perturbations or to environmental agents. On the other hand, it has been reported that in sleep apnea patients, the inflammation induced by snoring is also present in the bronchi (Salerno et al., 2004;Devouassoux et al., 2004). Therefore, if snoring is also sensed by the bronchi, one can use bronchial epithelial cells to study the effects of a vibratory stimulus, and at the same time, one can use bronchial epithelial cells as representative cells from the upper airway. However, the conclusions derived from cell lines should be extrapolated to primary cells with caution.

BEAS-2B cell line is one of the bronchial epithelial cell lines available. In 1988, Reddel R.R. et al. exposed normal human bronchial epithelial cells from explants of necropsy tracheobronchial specimens from noncancerous individuals to an adenovirus hybrid virus (12-SV40 or Ad12SV40) to provide non-tumorigenic human cell lines. These cells proliferate for more than 2 years and maintain typical epithelial morphology and many epithelial functional characteristics to normal human bronchial epithelial (NHBE) cells (Ke et al., 1988;Reddel et al., 1988). BEAS-2B cells retain the ability to undergo squamous differentiation in response to serum, as their normal counterpart cells. TGF-β1 known as a major serum-borne differentiation inducing signal, inhibits epithelial cell growth and induces squamous differentiation in NHBE cells (Thompson et al., 1995) as in BEAS-2B cells, which are also sensitive to induction of squamous differentiation by this agent (Ke et al., 1988). BEAS-2B cells express a large number of surface molecules under basal conditions, such as β1, β2, β3 and CD44 integrins, and after stimulation with cytokines, which induce vascular cell adhesion molecule-1 (VCAM-1) expression, also detectable in primary human bronchial epithelial cells ((Atsuta et al., 1997). Bronchial epithelial cells also produce a wide variety of proinflammatory cytokines, such as IL-1, IL-6, IL-8, IL-16, GM-CSF and tumor necrosis factor (TNF) (Levine et al., 1993;Arima et al., 1999;Devouassoux et al., 2004). BEAS-2B cells are very similar to NHBE cells, are easily cultivable and they come from a human source. This cell line has been used in many studies as a human bronchial epithelium model (Oudin and Pugin, 2002;Thomas et al., 2006). Therefore, we considered that BEAS-2B cells were a suitable model to study the effects of a vibratory stimulus on airway epithelial cells.

III.5.2 Vibratory stimulation device

The system implemented in this work to apply cell-vibration stimuli is based on a loudspeaker. In contrast with other complex systems previously employed for applying high-frequency mechanical displacements in chondrocythes and annular cells (Liu et al., 2001;Yamazaki et al., 2002) or for stimulating osteoblasts with high-frequency oscillatory strain (Tanaka et al., 2003), the loudspeaker-based system is simple to implement and readily usable. This system allows an easy adjustment of the amplitude and frequency of vibration in sinusoidal oscillation. Moreover, given its excellent dynamic response, the device could be used to reproduce more realistic patterns of vibration: inclusion of snoring pauses (corresponding to inspiration/expiration time), vibration at varying amplitude along inspiration, or vibration with complex frequency spectra. To this end, the vibration signals recorded with an accelerometer/microphone placed on the neck of the snoring patient could be used to drive the loudspeaker amplifier.

To investigate the potential effects of vibration on airway epithelial cells, we used a single oscillation with a frequency of 60Hz. Although snoring produces a complex sound extended up to high frequencies (Osborne et al., 1999;Hill et al., 1999;Rembold and Suratt, 2005), spectrum analysis has shown a high-amplitude vibration at low frequencies (50-100 Hz) (Osborne et al., 1999;Hill et al., 1999). The spectrum analysis of the snoring sound confirms previous data obtained by direct measurement of upper airway vibration images by means of cineradiography. Given that the typical vibration frequencies are around 30 Hz and 80 Hz for mouth and nasal snoring, respectively, (Liistro et al., 1991) we selected a frequency of 60 Hz to study the response of airway epithelial cells to vibration. The amplitude of the vibration applied in this work ($\pm$ 0.3 mm) is on the order of the upper airway snoring oscillations that can be derived from cineradiography images (Liistro et al., 1991). The duration of the applied vibration in the present study lasted several hours, which is a time period on the order of a night sleep. Although the sinusoidal oscillation applied to cultured cells did not exactly reproduce the vibration pattern in snoring patients, its main parameters (frequency, amplitude, and time) reasonably mimicked the basic features of snoring.

III.5.3 The role of IL-8 in inflammation

Among the different markers of inflammation (Kracht and Saklatvala, 2002), we focused on IL-8 to assess the potential injurious effects of cell vibration. IL-8 is a proinflammatory cytokine that is upregulated by different cellular stress stimuli (Hoffmann et al., 2002). This cytokine plays an important role in the pathogenic response because it is a potent chemoattractant and activator of neutrophils, promoting their infiltration from the blood capillaries to the tissue subjected to the inflammatory challenge. Human cells are characterized by their marked capacity for varying the expression levels of IL-8, allowing to modulate the concentration of this cytokine to control the degree of neutrophil infiltration in the injured tissue (Hoffmann et al., 2002). The expression of IL-8 is regulated at both transcriptional and posttranscriptional levels (Kracht and Saklatvala, 2002), and the main MAPK pathways (p38, MEK1/2 and JNK) play a significant role in the release of IL-8 during the inflammatory process (Hoffmann et al., 2002). In this work, we focused on IL-8 as a biomarker of inflammation in response to vibration, given that this cytokine shows a considerable upregulation when airway epithelial cells were subjected to other mechanical stimuli (Pugin, 2003;Vlahakis and Hubmayr, 2003).

III.5.4 Inflammatory effects of vibration

The supernatant IL-8 concentration after 40 hours of the start of the experiment increased with the duration of the vibration stimulus (Figure III.4). Both the magnitude of IL-8 increase and its time dependence are in keeping with the data previously reported when bronchial (Oudin and Pugin, 2002) and alveolar (Vlahakis et al., 1999) epithelial cells were subjected to realistic stretch deformations. In addition, the data in Figure III.5 show that the MAPK pathways played a significant role in the upregulation of IL-8 (Figure III.2). First, the use of genistein for non-specifically inhibiting tyrosine kinase, which is upstream of MAPK, considerably reduced the release of IL-8 in vibrated cells to a value below the untreated control, probably because this drug interfered with the physiologic production of the interleukin. The inhibition of the pathways of p38, MEK1/2, and JNK MAPKs significantly reduced the increase in IL-8 release induced by vibration (Figure III.5). Given that none of the inhibitors nor the DMSO solvent affected cell viability when are compared with control data ($p>0.05$ in all cases) and given that, according to Figure III.5 (control vs untreated), a 0.1% DMSO final concentration did not inhibit the

overexpression of IL-8 in these cells (Wong et al., 2005), our results indicate that the MAPK pathways are involved in the increase in IL-8 production induced by vibration. These results are in agreement with those reported when the same cell type was subjected to stretch (Oudin and Pugin, 2002), suggesting that similar mechanotransduction pathways are triggered by vibration and stretch. Further detailed studies should provide more insights into the similarities and differences in the triggering of inflammatory cascades by vibration and stretch.

III.5.5 Conclusions

In conclusion, we have shown that application of well-defined vibration stimulus simulating snoring to cultured airway epithelial cells initiates a proinflammatory response. This result lends support to the hypothesis that snoring could be an important factor contributing to the airway inflammation observed in patients with obstructive respiratory disorders during sleep. The simple experimental setting developed in this work can be applied to studying the effects of vibration in other cells of the airway wall and surrounding tissues that are affected by snoring vibration (endothelial, neuromuscular, macrophages, etc). Such experiments could help in interpreting the cellular processes that determine the airway dysfunctions in patients with obstructive breathing disturbances during sleep (Larsson et al., 1992;Kimoff et al., 2001;Paulsen et al., 2002;Carpagnano et al., 2003;Boyd et al., 2004;Series et al., 2004;Nguyen et al., 2005). A better understanding of the basic mechanisms of cell damage owing to snoring could potentially facilitate the extension of future innovative anti-inflammatory therapies to patients with respiratory sleep disturbances (Saklatvala, 2004;Duan et al., 2005).

Chapter IV

Effect of stretch on structural integrity and micromechanics of human alveolar epithelial cell monolayers exposed to thrombin

This chapter corresponds to the following publication:

X.Trepat*, **F.Puig***, N.Gavara, J.J. Fredberg, R. Farre and D. Navajas. *Effect of stretch on structural integrity and micromechanics of human alveolar epithelial cell monolayers exposed to thrombin.* American Journal of Physiology- Lung Cellular and Molecular Physiology 290:1104-1110, 2006.
* X. Trepat and F. Puig contributed equally to this work.

IV.1 ABSTRACT

Alveolar epithelial cells in patients with acute lung injury subjected to mechanical ventilation are exposed to increased procoagulant activity and mechanical strain. Thrombin induces epithelial cell stiffening, contraction, and cytoskeletal remodeling, potentially compromising the balance of forces at the alveolar epithelium during cell stretching. This balance can be further compromised by the loss of integrity of cell-cell junctions in the injured epithelium. The aim of this work was to study the effect of stretch on the structural integrity and micromechanics of human alveolar epithelial cell monolayers exposed to thrombin. Confluent and subconfluent cells (A549) were cultured on collagen-coated elastic substrates. After exposure to thrombin (0.5 U/ml), a stepwise cell stretch (20%) was applied with a vacuum-driven system mounted on an inverted microscope. The structural integrity of the cell monolayers was assessed by comparing intercellular and intracellular

strains within the monolayer. Strain was measured by tracking beads tightly bound to the cell surface. Simultaneously, cell viscoelasticity was measured using optical magnetic twisting cytometry. In confluent cells, thrombin did not induce significant changes in transmission of strain from the substrate to overlying cells. By contrast, thrombin dramatically impaired the ability of subconfluent cells to follow imposed substrate deformation. Upon substrate unstretching, thrombin- treated subconfluent cells exhibited compressive strain (9%). Stretch increased stiffness (56–62%) and decreased cell hysteresivity (13–22%) of vehicle cells. By contrast, stretch did not increase stiffness of thrombin-treated cells, suggesting disruption of cytoskeletal structures. Our findings suggest that thrombin could exacerbate epithelial barrier dysfunction in injured lungs subjected to mechanical ventilation.

IV.2 INTRODUCTION

Mechanical ventilation is the basic treatment in support of patients with acute lung injury, ALI, and the acute respiratory distress syndrome, ARDS (Ware and Matthay, 2000). A number of studies, however, have shown that aside from its beneficial effects, mechanical ventilation may exacerbate lung injury (Dreyfuss and Saumon, 1998;Dos Santos and Slutsky, 2000). For example, an extensive multicenter trial from the ARDS network revealed that mechanical ventilation with low tidal volumes reduced the mortality of patients with ARDS by 22% when compared with traditional ventilation with high tidal volumes (The- ARDS-network, 2000). This condition, known as ventilator-induced lung injury, is characterized by the presence of protein-rich alveolar edema, which reflects structural failure of the alveolar epithelial barrier (Pinhu et al., 2003). The physical integrity of this barrier requires a dynamic force balance between centripetal cytoskeletal forces and centrifugal adhesion forces at cell-cell and cell-matrix adhesion sites.

The serine-protease thrombin is found in bronchoalveolar fluids in a variety of lung inflammatory conditions (Howell et al., 2002;Levi et al., 2003). However, its role in the pathogenesis and resolution of lung injury remains poorly understood. Recent studies have revealed that, in addition to its role in the coagulation cascade, thrombin causes a number of proinflammatory and profibrotic effects in the lung through activation of protease-activated receptors, PARs (Howell et al., 2002;Moffatt et al., 2004). Work from our

laboratory (Trepat et al., 2005;Gavara et al., 2006) and others (Kawkitinarong et al., 2004) suggest that thrombin alters the balance of forces at the alveolar epithelial cell level by means of at least three competing mechanisms. First, thrombin has been shown to increase centripetal contractile forces via phosphorylation of the myosin light chain (MLC) (Kawkitinarong et al., 2004;Gavara et al., 2006). Second, thrombin has also been reported to increase levels of tight junction-associated proteins and circumferential reorganization of the cytoskeleton, potentially leading to enhanced cell-cell adhesion as suggested by increased transepithelial resistance in confluent alveolar epithelial monolayers (Kawkitinarong et al., 2004). Finally, thrombin rapidly increases cell stiffness by threefold, leading to a similar increase in the centripetal tension that cell-cell and cell-matrix adhesions would need to withstand during lung expansion (Trepat et al., 2005).

The aim of this work was to study the effect of stretch on the structural integrity and micromechanics of human alveolar epithelial cell monolayers exposed to thrombin. We used a novel technique to subject thrombin-treated cell monolayers to stepwise stretch and to measure simultaneously cell strain and viscoelasticity (Trepat et al., 2004). The technique is based on binding ferromagnetic beads to cell surface receptors. Because the beads are tightly connected to cell surface and cytoskeleton, they can be used as markers to measure cell strain during substrate stretching. The structural integrity of the cell monolayer is assessed by comparing the intracellular and intercellular strains within the monolayer. In addition, the beads are twisted by an oscillatory magnetic field (Fabry et al., 2001) that allows us to measure cell viscoelasticity during stretch.

IV.3 MATERIALS AND METHODS

IV.3.1 Cell culture and sample preparation.

Human alveolar epithelial cells A549, culture line CCL-185 (American Type Culture Collection, Manassas, VA), were used at passages 5-20. Cells were cultured in RPMI 1640 media supplemented with 10% inactivated fetal bovine serum (GIBCO, Gaithersburg, MD), 1 mM L-glutamine, penicillin-streptomycin (50 U/ml, 50 μg/ml, respectively), 2.5 μg/ml amphotericin B and 10 mM HEPES (Sigma, St Louis, MO).

For experiments, cells were harvested with a brief exposure to trypsin EDTA (Sigma, St. Louis, MO) and plated (3×10^5 cells/well) on collagen I-coated flexible-bottomed culture wells (35 mm diameter; Bioflex, Flexcell International, PA). Measurements were performed in confluent cells (7 to 14 days after plating) and in subconfluent cells (2 to 4 days after plating).

On the day of experiments, 400 μg of coated ferrimagnetic beads (Fe_3O_4) of 4.5 μm diameter with magnetic moment 9×10^{-13} A•m^2 suspended in HEPES-buffered RPMI 1640 were added to each individual well. After 20 min incubation, the well was washed with HEPES-buffered RPMI 1640 to remove unbound beads and mounted on the experimental setup.

The beads were coated with a synthetic RGD (Arg-Gly-Asp) containing peptide (Peptite 2000, Integra life Sciences, San Diego, CA) at 50 μg of peptide/mg bead in 1 ml of carbonate buffer (pH 9.4).

IV.3.2 Stretching device

Experiments were performed with a stretching device mounted on an inverted optical microscope (Axiovert S100, Zeiss, Gottingen, Germany) placed on a vibration isolation table (Isostation, Newport, Irvine, CA). The cell-stretching device is based on deforming the cell substrate by applying vacuum underneath the flexible-bottomed well. A cylindrical loading post is located underneath the central region of the well, coaxial to the microscope objective, to obtain uniform and equibiaxial strains in the central region of the cell culture (Schaffer et al., 1994). When vacuum is applied underneath the outer annular region of the flexible cell substrate, the central region is stretched equi-biaxially and homogeneously while roughly remaining on the microscope focal plane (Figure IV.1). The rising and falling times of the applied negative pressure step are set to 4 seconds with a first-order pneumatic filter (Trepat et al., 2004). Previously to the experiment, the stretching device was calibrated as described in detail elsewhere (Schaffer et al., 1994;Trepat et al., 2004). Nine dots were drawing forming a square pattern on the flexible substrate, which was deformed with negative pressure steps up to 45 cm Hg in random order. The position of the geometrical center of the dots was measured in relaxed and stretched conformations using a progressive scan blackand- white charge-coupled device (CCD) camera (CV-M10 BX; JAI,

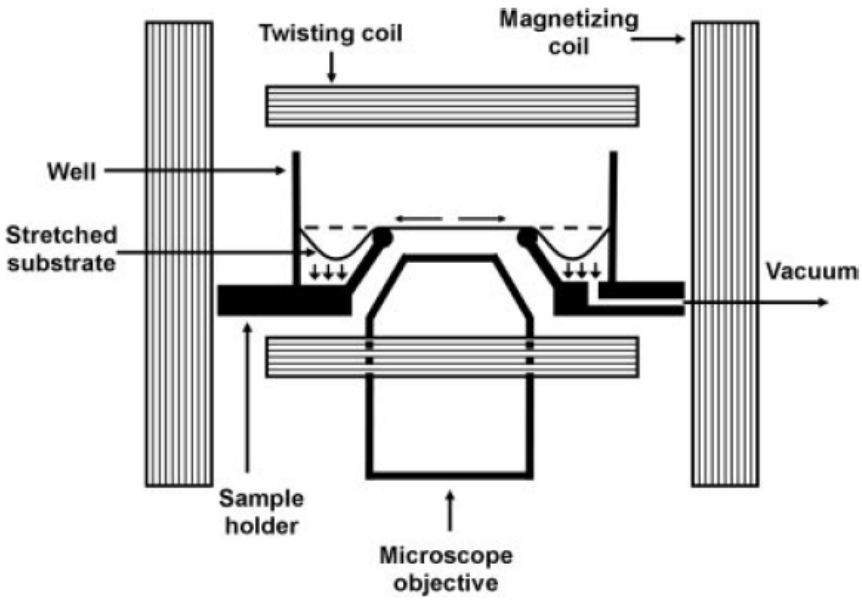

Figure IV.1: Scheme of the cell-stretching device coupled to two pairs of coaxial coils to perform magnetic twisting cytometry. From Trepat X et al., 2004.

Glostrup, Denmark) and a centroid algorithm (Trepat et al., 2003). Strain (ε_x) was computed for each pair of dots as:

$$\varepsilon_x = \frac{X_{STRETCH} - X_{RELAX}}{X_{RELAX}} \quad [1]$$

where X_{RELAX} and $X_{STRETCH}$ are the distances in the X direction between the dots in relaxed and stretched conformations, respectively. An equivalent expression was used to compute strain in the Y direction (ε_y). The mean strain of each substrate was calculated by averaging data from all pairs of dots. The calibration of the stretching device is reported in Figure IV.2. A linear relationship between pressure and strain was found with a maximum deformation of 28% for a vacuum pressure of 45 cm Hg. The error bars indicate the variability among wells (n = 3).

IV.3.3 Optical magnetic twisting cytometry (OMTC)

An optical magnetic twisting cytometer (Fabry et al., 2001) was coupled to the stretching device to measure cell mechanics, in particular, the complex elastic modulus of the cells G* (Trepat et al., 2004). In OMTC, ligand-coated ferrimagnetic beads are specifically bound to

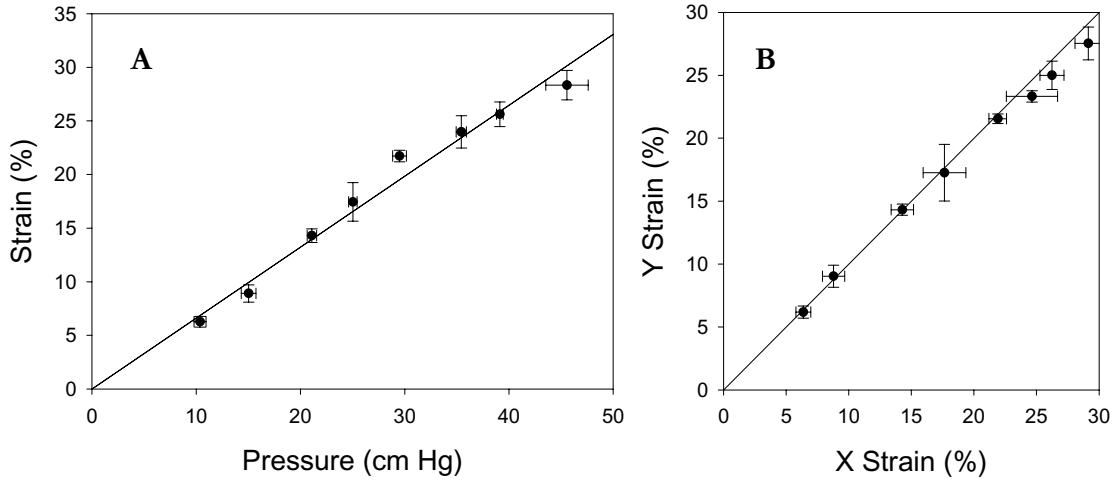

Figure IV. 2: The pressure-strain curve was linear (A) and biaxial (B) up to 25% deformation. Data are plotted as (mean ± SEM).

cell surface receptors. We used two orthogonal pairs of coaxial coils to magnetize and subsequently twist the beads (Figure IV.3). The beads are permanently magnetized with a brief (20 ms) and strong (120 mT) pulse of magnetic field in the horizontal direction of the cell monolayer and subsequently twisted in a weak sinusoidal magnetic field applied in the

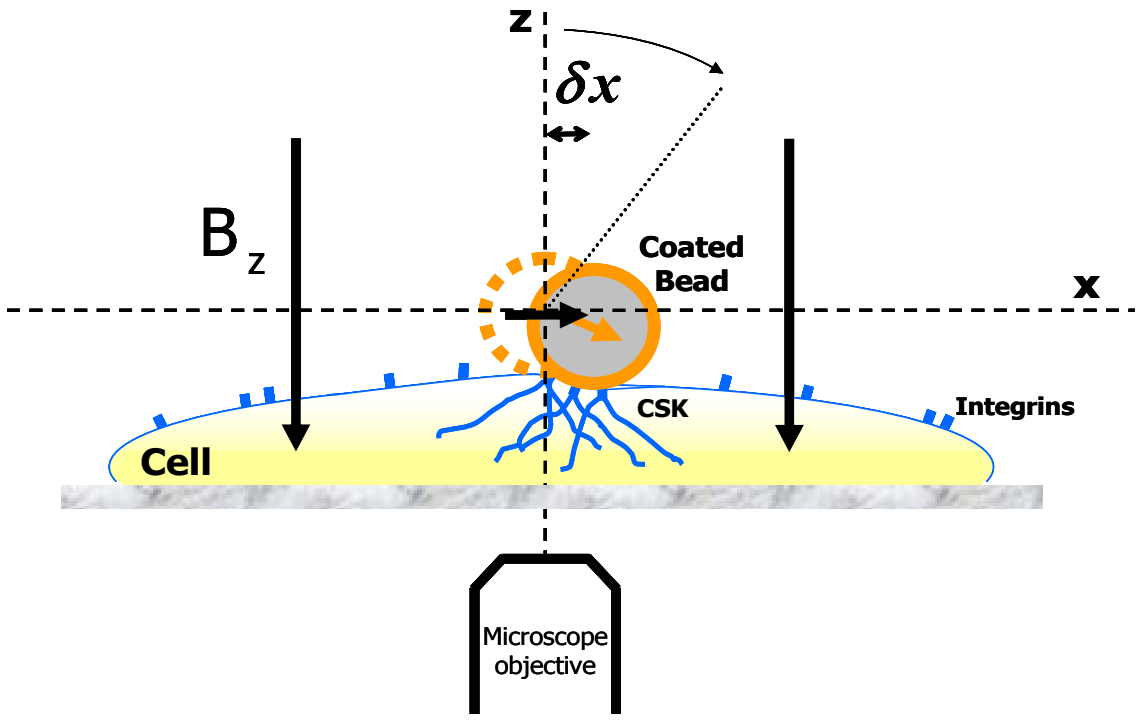

Figure IV. 3: Scheme of OMTC procedure to study cell viscoelasticity. RGD-coated beads (4.5 μm diameter) were attached to specific cell surface receptors (integrins). This coating forms focal adhesions and is able to bind tightly to the cytoskeleton. Ferromagnetic beads were then permanently magnetized in the horizontal direction (x) (150 mT,10ms) and sinusoidally twisted with a magnetic field Bz (3 mT, 0.1 Hz). The resulting bead displacement (δ_z) was measured with videomicroscopy.

vertical direction. The resulting lateral bead displacement is measured with nanometer resolution using videomicroscopy (Trepat et al., 2003). Images are obtained with a progressive scan black-and-white CCD camera (CV-M10 BX, JAI, Glostrup, Denmark) and digitized by an 8-bit resolution frame grabber (PC Eye4, Eltec, Mainz, Germany). In this study, microscope magnification was ×10 resulting in a field of view of 640 × 480 μm. The camera trigger and the current fed to the coils were controlled with an AD/DA PCI board (PCI-MIO-16XE-10, National Instruments, Austin, TX) driven by LabVIEW software (National Instruments, Austin, TX).

IV.3.4 Protocol

Confluent and subconfluent cell monolayers were subjected to the protocol illustrated in Figure IV.4. A first OMTC and cell strain measurement was performed by twisting the beads for 15 seconds in an oscillatory magnetic field of 5 mT amplitude and 1 Hz frequency (baseline). After 1 minute, thrombin (0.5 U/ml) or vehicle (HEPES-buffered RPMI 1640) was added to the well. Another measurement was carried out 5 minutes later as previously described. A stretch of 0% (control) or 20% of the substrate was then produced and the beads were twisted again 1.5 minutes after stretching (Figure IV.5). Stretch was held and the bead oscillation was repeated 5 minutes later. Finally, the substrate

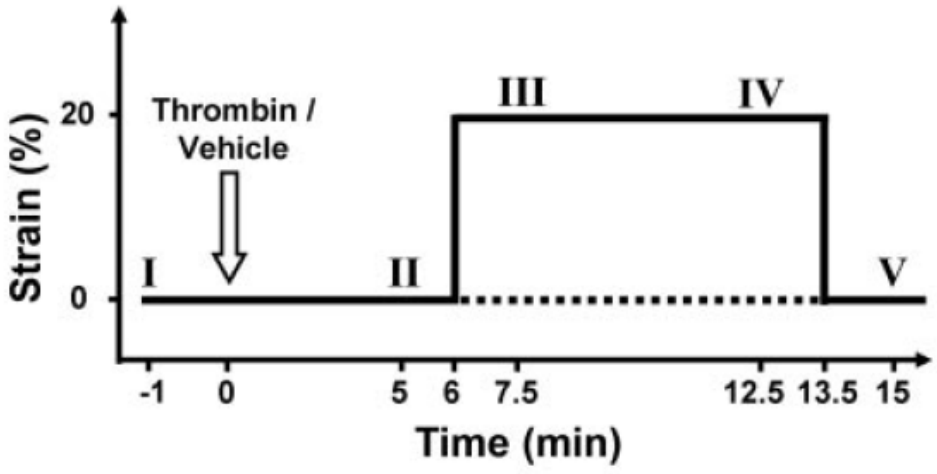

Figure IV.4: Experimental protocol. Cells were treated with thrombin or vehicle and subsequently subjected to a step of 20% equibiaxial strain (solid line) or to no strain (dashed line). The step was held for 7.5 min, and then the substrate was relaxed to its initial unstretched conformation. Measurements of cell viscoelasticity and strain were performed at time points indicated by Roman numerals. From Trepat et al., 2006

was relaxed to its initial unstretched conformation and the beads were twisted again 1.5 minutes after relaxation. The beads were magnetized before each measurement. For each experimental condition, N=7 wells were measured.

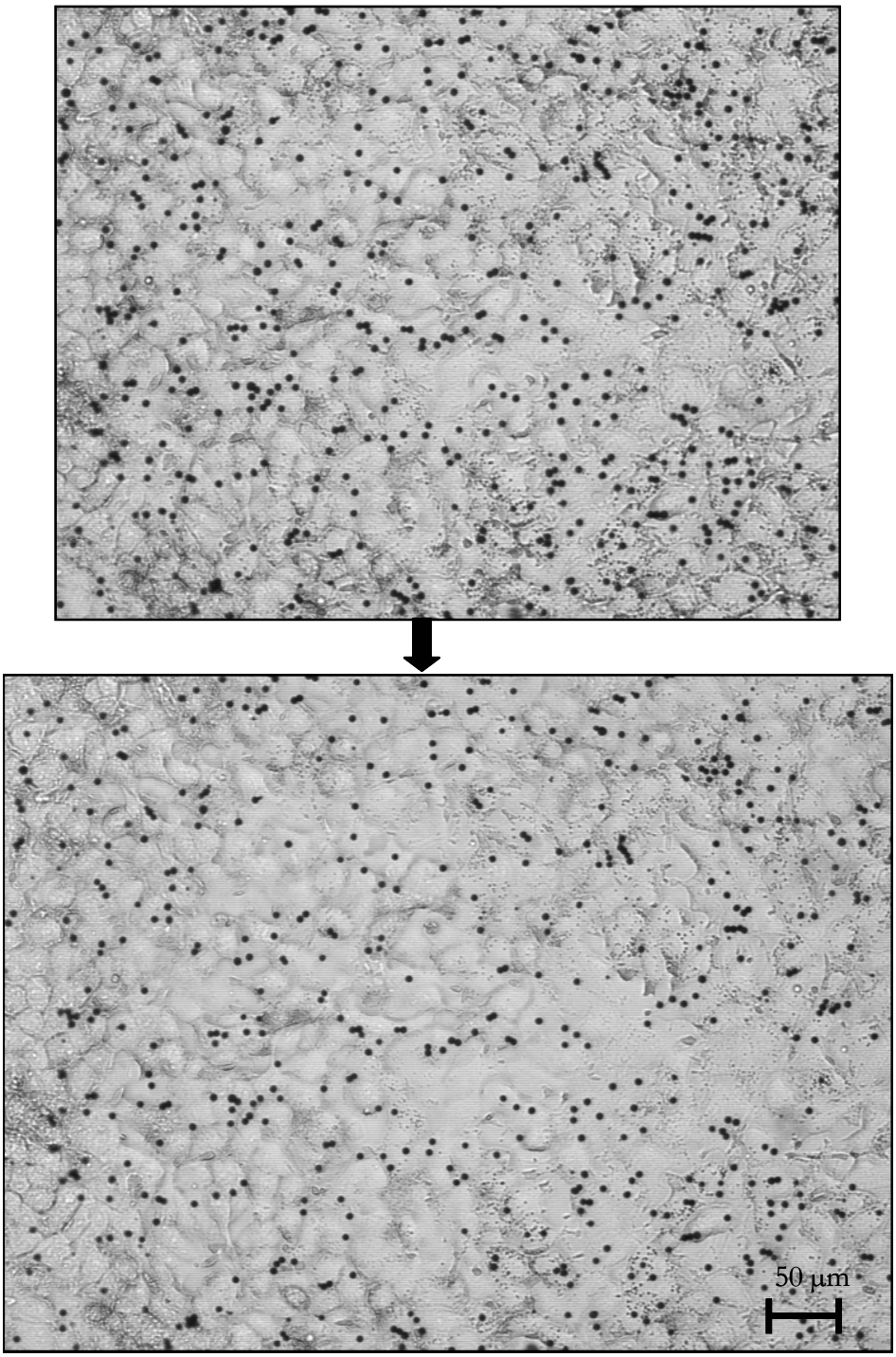

Figure IV.5: Alveolar epithelial cells (A549) under baseline conditions (top) and undergoing a stepwise deformation of 20% (bottom). Images correspond to the actual field of measurements. The black spots are ferrimagnetic beads (4.5 μm diameter).

IV.3.5 Data processing

Image analysis was performed with a multiple particle tracking software detailed elsewhere (Trepat et al., 2003). This software computed the position of each individual bead (~100-150 beads per well) throughout the experiments using a centroid algorithm.

We computed two indexes of strain to assess the extent to which cells followed the imposed substrate deformation (Figure IV.6) (Trepat et al., 2004). These indexes were obtained from the bead position in the first image of each OMTC measurement (no twisting field applied). The first index accounted for the intracellular deformation and was termed cell strain (ε_c). This index was defined as the fractional change of the distance (d) between beads bound to the same cell relative to the distance (d_{II}) before stretch application (time point II in Figure IV.4):

$$\varepsilon_c = 100 \times \frac{d - d_{II}}{d_{II}} \qquad [2]$$

ε_c was computed as the median of at least 15 pairs of beads in each well. The second index accounted for the intercellular deformation of the cell monolayer and was termed layer strain (ε_L). ε_L was calculated as the fractional change of the distance (D) between beads that were at least 200 pixels apart from each other (D>164 μm) relative to the distance before stretch application (D_{II}):

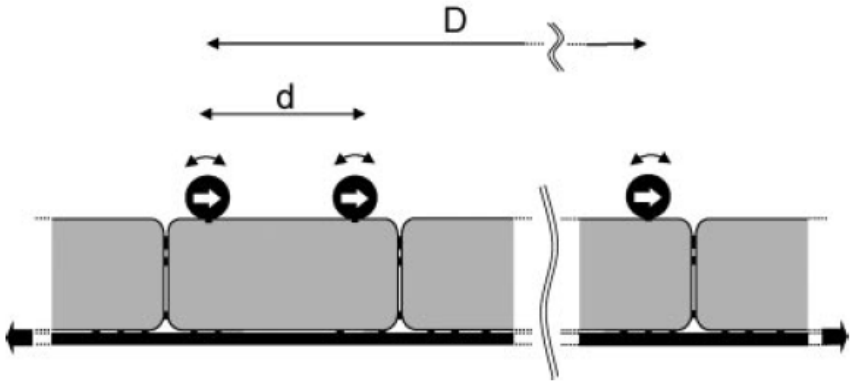

Figure IV.6: To measure cell viscoelasticity and strain, ferrimagnetic beads were specifically bound to the cell surface. The beads were permanently magnetized in the horizontal direction (white arrows indicate remanent magnetic moment) and then twisted in a sinusoidal vertical magnetic field. Cell viscoelasticity was measured from the applied magnetic field and the resulting oscillatory bead displacement. Cell strain (ε_c) was computed from the distance (d) between beads bound to the same cell. Layer strain (ε_L) was computed from the distance between beads that were separated by at least a distance (D) > 164μm. Bead position was determined with nanometer resolution using videomicroscopy. From Trepat et al., 2006

$$\varepsilon_L = 100 \times \frac{D - D_{II}}{D_{II}} \quad [3]$$

In a previous study we showed that ε_L matched the applied substrate strain (Trepat et al., 2004). To assess differences between bulk strain of the cell monolayer and strain of individual cells, we defined the loss of strain transmission ($\Delta\varepsilon$) as:

$$\Delta\varepsilon = \varepsilon_L - \varepsilon_c \quad [4]$$

$\Delta\varepsilon$ indicates the extent to which strain is transmitted from the substrate to overlying cells, and was taken as an index of paracellular monolayer disruption (see discussion). OMTC measurements were processed as follows. The specific torque applied to a bead was computed as:

$$T = \frac{m \cdot B}{V} \quad [5]$$

where V is the bead volume, m is the bead magnetic moment and B is the applied magnetic field. A complex elastic modulus of the cell G^* was computed from the Fourier transforms of the applied torque T^* and of the resulting bead displacement δ^*:

$$G^* = G' + j \cdot G'' = \frac{T^*}{\delta^*} \quad [6]$$

where we define G' as the storage modulus which we hereafter refer as stiffness and G'' as the loss modulus. j is the imaginary unit defined as $j^2 = -1$ (* indicates complex number). G' accounts for the energy stored in the cell during each oscillatory cycle and G'' for the energy dissipated into heat. G^* can also be expressed as:

$$G^* = G'(1 + j \cdot \eta) \quad [7]$$

where $\eta = G''/G'$ is the hysteresivity or loss tangent which reflects the balance between elastic and frictional stresses in the cell. When $\eta < 1$, cell mechanical behavior is predominantly elastic or solid-like. This mechanical property confers the cell with the ability to rapidly recover its shape in response to deformation. By contrast, when $\eta > 1$, the cell behavior is predominantly dissipative or liquid-like, which enables the cell to alter its shape and flow in functions such as crawling, spreading, division or contraction (Fabry et al., 2003). G^* was computed as the median of ~100-150 beads in each well.

IV.3.6 Statistics

Data are reported as means ± SEM. Statistical comparisons were performed by unpaired Student's t-test. Statistical significance was assumed at $P<0.05$.

IV.4 RESULTS

Figure IV.7 shows cell strain and layer strain in response to substrate stretch. When confluent cells were stretched, (Figure IV.7, top), ε_c was slightly smaller than ε_L, resulting in a small but significant $\Delta\varepsilon$ (inset). No significant differences were observed between cells treated with thrombin or with vehicle. When the substrate was returned to its unstretched conformation, ε_c of vehicle-treated cells recovered its baseline values while thrombin treated cells exhibited a tendency to maintain a small positive $\Delta\varepsilon$. The deformation of non-confluent cells in response to substrate stretch differed from that of confluent cells (Figure IV.7, bottom). When stretch was applied, ε_c was considerably smaller than ε_L in both vehicle-treated and thrombin-treated cells resulting in large $\Delta\varepsilon$, which was significantly larger in cells treated with thrombin than in cells treated with vehicle. When the substrate was unstretched, both groups exhibited negative ε_c, resulting in $\Delta\varepsilon > 0$. Holding the stretch for 5 minutes induced only minor changes in $\Delta\varepsilon$ of both confluent and non-confluent cells (not shown).

Baseline values for cell stiffness and hysteresivity were $G' = 1.20 \pm 0.06$ Pa/nm and $\eta = 0.344 \pm 0.007$ for confluent cells and $G' = 1.03 \pm 0.06$ Pa/nm and $\eta = 0.336 \pm 0.006$ for subconfluent cells. Thrombin markedly increased G' (192% ± 25% in confluent cells and 263% ± 22% in non-confluent cells) and decreased η (33% ± 3% in confluent cells and 36% ± 2% in non-confluent cells). Stretch application induced an increase in G' and a drop in η in vehicle-treated cells (Figure IV.8.A). By contrast, both G' and η of thrombin-treated cells remained roughly unchanged when the step of stretch was applied. Only minor changes were observed in G' and η after holding strain for 5 minutes (not shown). When the substrate was relaxed to its initial unstretched conformation, G' of thrombin-treated cells dropped to values close to the original baseline (Figure IV.8.B) whereas G' of thrombin treated cells that had not been stretched remained elevated. However, η of both stretched and unstretched thrombin-treated cells remained >25% lower than the baseline

value.

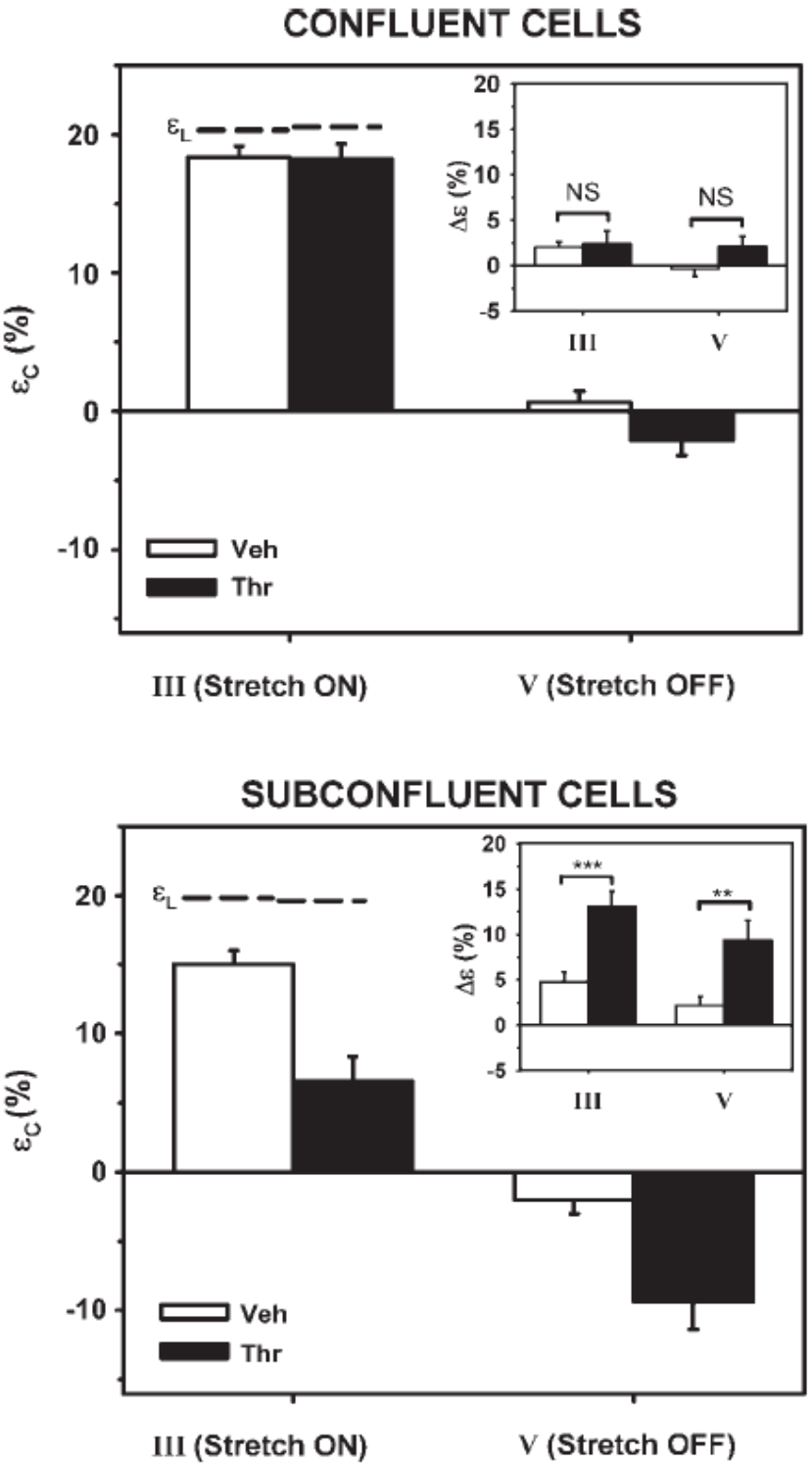

Figure IV.7: ε_c experienced by confluent cells (*top*) and subconfluent cells (*bottom*) in response to substrate stretch of 20% (*left*) and subsequent unstretch (*right*). Measurements were performed in $n = 7$ cell wells/group. Veh, vehicle-treated cells; Thr, thrombin-treated cells. NS, no significant differences; $\Delta\varepsilon$, loss of strain transmission. Dashed lines are the bulk ε_L. Roman numerals indicate time points in the protocol (see Figure IV.4). *Inset*: $\Delta\varepsilon = \varepsilon_L - \varepsilon_c$. $^{**}P < 0.01$, $^{***}P < 0.001$. From Trepat et al., 2006

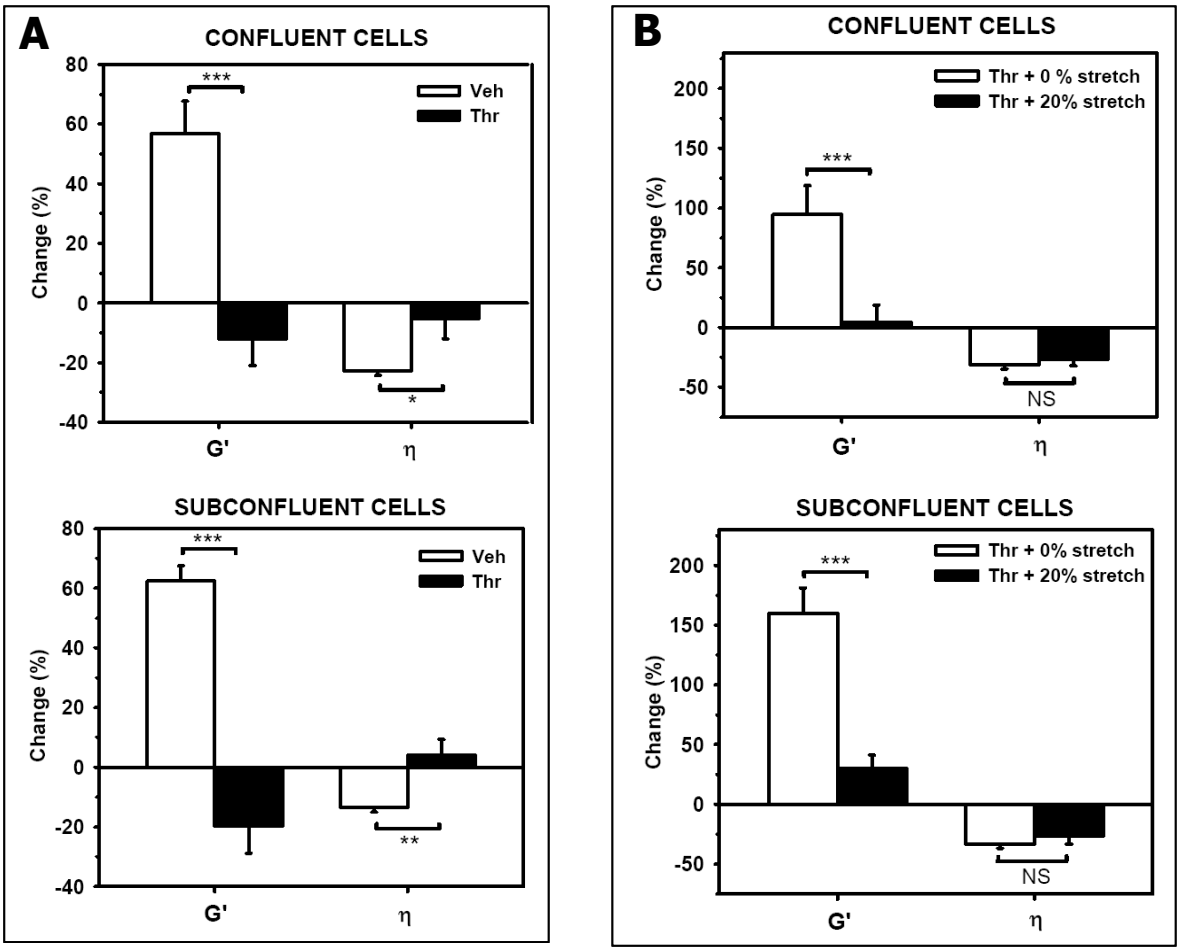

Figure IV.8: A: Relative changes induced by 20% stepwise stretch in *G'* (*left*) and η (*right*) of vehicle-treated cells (open bars) and thrombin-treated cells (filled bars). *Top*: confluent cells. *Bottom*: subconfluent cells. Data are relative changes between time points III and II (see Figure IV.4) of $n = 7$ wells/group. $^{*}P < 0.05$, $^{**}P < 0.01$, and $^{***}P < 0.001$. **B:** Relative changes from baseline in *G'* (*left*) and η (*right*) after relaxing the substrate to its initial unstretched conformation. Open bars are unstretched thrombin-treated cells, and filled bars are thrombin-treated cells that had been subjected to stretch. *Top*: confluent cells. *Bottom*: subconfluent cells. Data are relative changes between time points V and I of $n = 7$ wells/group. $^{***}P < 0.001$. From Trepat et al., 2006

IV.5 DISCUSSION

We measured the effect of stretch on the strain and micromechanics of confluent and subconfluent human alveolar epithelial cells exposed to thrombin. In confluent cells, we found that cell strain was slightly smaller than the imposed substrate strain. This effect was

independent of previous exposure to thrombin. By contrast, strain experienced by subconfluent cells was markedly smaller than substrate strain, and this effect was considerably exacerbated by thrombin. When the substrate was relaxed to its unstretched conformation, subconfluent cells exhibited negative strain. This negative strain was substantially larger in thrombin-treated cells. Stretch induced an increase in cell stiffness and a decrease in cell hysteresivity in vehicle cells but not in thrombintreated cells. Upon stretch removal, stiffness but not hysteresivity of thrombin-treated cells returned to their initial baseline value.

IV.5.1 Cell model

A major limitation of this study is that it does not include several essential features of the extracellular environment of the injured epithelium such as the presence of inflammatory cells and proinflammatory mediators, the deposition of fibrin, the inactivation of surfactant and the secretion of extracellular matrix (Ware and Matthay, 2000). In the absence of this pathophysiological environment, the simple extrapolation of our findings to "in vivo" conditions may be misleading. However, this simple model captures a central feature of the acutely injured epithelium, i.e., mechanical determinants of cell-cell junctions.

The study was carried out in human alveolar epithelial cells from the cell line A549. Although this cell line is extensively used (Vlahakis et al., 1999;Stroetz et al., 2001;Kawkitinarong et al., 2004), its appropriateness as a cultured model of alveolar epithelial cells remains controversial. The most suitable alveolar epithelial cells to study the effects of any deformation would be Type I cells because these cells cover substantially more surface area of the alveolus and have traditionally been thought to be more susceptible to injury than Type II cells, which are localized at the corners of alveolar spaces and might be protected from deforming injury. But establishment of primary Type I epithelial cultures have met with limited success. Isolation and culture of alveolar Type I cells is difficult, in part because their cytoplasmic extensions are thin and the intercellular junctions may be very tight (Crandall and Matthay, 2001) and also because there are technical difficulties inherent in isolating purified functional populations of Type I cells from adult lung. For these reasons it is very common to use Type II epithelial cells like an alveolar epithelium model. Exclusive monolayers of Type II pneumocytes may not completely mimic the pulmonary epithelium where Type I and Type II cells coexist, but

they have been useful for many studies. However, some investigators, due to Type II cells proliferate and differentiate into Type I cells, have used differentiated primary Type II cells as a Type I cell model (Paine, III and Simon, 1996). But although in some aspects it could be an advantage to use alveolar epithelial Type I cell-like monolayers obtained by culturing freshly isolated Type II, it should be taken into consideration that Type II cells cultured on tissue culture plastic or porous substrata cease to express the Type II cell phenotype avoiding the use of primary Type I cultures (Crandall and Matthay, 2001). In fact, when Type II cells are cultured in these manners, the cells flatten; they lose differentiated Type II cell morphologic features, and cease production of surfactant. Continuous cell lines are an alternative to primary Type II cultures.

A549 cell line was established in 1972 and has characteristic features of Type II cells of the pulmonary epithelium. Confluent monolayers consist of cuboidal and polygonal cells which appear closely packed and exhibit a clear and uniform distribution of lamellar bodies (Foster et al., 1998;Stroetz et al., 2001). These cells have been shown to express a variety of cytokine and growth factors, to exhibit intercellular adhesion molecule-1 surface receptor expression, to possess functioning proinflammatory signaling pathways and are able to synthesize lecithin and phosphatidylcholine (Vlahakis et al., 1999). A549 cell line has also been shown to exhibit metabolic and transport properties consistent with Type II pulmonary epithelial cells in vivo and does not functionally differentiate in culture to Type I epithelium-like (Foster et al., 1998). Moreover, unlike primary culture models, they are easy to maintain in culture. For these reasons this cell line has been used in many studies as a human alveolar epithelium model. But this cell line, as all cell culture systems, has some limitations. A549 cells have characteristic differences when are compared to rat and human Type II pulmonary epithelial cells. As an example, A549 cells secrete less phosphatidyl-glycerol, which is an important component of surfactant active material (Vlahakis et al., 1999). But one of the major criticisms of the A549 cell line has been that the monolayers formed by these cells are much leakier than other conventional cell lines if evaluated solely on the basis of TER (Foster et al., 1998). Specifically, the ability of A549 cells to establish functional tight junctions and to form non-permeable monolayers has been called into question (Winton et al., 1998;Stroetz et al., 2001) (See Appendix 2). A recent study, however, has provided evidence that A549 cells have the ability to form adherens junctions and thigh junctions when grown to confluence (Kawkitinarong et al., 2004). In addition, the authors showed that A549 monolayers exhibit significant transepithelial resistance, and

that this resistance can be modulated by thrombin. A549 cells have also been reported to express functional PARs and to respond to thrombin by releasing inflammatory mediators including IL-6, IL-8 and PGE2 (Asokananthan et al., 2002). Therefore, despite the limitations inherent in transformed cell lines, we considered that A549 cells were a suitable model to study the micromechanics and structural integrity of alveolar epithelial cell monolayers subjected to thrombin and stretch.

IV.5.2 The role of thrombin in the alveolar epithelium

Thrombin is well known for its key role in the coagulation cascade, in which it cleaves circulating fibrinogen to fibrin. In this function, thrombin is involved in coagulation abnormalities that lead to alveolar fibrin deposition and lung dysfunction in ALI (Laterre et al., 2003;Idell, 2003). In addition, thrombin also mediates cellular responses through proteolytic activation of the protease-activated receptor, PAR family (Coughlin, 2000;Hollenberg and Compton, 2002;Moffatt et al., 2004). PAR activation by thrombin has been comprehensively studied at the endothelial level (Moy et al., 1996;Van Nieuw Amerongen et al., 1998;Dudek and Garcia, 2001;Birukova et al., 2004). By contrast, the role of thrombin in the alveolar epithelium is only starting to be elucidated. In this connection, increasing evidence supports the notion that activation of PARs also mediates relevant cellular responses in the alveolar epithelium such as release of inflammatory mediators, MLC phosphorylation, increased levels and translocation of tight junction proteins and cytoskeletal remodeling (Asokananthan et al., 2002;Kawkitinarong et al., 2004;Trepat et al., 2005). However, the potential role of thrombin in the pathogenesis and resolution of ALI and ARDS under dynamic mechanical conditions remains elusive.

IV.5.3 Formation of paracellular gaps

We used a recently developed technique that allowed us to subject adherent cells to biaxial stretch of their substrate and to simultaneously measure their strain and viscoelasticity (Trepat et al., 2004). Cell strain was computed from changes in the distance between the ligand-coated ferrimagnetic beads tightly bound to cell surface via focal adhesions. If the cell were a mechanically homogenous body firmly attached to its substrate, the imposed substrate deformation would be wholly transmitted to the apical surface of the cell. In such case, strain of the cell monolayer ε_L and strain of individual cells ε_c would be equal and $\Delta\varepsilon$

=0. However, in the present study, we found significant differences between ε_L and ε_c (Figure IV.7). We reason that this loss of strain transmission might be attributable to two main factors: mechanical inhomogeneities in the cell body and partial detachment of the cell from the substrate. Mechanical inhomogeneities in the cell body could result in regional differences in cell stiffness (A-Hassan et al., 1998). In response to substrate strain, stiffer regions would deform less than the substrate, leading to $\Delta\varepsilon$ <0. Conversely, softer regions would deform more than the substrate and yield $\Delta\varepsilon$ >0. Given that ε_c and ε_L were computed over at least 15 pairs of beads in each well studied, and that the beads were randomly distributed over the cell surface, mechanical inhomogeneities probably do not account for the discrepancies between ε_L and ε_c. Underestimation of ε_c could also arise from basal to apical strain gradients. Such gradients could differ between confluent vs. subconfluent cells and between thrombin-contracted vs. non-contracted cells, thus partially explaining the different values of $\Delta\varepsilon$ between these different experimental conditions. However, if the values of $\Delta\varepsilon$ during stretching arised from basal to apical strain gradients, they would vanish once the substrate is unstretched to its initial conformation. This was not case in our experiments (Figure IV.7, inset). Indeed, upon substrate unstretching, $\Delta\varepsilon$ remained significantly positive with values similar to those obtained during stretching. Therefore, we conclude that the contribution of basal to apical inhomogeneities to the average $\Delta\varepsilon$ during stretching, if any, is small. Instead, discrepancies between ε_L and ε_c are more likely to be due to the breakdown of cell-cell and cell-substrate adhesions during cell distention. As a result of this loss in attachments, cells retracted from their substrate and paracellular gaps formed or increased in size. This interpretation is consistent with the fact that $\Delta\varepsilon$ remained elevated after stretch cessation. Given the aforementioned considerations, the index $\Delta\varepsilon$ was assumed as an index of formation or change in size of paracellular gaps.

IV.5.4 Effect of stretch on the strain of confluent and sub-confluent monolayers exposed to thrombin

The structural integrity of the alveolar epithelium is determined by a force balance between centripetal cytoskeletal tension and centrifugal cell-cell and cell-matrix tethering forces. Given that the epithelium undergoes stretch during breathing and mechanical ventilation, cell stiffness is a central determinant of this dynamic balance: the stiffer the cell, the larger centripetal tension that cell-cell and cell-matrix adhesions need to withstand during lung expansion. Prompted by the findings that thrombin induced a prolonged 3-fold increase in

cell stiffness (Trepat et al., 2005), we studied whether exposure with thrombin followed by a single mechanical stretch with an amplitude characteristic of mechanical ventilation (20%) (Tschumperlin and Margulies, 1999) induced changes in epithelial barrier integrity. We found that strain experienced by thrombin-treated and vehicle-treated confluent cells differed from imposed substrate strain (Figure IV.7). These results suggest that cell-cell and cell-matrix adhesions were not able to completely withstand the increased centripetal tension induced by stretching, leading to gap formation as reflected by $\Delta\varepsilon > 0$. Interestingly, we did not find significant differences in $\Delta\varepsilon$ between thrombin-treated and vehicle-treated confluent cells, indicating that the increase in centripetal tension induced by thrombin did not significantly contribute to gap formation. This apparent paradox could be explained by the fact that, in addition to increase cell stiffness, thrombin also increases the levels of tight-junction proteins (ZO-1 and occludin) and induces peripheral actin remodeling in A549 cells (Kawkitinarong et al., 2004;Trepat et al., 2005). Our findings suggest that this peripheral remodeling of the cortical cytoskeleton and of cell junctions induced an increase in tethering forces. As a result, the confluent cell monolayer was able to balance the increase in centripetal force caused by cell stiffening and contraction, thus preventing paracellular gaps to form or increase in size.

In contrast to confluent cells, non-confluent cells exhibited substantial retraction from the substrate as shown by the large $\Delta\varepsilon$ we found. This reveals a critical mechanical role of cell-cell junctions in counterbalancing increased centripetal forces during stretching. $\Delta\varepsilon$ was dramatically increased in subconfluent cells that had been exposed to thrombin indicating a substantial rise in the size of paracellular gaps. The differential behavior we found between confluent and subconfluent cells can be explained in terms of a simple force balance. In confluent cells, the increase in centripetal force caused by stretch was balanced by the reinforcement of cell-cell junctions induced by thrombin. However, in subconfluent cells where anchorages to adjacent cells are reduced or absent, cell substrate adhesions failed to withstand centripetal tension leading to partial cell retraction from the substrate. Given that ALI and ARDS are characterized by widespread epithelial disruption, impairment of cell-cell junctions is a hallmark of disease progression (Bachofen and Weibel, 1982;Ware and Matthay, 2000). In this context, our results suggest that the combined effect of cell-cell junction impairment and cell stretching can result in further paracellular gap formation and increased epithelial permeability. This effect might be dramatically exacerbated by the presence of thrombin.

When the cell substrate was relaxed to its initial unstretched conformation, subconfluent thrombin-treated cells exhibited significant compressive strain. This negative strain could be a consequence of cell detachment and retraction during stretching that turned into negative strain after stretch removal. To the best of our knowledge the response of alveolar epithelial cells to compressive stress has not been studied. However, compressive stress has been shown to slow wound healing and to trigger profibrotic responses in cultured bronchial epithelial cells (Savla and Waters, 1998;Tschumperlin et al., 2003). Similar responses could occur in the alveolar epithelium as a result of the combined effect of thrombin and stretch and could contribute to the profibrotic environment of acutely injured lungs (Howell et al., 2002;Idell, 2003).

IV.5.5 Effect of micromechanics of confluent and sub-confluent monolayers exposed to thrombin

Simultaneously with global cell deformation, we measured cell stiffness G' and hysteresivity η with OMTC. In line with a previous study (Trepat et al., 2004), vehicle cells experienced significant stiffening and a drop in η in response to stretch (Figure IV.8.A). By contrast, stretch had little effect in G' and η in thrombin-treated cells. This differential behavior could be attributed to stretch-induced changes in cytoskeletal tension (prestress). Cytoskeletal prestress is thought to be carried by actin microfilaments and intermediate filaments and mainly modulated by cell adhesions to adjacent cells and to the extracellular matrix and by the cell contractile apparatus (Stamenovic and Wang, 2000;Ingber, 2003). A number of studies in different cell types have demonstrated that increased prestress is paralleled by increased G' and decreased η (Pourati et al., 1998;Trepat et al., 2004;Stamenovic et al., 2004). Given that we observed similar viscoelastic response to stretch in confluent and non-confluent cells, the differential behavior of vehicle and thrombin-treated cells does not seem to lie in cell-cell and cell-matrix adhesion forces. Indeed, G' and η of confluent and non-confluent cells exhibited parallel behavior in response to stretch. Instead, the absence of stretch-induced stiffening in thrombin-treated cells probably arises from structural changes at the cytoskeleton level. Thrombin has been shown to enhance MLC phosphorylation, which is indicative of an increased number of actinmyosin interactions (Kawkitinarong et al., 2004). Disruption of these interactions by cell distention could explain the differential response to stretch of thrombin-treated and

vehicle-treated cells. Indeed, in thrombin-treated cells, the increase in prestress resulting from cytoskeletal distention could be counterbalanced by a loss of cell contractile stress due to detachment of myosin from actin, ultimately leading to unchanged stiffness and hysteresivity after stretch. By contrast, in vehicle-treated cells were levels of MLC phosphorylation are lower (Kawkitinarong et al., 2004), the fall in prestress due to myosin disruption would be smaller than the increase in prestress caused by cytoskeletal distention, resulting in the stretch-induced cell stiffening observed. Disruption of actin-myosin interactions has been postulated as a cause of stretch-induced softening in airway smooth muscle tissues (Fredberg et al., 1997), but has not yet been observed at the single cell level. Our data suggest that this phenomenon could be not only inherent in smooth muscle cells but also to other cell types. In addition to detachment of actin-myosin interactions, stretch could also provide enough mechanical energy to disrupt or unfold cytoskeletal crosslinks, which might be more abundant in the cortical cytoskeleton of thrombin-treated cells than in untreated cells (Kawkitinarong et al., 2004;Trepat et al., 2005). The structural rearrangements discussed above are consistent with the observed drop of G' upon release of the substrate stretch (Figure IV.8.B). Indeed, G' of thrombin-treated cells recovered the untreated baseline levels after stretch release, suggesting that stretch disrupted the cytoskeletal structures that determined thrombin-induced stiffening.

The potential implications of the disruption and rearrangement of cytoskeletal structures induced by a single stretch in cells exposed to thrombin are at least two-fold. First, it is well-known that the cytoskeleton is the scaffold that interconnects organelles in the cell and provides a large surface area for proteins to bind. Mechanical breakdown of this scaffold has been shown to influence relevant cellular functions, including apoptosis, which is believed to be a major cause of epithelial cell death in lung injury (Janmey, 1998;Martin et al., 2003). Second, the observation that application of stretch reversed thrombin-induced stiffening is a new factor to take into account in the balance of forces at the alveolar-capillary barrier. Our results suggest that the force balance paradigm (Moy et al., 1996;Dudek and Garcia, 2001) cannot be interpreted in terms of static forces because some of its mechanical determinants, i.e., cell stiffness and contraction, are substantially altered by stretch.

Although the stiffness of thrombin-treated cells recovered a value close to baseline after substrate relaxation, cell hysteresivity remained 20–25% lower than its original untreated

baseline (Figure IV.8.B). Cell hysteresivity reflects the degree of solid-like vs. liquid-like behaviour of the cell. In addition, recent findings suggest that η is a robust measure of cytoskeleton dynamics and remodeling (Sollich et al., 1997;Fabry et al., 2003;Bursac et al., 2005). In the light of these studies, our findings that thrombin induces a sustained decrease in η suggest that thrombin could impair essential functions of alveolar epithelial cells such as migration and proliferation, in which cells require high η to change their shape and flow.

IV.5.6 Conclusions

In summary, we showed that thrombin impairs the ability of alveolar epithelial cells to follow imposed substrate deformations when cell-cell junctions are reduced or absent, which could result in increased epithelial permeability. This effect was absent in confluent cell monolayers, which highlights the central role of cell-cell junctions in withstanding increased tension in the presence of thrombin and mechanical stretch. Stretching thrombin-treated cells resulted in profound changes in cell mechanics possibly due to disruption and rearrangement of cytoskeletal structures. Overall, our findings suggest that thrombin has a potential role in the pathogenesis and resolution of ALI and ARDS in patients subjected to mechanical ventilation. Our novel experimental approach can be used to assess the contribution of inflammatory mediators to the structural integrity of the alveolar capillary barrier in mechanically stimulated cell monolayers.

Chapter V

Conclusions of the thesis

Effect of a vibratory stimulus on airway epithelial cells

1. A cell-vibration stimuli system was developed to apply high frequency oscillatory perturbations to cultured cells. This system allows an easy adjustment of the amplitude and frequency of vibration in sinusoidal oscillation and is potentially applicable to study the effects of vibration due to snoring in the different cell types (epithelial, endothelial, neuromuscular, neuronal, macrophages, etc) involved in airway pathophysiology during respiratory sleep disturbances (Aim 1).

2. A vibratory stimulus at 60 Hz and ±0.3 mm applied to cultured bronchial epithelial cells did not affect cell proliferation up to 24h, indicating that this stimulus did not detach the cells from their substrate. (Aim 2).

3. A mechanical vibration with amplitude and frequency that simulate snoring triggered an inflammatory cascade, as reflected by the time-dependent increase in the release of the inflammatory cytokine IL-8 (46% at 12h (P= 0.029) and 56% at 24h (P= 0.013). (Aim 3).

4. The inhibition of the pathways of p38, ERK, and JNK MAPKs significantly reduced the increase in IL-8 release induced by vibration, indicating that the upregulation of IL-8 is mediated by MAPK signaling cascades. (Aim 4).

5. These results in an in vitro model support the hypothesis that the snoring vibration may be an important source of cell injury in the airway of patients suffering respiratory sleep disturbances such as the obstructive sleep apnea/hypopnea syndrome and the

upper airway resistance syndrome.

Effect of stretch on the structural integrity and micromechanics of human alveolar epithelial cell monolayers exposed to thrombin.

6. An index to evaluate loss in cell-substrate adhesion was defined. This index computed from the changes in the distance between beads tightly bound to cell surface via focal adhesions can determine the formation or change in size of paracellular gaps. (Aim 5).

7. Thrombin did not compromise the physical integrity of the confluent alveolar epithelial barrier. In confluent cells, cell strain and layer strain were very similar and this result was independent of the treatment. This result indicates that thrombin did not contribute to gap formation in confluent cells. (Aim 6).

8. Cell strain experienced by subconfluent cells was markedly smaller than layer strain, and this effect was considerably exacerbated by thrombin, indicating a substantial rise in the formation or size of paracellular gaps. (Aim 7).

9. In subconfluent cells, as the presence of cell-cell and cell-matrix adhesions is limited, tethering forces can not balance the centripetal tension due to stretch, compromising the physical integrity of the barrier (Aim 8).

10. Stretch increased stiffness and decreased cell hysteresivity of vehicle-treated cells. By contrast, stretch did not increase stiffness of thrombin-treated cells. This different behavior between vehicle and thrombin-treated cells can not be attributed to cell detachment since this behavior exists in both confluent and non-confluent cells. These results suggest disruption and rearrangement of cytoskeletal structures. (Aim 9).

11. These findings suggest that thrombin could exacerbate epithelial barrier dysfunction in injured lungs subjected to mechanical ventilation.

Reference list

A-Hassan,E., W.F.Heinz, M.D.Antonik, N.P.D'Costa, S.Nageswaran, C.A.Schoenenberger, and J.H.Hoh. 1998. Relative microelastic mapping of living cells by atomic force microscopy. *Biophys. J.* 74:1564-1578.

Alcaraz,J. 2001. Tesi doctoral: Micromechanics of Cultured Human Bronchial Epithelial Cells Measured with Atomic Force Microscopy. *Universitat Barcelona.*

Alzoghaibi,M.A. and A.S.Bahammam. 2005. Lipid peroxides, superoxide dismutase and circulating IL-8 and GCP-2 in patients with severe obstructive sleep apnea: a pilot study. *Sleep Breath.* 9:119-126.

Amin,K., D.Ludviksdottir, C.Janson, O.Nettelbladt, E.Bjornsson, G.M.Roomans, G.Boman, L.Seveus, and P.Venge. 2000. Inflammation and structural changes in the airways of patients with atopic and nonatopic asthma. BHR Group. *Am J Respir. Crit Care Med.* 162:2295-2301.

Ando,H. and R.Noguchi. 2003. Dependence of palmar sweating response and central nervous system activity on the frequency of whole-body vibration. *Scand. J. Work Environ. Health* 29:216-219.

Arima,M., J.Plitt, C.Stellato, C.Bickel, S.Motojima, S.Makino, T.Fukuda, and R.P.Schleimer. 1999. Expression of interleukin-16 by human epithelial cells. Inhibition by dexamethasone. *Am. J. Respir. Cell Mol. Biol.* 21:684-692.

Asokananthan,N., P.T.Graham, J.Fink, D.A.Knight, A.J.Bakker, A.S.McWilliam, P.J.Thompson, and G.A.Stewart. 2002. Activation of protease-activated receptor (PAR)-1, PAR-2 and PAR-4 stimulates IL-6, IL-8 and prostaglandin E2 release from human respiratory epithelial cells. *J. Immunol.* 168:3577-3585.

Atsuta,J., S.A.Sterbinsky, J.Plitt, L.M.Schwiebert, B.S.Bochner, and R.P.Schleimer. 1997. Phenotyping and cytokine regulation of the BEAS-2B human bronchial epithelial cell: demonstration of inducible expression of the adhesion molecules VCAM-1 and ICAM-1. *Am. J. Respir. Cell Mol. Biol.* 17:571-582.

Ayappa,I. and D.M.Rapoport. 2003. The upper airway in sleep: physiology of the pharynx. *Sleep Medicine Reviews* 7:9-33.

Bachofen,H., S.Schurch, M.Urbinelli, and E.R.Weibel. 1987. Relations among alveolar surface tension, surface area, volume, and recoil pressure. *J. Appl. Physiol* 62:1878-1887.

Bachofen,M. and E.R.Weibel. 1982. Structural alterations of lung parenchyma in the adult respiratory distress syndrome. *Clin. Chest Med.* 3:35-56.

Back,G.W., S.Nadig, S.Uppal, and A.P.Coatesworth. 2004. Why do we have a uvula?: literature review and a new theory. *Clin. Otolaryngol.* 29:689-693.

Bausch,A.R., U.Hellerer, M.Essler, M.Aepfelbacher, and E.Sackmann. 2001. Rapid stiffening of integrin receptor-actin linkages in endothelial cells stimulated with thrombin: a magnetic bead microrheology study. *Biophys. J* 80:2649-2657.

Birukova,A.A., K.G.Birukov, K.Smurova, D.Adyshev, K.Kaibuchi, I.Alieva, J.G.Garcia, and A.D.Verin. 2004. Novel role of microtubules in thrombin-induced endothelial barrier dysfunction. *The FASEB Journal* 18:1879-1890.

Bitterman,P.B. 1992. Pathogenesis of fibrosis in acute lung injury. *Am. J. Med.* 92:39S-43S.

Bove,M., A.Nardone, and M.Schieppati. 2003. Effects of leg muscle tendon vibration on group Ia and group II reflex responses to stance perturbation in humans. *J. Physiol* 550:617-630.

Boyd,J.H., B.J.Petrof, Q.Hamid, R.Fraser, and R.J.Kimoff. 2004. Upper airwaymuscle inflammation and denervation changes in Obstructive Sleep Apnea. *Am. J. Respir. Crit. Care Med.* 170:541-546.

Breeze,R.G. and E.B.Wheeldon. 1977. The cells of the pulmonary airways. *Am Rev. Respir. Dis.* 116:705-777.

Bursac,P., G.enormand, B.Fabry, M.Oliver, D.A.Weitz, V.Viasnoff, J.P.Butler, and

J.J.Fredberg. 2005. Cytoskeletal remodelling and slow dynamics in the living cell. *Nat. Mat.* 4:557-561.

Buscemi,L. 2004. Tesi doctoral: Estudi mitjançant microcòpia de força atòmica de la mecànica de cèl·lules epitelials alveolars en resposta a trombina. *Universitat Barcelona.*

Carpagnano,G.E., S.A.Kharitonov, O.Resta, M.P.Foschino-Barbaro, E.Gramiccioni, and P.J.Barnes. 2002. Increased 8-isoprostane and interleukin-6 in breath condensate of obstructive sleep apnea patients. *Chest* 122:1162-1167.

Carpagnano,G.E., S.A.Kharitonov, O.Resta, M.P.Foschino-Barbaro, E.Gramiccioni, and P.J.Barnes. 2003. 8-Isoprostane, a marker of oxidative stress, is increased in exhaled breath condensate of patients with obstructive sleep apnea after night and is reduced by continuous positive airway pressure therapy. *Chest* 124:1386-1392.

Chan,C.S., A.J.Woolcock, and C.E.Sullivan. 1988. Nocturnal asthma: role of snoring and obstructive sleep apnea. *Am. Rev. Respir. Dis.* 137:1502-1504.

Chan,J., J.C.Edman, and P.J.Koltai. 2004. Obstructive Sleep Apnea in Children. *Am. Fam. Physician.* 69:1147-1154.

Chess,P.R., L.Toia, and J.N.Finkelstein. 2000. Mechanical strain-induced proliferation and signaling in pulmonary epithelial H441 cells. *Am. J. Physiol Lung Cell Mol. Physiol* 279:L43-L51.

Chicurel,M.E., C.S.Chen, and D.E.Ingber. 1998. Cellular control lies in the balance of forces. *Curr. Opin. Cell Biol.* 10:232-239.

Chilvers,M.A. and C.O'Callaghan. 2000. Local mucociliary defence mechanisms. *Paediatr. Respir. Rev.* 1:27-34.

Chow,C.W., M.T.Herrera Abreu, T.Suzuki, and G.P.Downey. 2003. Oxidative stress and acute lung injury. *Am J Respir. Cell Mol. Biol.* 29:427-431.

Chu,E.K., J.S.Foley, J.Cheng, A.S.Patel, J.M.Drazen, and D.J.Tschumperlin. 2005. Bronchial epithelial compression regulates epidermal growth factor receptor family ligand expression in an autocrine manner. *Am. J. Respir. Cell Mol. Biol.* 32:373-380.

Cirino,G., C.Napoli, M.Bucci, and C.Cicala. 2000. Inflammation-coagulation network: are

serine protease receptors the knot? *Trends Pharmacol. Sci.* 21:170-172.

Clark,P.A., A.Rodriguez, D.R.Sumner, M.A.Hussain, and J.J.Mao. 2005. Modulation of bone ingrowth of rabbit femur titanium implants by in vivo axial micromechanical loading. *J. Appl. Physiol* 98:1922-1929.

Coughlin,S.R. 2000. Thrombin signalling and protease-activated receptors. *Nature* 407:258-264.

Crandall,E.D. and M.A.Matthay. 2001. Alveolar epithelial transport. Basic science to clinical medicine. *Am J Respir. Crit Care Med.* 163:1021-1029.

Crapo,J.D., B.E.Barry, P.Gehr, M.Bachofen, and E.R.Weibel. 1982. Cell number and cell characteristics of the normal human lung. *Am Rev. Respir. Dis.* 126:332-337.

Crouch,E.C., G.R.Martin, J.S.Brody, and G.W.Laurie. 1997. Basement membranes. *In: The Lung: Scientific Foundations, editedby Crystal RG, West JB, Weibel ER, and Barnes PJ. Philadelphia,PA: Lippincott-Raven*769-791.

Cunningham,K.S. and A.I.Gotlieb. 2005. The role of shear stress in the pathogenesis of atherosclerosis. *Lab. Invest.* 85:9-23.

Currant-Everett,D. 2000. Multiple comparisons: philosophies and illustrations. *Am. J. Physiol. Regulatory Integr. Comp. Physiol.* 279:R1-R8.

Currant-Everett,D. and D.J.Benos. 2004. Guidelines for reporting statistics in journals published by the American Physiological Society. *J. Appl. Physiol.* 97:457-459.

Curry,B.D., J.L.Bain, J.G.Yan, L.L.Zhang, M.Yamaguchi, H.S.Matloub, and D.A.Riley. 2002. Vibration injury damages arterial endothelial cells. *Muscle Nerve* 25:527-534.

Curry,B.D., S.R.Govindaraju, J.L.Bain, L.L.Zhang, J.G.Yan, H.S.Matloub, and D.A.Riley. 2005. Evidence for frequency-dependent arterial damage in vibrated rat tails. *Anat. Rec. A Discov. Mol. Cell Evol. Biol.* 284:511-521.

Devouassoux,G., E.Rossini, M.Fior-Gozlan, M.Henry, P.Levy, and J.L.Pepin. 2004. Sleep apnea syndrome (SAS) is associated with bronchial neutrophilrecruitment. *Am. J. Respir. Crit. Care Med.* 169:A686.

Dos Santos,C.C. and A.S.Slutsky. 2000. Invited review: mechanisms of ventilator-induced lung injury: a perspective. *J. Appl. Physiol.* 89:1645-1655.

Dreyfuss,D. and G.Saumon. 1998. Ventilator-induced lung injury: lessons from experimental studies. *Am. J. Respir. Crit. Care Med.* 157:294-323.

Duan,W., J.H.Chan, K.McKay, J.R.Crosby, H.H.Choo, B.P.Leung, J.G.Karras, and W.S.Wong. 2005. Inhaled p38alpha mitogen-activated protein kinase antisense oligonucleotide attenuates asthma in mice. *Am. J. Respir. Crit. Care Med.* 171:571-578.

Dudek,S.M. and J.G.Garcia. 2001. Cytoskeletal regulation of pulmonary vascular permeability. *J. Appl. Physiol.* 91:1487-1500.

Duran,J., S.Esnaola, R.Rubio, and A.Iztueta. 2001. Obstructive sleep apnea-hypopnea and related clinical features in a population-based sample of subjects aged 30 to 70 yr. *Am. J. Respir. Crit. Care Med.* 163:685-689.

Evans,M.J., L.J.Cabral, R.J.Stephens, and G.Freeman. 1973. Renewal of alveolar epithelium in the rat following exposure to NO2. *Am. J. Pathol.* 70:175-198.

Evans,M.J., L.V.Johnson, R.J.Stephens, and G.Freeman. 1976. Renewal of the terminal bronchiolar epithelium in the rat following exposure to NO2 or O3. *Lab. Invest.* 35:246-257.

Fabry,B. and J.J.Fredberg. 2003. Remodeling of the airway smooth muscle cell: are we built of glass? *Respir. Physiol Neurobiol.* 137:109-124.

Fabry,B., G.N.Maksym, J.P.Butler, M.Glogauer, D.Navajas, N.A.Taback, E.J.Millet, and J.J.Fredberg. 2003. Time scale and other invariants of integrative mechanical behavior in living cells. *Phys. Rev. E Stat. Nonlin. Soft. Matter Phys.* 68:041914.

Fabry,B., G.N.Maksym, S.A.Shore, P.E.Moore, R.A.Panettieri, Jr., J.P.Butler, and J.J.Fredberg. 2001. Selected contribution: time course and heterogeneity of contractile responses in cultured human airway smooth muscle cells. *J. Appl. Physiol* 91:986-994.

Fehrenbach,H. 2001. Alveolar epithelial type II cell: defender of the alveolus revisited. *Respir. Res.* 2:33-46.

Ferreira,A.M., V.Clemente, D.Gozal, A.Gomes, C.Pissarra, H.César, I.Coelho, C.F.Silva, and M.H.P.Azevedo. 2000. Snoring in Portuguese Primary School Children. *Pediatrics*

106:1-6.

Fitzpatrick,M.F., K.Martin, E.Fossey, C.M.Shapiro, R.A.Elton, and N.J.Douglas. 1993. Snoring, asthma and sleep disturbance in Britain: a community-based survey. *Eur. Respir. J.* 6:531-535.

Fokkens,W.J. and R.A.Scheeren. 2000. Upper airway defence mechanisms. *Paediatr. Respir. Rev.* I:336-341.

Foster,K.A., C.G.Oster, M.M.Mayer, M.L.Avery, and K.L.Audus. 1998. Characterization of the A549 cell line as a type II pulmonary epithelial cell model for drug metabolism. *Exp. Cell Res.* 243:359-366.

Fredberg,J.J., D.Inouye, B.Miller, M.Nathan, S.Jafari, S.H.Raboudi, J.P.Butler, and S.A.Shore. 1997. Airway smooth muscle, tidal stretches, and dynamically determined contractile states. *Am. J. Respir. Crit Care Med.* 156:1752-1759.

Friberg,D. 1999. Heavy snorer's disease: a progressive local neuropathy. *Acta Otolaryngol.* 119:925-933.

Friberg,D., B.Gazelius, T.Hokfelt, and B.Nordlander. 1997. Abnormal afferent nerve endings in the soft palatal mucosa of sleep apnoics and habitual snorers. *Regul. Pept.* 71:29-36.

Gavara,N., R.Sunyer, P.Roca-Cusachs, R.Farre, M.Rotger, and D.Navajas. 2006. Thrombin-induced contraction in alveolar epithelial cells probed by traction microscopy. *J. Appl. Physiol* 101:512-520.

Goeckeler,Z.M. and R.B.Wysolmerski. 1995. Myosin light chain kinase-regulated endothelial cell contraction: the relationship between isometric tension, actin polymerization, and myosin phosphorylation. *J. Cell Biol.* 130:613-627.

Greene,K.E., J.R.Wright, K.P.Steinberg, J.T.Ruzinski, E.Caldwell, W.B.Wong, W.Hull, J.A.Whitsett, T.Akino, Y.Kuroki, H.Nagae, L.D.Hudson, and T.R.Martin. 1999. Serial changes in surfactant-associated proteins in lung and serum before and after onset of ARDS. *Am. J. Respir. Crit Care Med.* 160:1843-1850.

Hill,P.D., B.W.Lee, J.E.Osborne, and E.Z.Osman. 1999. Palatal snoring identified by

acoustic crest factor analysis. *Physiol. Meas.* 20:167-174.

Hoffmann,E., O.Dittrich-Breiholz, H.Holtmann, and M.Kratcht. 2002. Multiple control of interleukin-8 gene expression. *J. Leukoc. Biol.* 72:847-855.

Hollenberg,M.D. and S.J.Compton. 2002. International Union of Pharmacology. XXVIII. Proteinase-activated receptors. *Pharmacol. Rev.* 54:203-217.

Hori,Y., H.Shizuku, A.Kondo, H.Nakagawa, B.Kalubi, and N.Takeda. 2006. Endoscopic evaluation of dynamic narrowing of the pharynx by the Bernouilli effect producing maneuver in patients with obstructive sleep apnea syndrome. *Auris Nasus Larynx* 33:429-432.

Howell,D.C., G.J.Laurent, and R.C.Chambers. 2002. Role of thrombin and its major cellular receptor, protease-activated receptor-1, in pulmonary fibrosis. *Biochem. Soc. Trans.* 30:211-216.

Idell,S. 2003. Coagulation, fibrinolysis, and fibrin deposition in acute lung injury. *Crit. Care Med.* 31:S213-S220.

Ingber,D.E. 2003. Tensegrity. I. Cell structure and hierarchical systems biology. *J. Cell Sci.* 116:1157-1173.

Ishizaka,A., T.Matsuda, K.H.Albertine, H.Koh, S.Tasaka, N.Hasegawa, N.Kohno, T.Kotani, H.Morisaki, J.Takeda, M.Nakamura, X.Fang, T.R.Martin, M.A.Matthay, and S.Hashimoto. 2004. Elevation of KL-6, a lung epithelial cell marker, in plasma and epithelial lining fluid in acute respiratory distress syndrome. *Am J Physiol Lung Cell Mol. Physiol* 286:L1088-L1094.

Janmey,P.A. 1998. The cytoskeleton and cell signaling: component localization and mechanical coupling. *Physiol. Rev.* 78:763-781.

Kawkitinarong,K., L.Linz-McGillem, K.G.Birukov, and J.G.Garcia. 2004. Differential Regulation of Human Lung Epithelialand Endothelial Barrier Function by Thrombin. *Am. J. Respir. Cell Mol. Biol.* 31:517-527.

Ke,Y., R.R.Reddel, B.I.Gerwin, M.Miyashita, M.McMenamin, J.F.Lechner, and C.C.Harris. 1988. Human bronchial epithelial cells with integrated SV40 virus T antigen genes retain

the ability to undergo squamous differentiation. *Differentiation* 38:60-66.

Kennedy,G., F.Khan, M.McLaren, and J.J.Belch. 1999. Endothelial activation and response in patients with hand arm vibration syndrome. *Eur. J. Clin. Invest.* 29:577-581.

Kimoff,R.J., E.Sforza, V.Champagne, L.Ofiara, and D.Gendron. 2001. Upper airway sensation in snoring and obstructive sleep apnea. *Am. J. Respir. Crit. Care Med.* 164:250-255.

Kracht,M. and J.Saklatvala. 2002. Transcriptional and post-transcriptional control of gene expression in inflammation. *Cytokine* 20:91-106.

Larsson,H., B.Carlsson-Nordlander, L.E.Lindblad, O.Norbeck, and E.Svanborg. 1992. Temperature thresholds in the oropharynx of patientswith obstructive sleep apnea syndrome. *Am. Rev. Respir. Dis.* 146:1246-1249.

Larsson,L.G., A.Lindberg, K.A.Franklin, and B.Lundback. 2001. Symptoms related to obstructive sleep apnoea are common in subjects with asthma, chronic bronchitis and rhinitis in a general population. *Respir. Med.* 95:423-429.

Laterre,P.F., X.Wittebole, and J.F.Dhainaut. 2003. Anticoagulant therapy in acute lung injury. *Crit Care Med.* 31:S329-S336.

Levi,M., M.J.Schultz, A.W.Rijneveld, and P.T.van der. 2003. Bronchoalveolar coagulation and fibrinolysis in endotoxemia and pneumonia. *Crit. Care Med.* 31:S238-S242.

Levine,S.J., P.Larivee, C.Logun, C.W.Angus, and J.H.Shelhamer. 1993. Corticosteroids differentially regulate secretion of IL-6, IL-8, and G-CSF by a human bronchial epithelial cell line. *Am J Physiol* 265:L360-L368.

Liistro,G., D.Stanescu, and C.Veriter. 1991. Pattern of simulated snoring is different through mouth and nose. *J. Appl. Physiol.* 70:2736-2741.

Liu,J., I.Sekiya, K.Asai, T.Tada, T.Kato, and N.Matsui. 2001. Biosynthetic response of cultured articular chondrocytes to mechanical vibration. *Res. Exp. Med. (Berl).* 200:183-193.

Liu,M., A.K.Tanswell, and M.Post. 1999. Mechanical force-induced signal transduction in lung cells. Am J Physiol 1999;277:L667-83. *Am. J. Physiol. Lung Cell. Mol. Physiol.* 277:L667-L683.

Lu,L.R., J.K.Peat, and C.E.Sullivan. 2003. Snoring in preschool children: prevalence and association with nocturnal cough and asthma. *Chest* 124:587-593.

Lugaresi,E., S.Mondini, M.Zucconi, P.Montagna, and F.Cirignotta. 1983. Staging of heavy snorers' disease. A proposal. *Bull. Eur. Physiopathol. Respir.* 19:590-594.

Lum,H. and A.B.Malik. 1996. Mechanisms of increased endothelial permeability. *Can. J. Physiol. Pharmacol.* 74:787-800.

Lundborg,G., L.B.Dahlin, H.A.Hansson, M.Kanje, and L.E.Necking. 1990. Vibration exposure and peripheral nerve fiber damage. *J. Hand Surg. [Am.]* 15:346-351.

Luster,A.D. 1998. Chemokines--chemotactic cytokines that mediate inflammation. *N. Engl. J Med.* 338:436-445.

Mackli,C.C. 1954. The pulmonary alveolar mucoid film and the pneumonocytes. *Lancet* 266:1099-1104.

Martin,T.R. 2002. Neutrophils and lung injury: getting it right. *J Clin. Invest* 110:1603-1605.

Martin,T.R., M.Nakamura, and G.Matute-Bello. 2003. The role of apoptosis in acute lung injury. *Crit. Care Med.* 31:S184-S188.

Mason,R.J. and M.C.Williams. 1977. Type II alveolar cell. Defender of the alveolus. *Am. Rev. Respir. Dis.* 115:81-91.

Matthay,M.A., G.A.Zimmerman, C.Esmon, J.Bhattacharya, B.Coller, C.M.Doerschuk, J.Floros, M.A.Gimbrone, Jr., E.Hoffman, R.D.Hubmayr, M.Leppert, S.Matalon, R.Munford, P.Parsons, A.S.Slutsky, K.J.Tracey, P.Ward, D.B.Gail, and A.L.Harabin. 2003. Future research directions in acute lung injury: summary of a National Heart, Lung, and Blood Institute working group. *Am J Respir. Crit Care Med.* 167:1027-1035.

Mitic,L.L. and J.M.Anderson. 1998. Molecular architecture of tight junctions. *Annu. Rev. Physiol* 60:121-142.

Moffatt,J.D., C.P.Page, and G.J.Laurent. 2004. Shooting for PARs in lung diseases. *Curr. Opin. Pharm.* 4:221-229.

Moorhead,P.S. 1965. Human tumor cell line with a quasi-diploid karyotype (RPMI 2650).

Exp. Cell Res. 39:190-196.

Moy,A.B., J.Van Engelenhoven, J.Bodmer, J.Kamath, C.Keese, I.Giaever, S.Shasby, and D.M.Shasby. 1996. Histamine and thrombin modulate endothelial focal adhesion through centripetal and centrifugal forces. *J. Clin. Invest* 97:1020-1027.

Murphy,J.T., S.L.Duffy, D.L.Hybki, and K.Kamm. 2001. Thrombin-mediated permeability of human microvascular pulmonary endothelial cells is calcium dependent. *J. Trauma* 50:213-222.

Musch,M.W., M.M.Walsh-Reitz, and E.B.Chang. 2006. Roles of ZO-1, occludin, and actin in oxidant-induced barrier disruption. *Am. J. Physiol. Gastrointest. Liver Physiol.* 290:G222-G231.

Necking,L.E., G.Lundborg, R.Lundstrom, L.E.Thornell, and J.Friden. 2004. Hand muscle pathology after long-term vibration exposure. *J. Hand Surg. [Br.]* 29:431-437.

Nguyen,A.T., V.Jobin, R.Payne, J.Beauregard, N.Naor, and R.J.Kimoff. 2005. Laryngeal and velopharyngeal sensory impairment in obstructive sleep apnea. *Sleep* 28:585-593.

Ni,C.W., H.J.Hsieh, Y.J.Chao, and D.L.Wang. 2004. Interleukin-6-induced JAK2/STAT3 signaling pathway in endothelial cells is suppressed by hemodynamic flow. *Am. J. Physiol. Cell Physiol.* 287:C771-C780.

O'Brien,L.M., C.R.Holbrook, C.B.Mervis, C.J.Klaus, J.L.Bruner, T.J.Raffield, J.Rutherford, R.C.Mehl, M.Wang, A.Tuell, B.C.Hume, and D.Gozal. 2003. Sleep and Neurobehavioral Characteristics of 5- to 7-Year-Old Children With Parentally Reported Symptoms of Attention-Deficit/Hyperactivity Disorder. *Pediatrics* 111:554-563.

Ohga,E., T.Tomita, H.Wada, H.Yamamoto, T.Nagase, and Y.Ouchi. 2003. Effects of obstructive sleep apnea on circulating ICAM-1, IL-8, and MCP-1. *J Appl. Physiol* 94:179-184.

Oksenberg,A. and D.S.Silverberg. 1998. The effect of body posture on sleep-related breathing disorders: facts and therapeutic implications. *Sleep Med. Rev.* 2:139-162.

Osborne,J.E., E.Z.Osman, P.D.Hill, B.V.Lee, and C.Sparkes. 1999. A new acoustic method of differentiating palatal from non-palatal snoring. *Clin. Otolaryngol. Allied Sci.* 24:130-133.

Oudin,S. and J.Pugin. 2002. Role of MAP Kinase Activation in interleukin-8 production by

human beas-2b bronchial epithelial cells submitted to cyclic stretch. *Am. J. Respir. Cell Mol. Biol.* 27:107-114.

Paine,R., III and R.H.Simon. 1996. Expanding the frontiers of lung biology through the creative use of alveolar epithelial cells in culture. *Am. J. Physiol* 270:L484-L486.

Patel,A.S., D.Reigada, C.H.Mitchell, S.R.Bates, S.S.Margulies, and M.Koval. 2005. Paracrine stimulation of surfactant secretion by extracellular ATP in response to mechanical deformation. *Am. J. Physiol Lung Cell Mol. Physiol* 289:L489-L496.

Paulsen,F.P., P.Steven, M.Tsokos, K.Jungmann, A.Mu¨ller, T.Verse, and W.Pirsig. 2002. Upper Airway Epithelial Structural Changes in Obstructive Sleep-disordered Breathing. *Am. J. Respir. Crit. Care Med.* 166:501-509.

Peker,Y., H.Kraiczi, J.Hedner, S.Loth, A.Johansson, and M.Bende. 1999. An independent association between obstructive sleep apnoea and coronary artery disease. *Eur. Respir. J* 14:179-184.

Pendlebury,S.T., J.L.Pepin, D.Veale, and P.Levy. 1997. Natural evolution of moderate sleep apnoea syndrome: significant progression over a mean of 17 months. *Thorax* 52:872-878.

Pinhu,L., T.Whitehead, T.Evans, and M.Griffiths. 2003. Ventilator-associated lung injury. *Lancet* 361:332-340.

Pourati,J., A.Maniotis, D.Spiegel, J.L.Schaffer, J.P.Butler, J.J.Fredberg, D.E.Ingber, D.Stamenovic, and N.Wang. 1998. Is cytoskeletal tension a major determinant of cell deformability in adherent endothelial cells? *Am. J. Physiol. Cell Physiol.* 274:C1283-C1289.

Pugin,J. 2003. Molecular mechanisms of lung cell activation induced by cyclic stretch. *Crit. Care Med.* 31 [Suppl]:S200-S206.

Puig,F., F.Rico, I.Almendros, J.M.Montserrat, D.Navajas, and R.Farre. 2005. Vibration enhances interleukin-8 release in a cell model of snoring-induced airway inflammation. *Sleep* 28:1312-1316.

Reddel,R.R., Y.Ke, B.I.Gerwin, M.G.McMenamin, J.F.Lechner, R.T.Su, D.E.Brash, J.B.Park, J.S.Rhim, and C.C.Harris. 1988. Transformation of human bronchial epithelial cells by infection with SV40 or adenovirus-12 SV40 hybrid virus, or transfection via

strontium phosphate coprecipitation with a plasmid containing SV40 early region genes. *Cancer Res.* 48:1904-1909.

Rembold,C.M. and P.M.Suratt. 2005. An upper airway resonator model of high-frequency inspiratory sounds in children with sleep-disordered breathing. *J. Appl. Physiol.* 98:1855-1861.

Ricard,J.D., D.Dreyfuss, and G.Saumon. 2003. Ventilator-induced lung injury. *Eur. Respir. J. Suppl.* 42:2s-9s.

Rubinstein,I. 1995. Nasal inflammation in patients with obstructive sleep apnea. *Laryngoscope* 105:175-177.

Sacco,O., M.Silvestri, F.Sabatini, R.Sale, A.C.Defilippi, and G.A.Rossi. 2004. Epithelial cells and fibroblasts: structural repair and remodelling in the airways. *Paediatr. Respir. Rev.* 5 Suppl A:S35-S40.

Saklatvala,J. 2004. The p38 MAP kinase pathway as a therapeutic target in inflammatory disease. *Curr. Opin. Pharm.* 4:372-377.

Salerno,F.G., E.Carpagnano, P.Guido, M.R.Bonsignore, A.Roberti, M.Aliani, A.M.Vignola, and A.Spanevello. 2004. Airway inflammation in patients affected by obstructive sleep apnea syndrome. *Respir. Med.* 98:25-28.

Savla,U. and C.M.Waters. 1998. Mechanical strain inhibits repair of airway epithelium in vitro. *Am. J. Physiol. Lung Cell. Mol. Physiol.* 274:L883-L892.

Schaffer,J.L., M.Rizen, G.J.L'Italien, A.Benbrahim, J.Megerman, L.C.Gerstenfeld, and M.L.Gray. 1994. Device for the application of a dynamic biaxially uniform and isotropic strain to a flexible cell culture membrane. *J. Orthop. Res.* 12:709-719.

Sekosan,M., M.Zakkar, B.L.Wenig, C.O.Olopade, and I.Rubinstein. 1996. Inflammation in the uvula mucosa of patients with obstructive sleep apnea. *Laryngoscope* 106:1018-1020.

Series,F., J.Chakir, and D.Boivin. 2004. Influence of weight and sleep apnea status on immunologic and structural features of the uvula. *Am. J. Respir. Crit. Care Med.* 170:1114-1119.

Shamsuzzaman,A.S., M.Winnicki, P.Lanfranchi, R.Wolk, T.Kara, V.Accurso, and

V.K.Somers. 2002. Elevated C-reactive protein in patients with obstructive sleep apnea. *Circulation* 105:2462-2464.

Silverthorn,D.U. 2001. Human Physiology: an integrated approach. *Prentice-Hall, New Jersey.*

Sollich,P., F.Lequeux, P.Hebraud, and M.E.Cates. 1997. Rheology of soft glassy materials. *Phys. Rev. Lett.* 78:2020-2023.

Stamenovic,D., B.Suki, B.Fabry, N.Wang, and J.J.Fredberg. 2004. Rheology of airway smooth muscle cells is associated with cytoskeletal contractile stress. *J. Appl. Physiol* 96:1600-1605.

Stamenovic,D. and N.Wang. 2000. Invited review: engineering approaches to cytoskeletal mechanics. *J. Appl. Physiol* 89:2085-2090.

Stoyneva,Z., M.Lyapina, D.Tzvetkov, and E.Vodenicharov. 2003. Current pathophysiological views on vibration-induced Raynaud's phenomenon. *Cardiovasc. Res.* 57:615-624.

Stroetz,R.W., N.E.Vlahakis, B.J.Walters, M.A.Schroeder, and R.D.Hubmayr. 2001. Validation of a new live cell strain system: characterization of plasma membrane stress failure. *J Appl. Physiol* 90:2361-2370.

Suratt,P.M., P.Dee, R.L.Atkinson, P.Armstrong, and S.C.Wilhoit. 1983. Fluoroscopic and computed tomographic features of the pharyngeal airway in obstructive sleep apnea. *Am Rev. Respir. Dis.* 127:487-492.

Tanaka,S.M., J.Li, R.L.Duncan, H.Yokota, D.B.Burr, and C.H.Turner. 2003. Effects of broad frequency vibration on cultured osteoblasts. *J. Biomech.* 36:73-80.

The- ARDS- network. 2000. Ventilation with lower tidals volumes as compared with traditional tidal volumes for acute lung injury and the acute respiratory distress syndrome. The- ARDS- network. *N. Engl. J. Med.* 342:1301-1308.

Thomas,R.A., J.C.Norman, T.T.Huynh, B.Williams, S.J.Bolton, and A.J.Wardlaw. 2006. Mechanical stretch has contrasting effects on mediator release from bronchial epithelial cells, with a rho-kinase-dependent component to the mechanotransduction pathway. *Respir. Med.* 100:1588-1597.

Thompson,A.B., R.A.Robbins, D.J.Romberger, J.H.Sisson, J.R.Spurzem, H.Teschler, and S.I.Rennard. 1995. Immunological functions of the pulmonary epithelium. *Eur. Respir. J.* 8:127-149.

Tjandrawinata,R.R., V.L.Vincent, and M.Hughes-Fulford. 1997. Vibrational force alters mRNA expression in osteoblasts. *FASEB J.* 11:493-497.

Trepat,X., M.Grabulosa, L.Buscemi, F.Rico, B.Fabry, J.J.Fredberg, and R.Farre. 2003. Oscillatory magnetic tweezers based on ferromagnetic beads and simple coaxial coils. *Rev. Sci. Instrum.* 74:4012-4020.

Trepat,X., M.Grabulosa, L.Buscemi, F.Rico, R.Farre, and D.Navajas. 2005. Thrombin and histamine induce stiffening of alveolar epithelial cells. *J. Appl. Physiol.* 98:1567-1574.

Trepat,X., M.Grabulosa, F.Puig, G.N.Maksym, D.Navajas, and R.Farre. 2004. Viscoelasticity of human alveolar epithelial cells subjected to stretch. *Am. J. Physiol. Lung Cell. Mol. Physiol.* 287:L1025-L1034.

Trepat,X., F.Puig, N.Gavara, J.J.Fredberg, R.Farre, and D.Navajas. 2006. Effect of stretch on structural integrity and micromechanics of human alveolar epithelial cell monolayers exposed to thrombin. *Am. J. Physiol. Lung Cell. Mol. Physiol.* 290:L1104-L1110.

Tschumperlin,D.J. and S.S.Margulies. 1999. Alveolar epithelial surface area volume relationship in isolated rat lungs. *J. Appl. Physiol.* 86:2026-2033.

Tschumperlin,D.J., J.Oswari, and A.S.Margulies. 2000. Deformation-induced injury of alveolar epithelial cells. Effect of frequency, duration, and amplitude. *Am. J. Respir. Crit Care Med.* 162:357-362.

Tschumperlin,D.J., J.D.Shively, T.Kikuchi, and J.M.Drazen. 2003. Mechanical stress triggers selective release of fibrotic mediators from bronchial epithelium. *Am. J. Respir. Cell Mol. Biol.* 28:142-149.

Tschumperlin,D.J., J.D.Shively, M.A.Swartz, E.S.Silverman, K.J.Haley, G.Raab, and J.M.Drazen. 2002. Bronchial epithelial compression regulates MAP kinase signaling and HB-EGF-like growth factor expression. *Am. J. Physiol. Lung Cell. Mol. Physiol.* 282:L904-L911.

Van Nieuw Amerongen,G.P., R.Draijer, M.A.Vermeer, and V.W.van Hinsbergh. 1998. Transient and prolonged increase in endothelial permeability induced by histamine and thrombin: role of protein kinases, calcium, and RhoA. *Circ. Res.* 83:1115-1123.

Vestweber,D. 2000. Molecular mechanisms that control endothelial cell contacts. *J. Pathol.* 190:281-291.

Vgontzas,A.N., D.A.Papanicolaou, E.O.Bixler, A.Kales, K.Tyson, and G.P.Chrousos. 1997. Elevation of plasma cytokines in disorders of excessive daytime sleepiness: role of sleep disturbance and obesity. *J Clin. Endocrinol. Metab* 82:1313-1316.

Victor,L.D. 1999. Obstructive sleep apnea. *Am. Fam. Physician* 60:2279-2286.

Vlahakis,N.E. and R.D.Hubmayr. 2003. Response of alveolar cells to mechanical stress. *Curr. Opin. Crit. Care* 9:2-8.

Vlahakis,N.E., M.A.Schroeder, A.H.Limper, and R.D.Hubmayr. 1999. Stretch induces cytokine release by alveolar epithelial cells in vitro. *Am. J. Physiol. Lung Cell. Mol. Physiol.* 277:L167-L173.

von Bethmann,A.N., F.Brasch, R.Nusing, K.Vogt, H.D.Volk, K.M.Muller, A.Wendel, and S.Uhlig. 1998. Hyperventilation induces release of cytokines from perfused mouse lung. *Am. J. Respir. Crit Care Med.* 157:263-272.

Ware,L.B. and M.A.Matthay. 2000. The acute respiratory distress syndrome. *N. Engl. J. Med.* 342:1334-1349.

West,J.B. 2000. Invited review: pulmonary capillary stress failure. *J Appl. Physiol* 89:2483-2489.

West,J.B. and O.Mathieu-Costello. 1999. Structure, strength, failure, and remodeling of the pulmonary blood-gas barrier. *Annu. Rev. Physiol* 61:543-572.

Wiener-Kronish,J.P., K.H.Albertine, and M.A.Matthay. 1991. Differential responses of the endothelial and epithelial barriers of the lung in sheep to Escherichia coli endotoxin. *J. Clin. Invest* 88:864-875.

Winton,H.L., H.Wan, M.B.Cannell, D.C.Gruenert, P.J.Thompson, D.R.Garrod, G.A.Stewart, and C.Robinson. 1998. Cell lines of pulmonary and non-pulmonary origin as

tools to study the effects of house dust mite proteinases on the regulation of epithelial permeability. *Clin. Exp. Allergy* 28:1273-1285.

Wirtz,H.R. and L.G.Dobbs. 1990. Calcium mobilization and exocytosis after one mechanical stretch of lung epithelial cells. *Science* 250:1266-1269.

Wirtz,H.R. and L.G.Dobbs. 2000. The effects of mechanical forces on lung functions. *Respir. Physiol* 119:1-17.

Wong,C.K., C.B.Wang, W.K.Ip, Y.P.Tian, and C.W.Lam. 2005. Role of p38 MAPK and NF-kB for chemokine release in coculture of human eosinophils and bronchial epithelial cells. *Clin. Exp. Immunol.* 139:90-100.

Woodson,B.T., J.C.Garancis, and R.J.Toohill. 1991. Histopathologic changes in snoring and obstructive sleep apnea syndrome. *Laryngoscope* 101:1318-1322.

Yamazaki,S., A.J.Banes, P.S.Weinhold, M.Tsuzaki, M.Kawakami, and J.T.Minchew. 2002. Vibratory loading decreases extracellular matrix and matrix metalloproteinase gene expression in rabbit annulus cells. *Spine J.* 2:415-420.

Young,T., J.Skatrud, and P.E.Peppard. 2004. Risk factors for obstructive sleep apnea in adults. *JAMA* 291:2013-2016.

Zhu,C., G.Bao, and N.Wang. 2000. Cell mechanics: mechanical response, cell adhesion, and molecular deformation. *Annu. Rev. Biomed. Eng* 2:189-226.

Appendix 1

ELISA test

The kit of ELISA used in the study consist of an ELISA variant called Sandwich ELISA. In our case, it quantitates recombinant human IL-8 antigen using a standard curve, which is based on known concentrations of antigen, from which the unknown concentration of the sample can be detected. In this technique a mouse monoclonal antibody specific for IL-8 had been pre-coated onto a 96 well polystyrene microplate. An assay diluent, a buffered

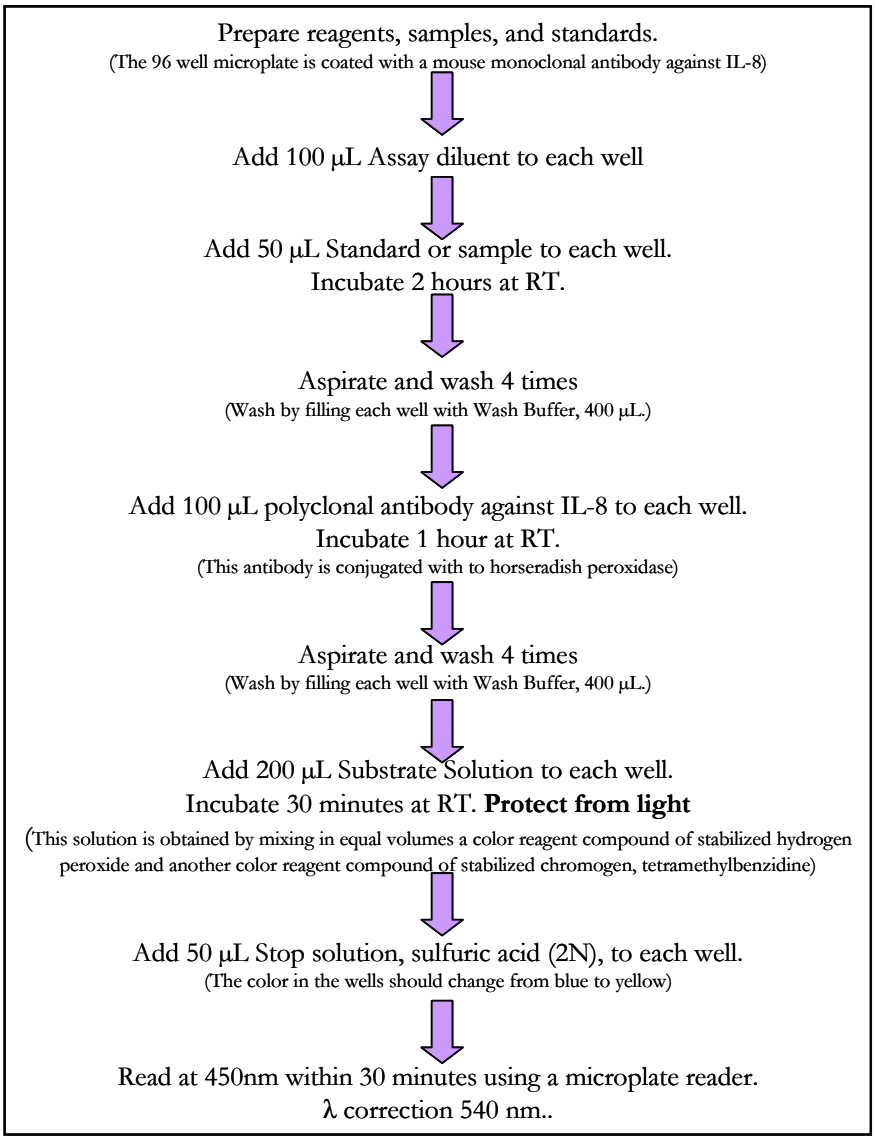

Figure: ELISA protocol summary. Modified from human IL-8 ELISA manual (Quantikine, R&D Systems, Minneapolis, Minn)

protein base with blue dye and preservatives, was firstly added to each well. Then, the sample or the standards (recombinant human IL-8 in a buffered protein base with preservatives, lyophilized) containing the antigen IL-8 were pipetted into the wells and any IL-8 present was bound by the immobilized antibody. After the wells were washed to remove unbound substances using a wash buffer, a second enzyme-linked polyclonal antibody specific for IL-8 conjugated to horseradish peroxidase with red dye and preservatives was added to the wells. After any free second antibody was removed by washing, a substrate solution was added to the wells, and color developed in proportion to the amount of IL-8 bound. This substrate solution was obtained by mixing in equal volumes a color reagent compound of stabilized hydrogen peroxide and another color reagent compound of stabilized chromogen (tetramethylbenzidine). The reaction was stopped with sulfuric acid (2N) and the intensity of the color was measured using a microplate reader (Multiskan RC, ThermoLabsystems, Helsinki, Finland). In this experiment the reader was set to 450 nm to determine the optical density of each well. The protocol is shown schematically in the figure.

Appendix 2

ZO-1 immunofluoresce

The tight junction creates a regulated barrier in the paracellular pathway. Tight junctions with the actin-rich adherens junction, form a functional unit called the apical junction complex. In contrast with the epithelium, the endothelium does not show a clear morphologic differentiation between adherens and tight junctions (Vestweber, 2000). A growing number of tight junction–associated proteins have been identified, but functions are defined for only a few. ZO-1 is one of the major cytoplasmatic proteins of the tight junctions and it is bound to the transmembrane protein occludin and to the actin-based cytoskeleton. Rows of the protein occludin form the intercellular barrier between two cells. (Mitic and Anderson, 1998).

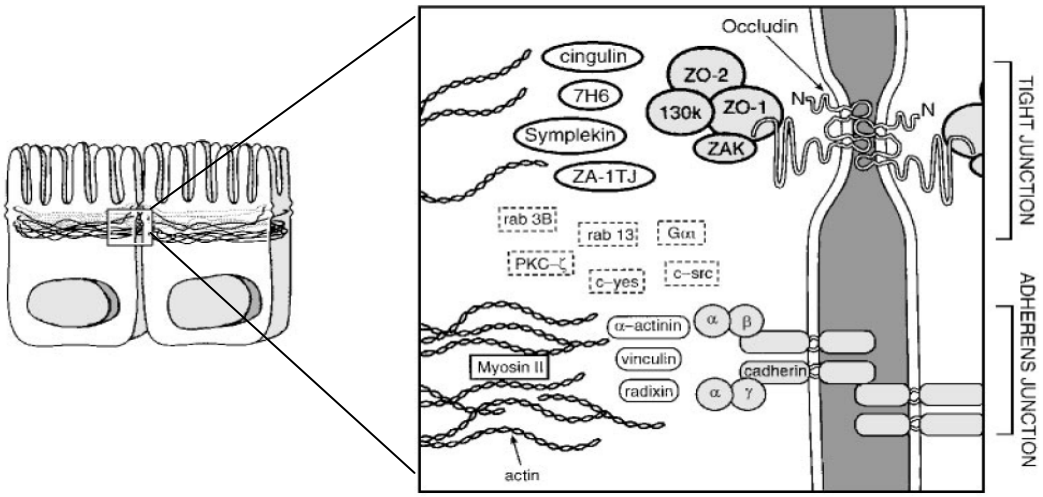

Figure: Model showing the protein components of the apical junction complex, the tight and adherens junctions, in a highly polarized epithelial cell (left). The boxed region at the right side of the figure is a higher magnification of the boxed region at the left side. It shows dentified proteins and their protein associations. Some proteins are specific to one junction; others may be shared (broken boxes). Adapted from Mitic and Andeerson, 1998

It has been reported that A549 cells have not the ability to establish functional tight junctions and to form non-permeable monolayers (Winton et al., 1998;Stroetz et al., 2001), although a recent study has provided opposite evidence (Kawkitinarong et al., 2004).

In this work we have used three different indirect immunofluorescence protocols to assess whether A549 cells could establish tight junction, in particular ZO-1 protein. We observed that protocol 2 (see below) was the most adequate to stain ZO-1 in A549 cells. However, in agreement with the literature (Winton et al., 1998;Stroetz et al., 2001) we observed that these cells do not establish clear tight junctions as shown in the example of the figure:

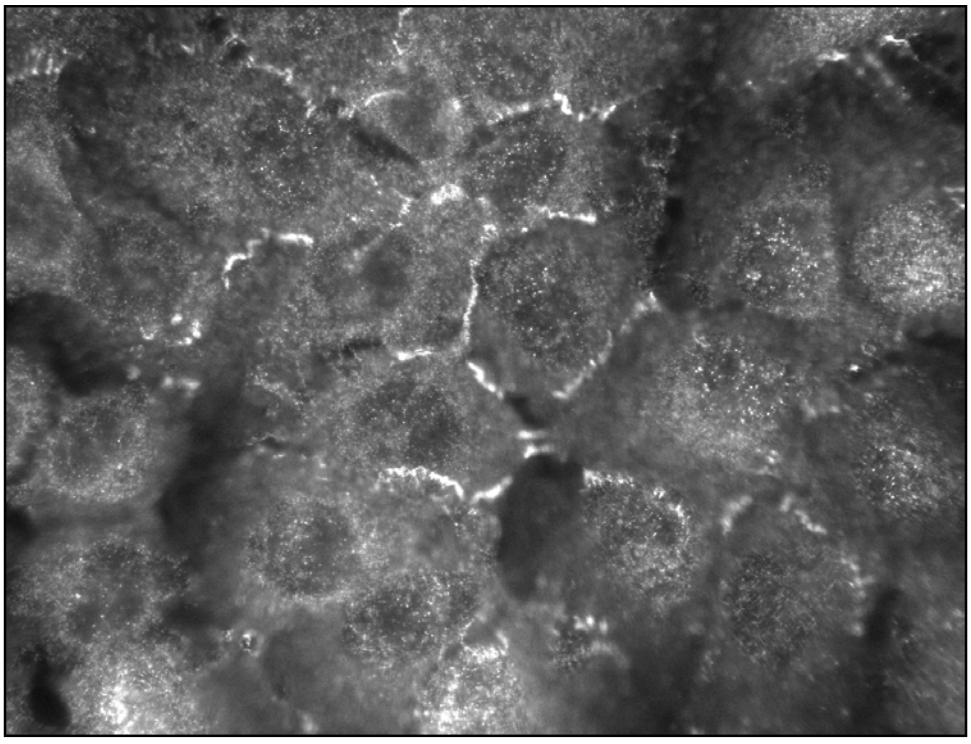

Figure: ZO-1 staining using protocol 2. Imaging was performed with an inverted microscope (Eclipse TE2000, Nikon, Japan) placed on a vibration isolation table (Isostation, Newport, Irrine, Ca). Fluorescence images were adquired with a 12-bit resolution cooled camera (Orca AG, Mamamatsu Photonics, Japan). The apparent pixel size after magnification (60 ×) was 0.107 μm with a resulting field of views of 216 × 143 μm^2 and with a depth focus of a 0.3 μm.

PROTOCOL 1 (Obtained from INVITROGEN catalog)

1. Wash cells twice with prewarmed PBS 1X (phosphate-buffered-saline) pH 7.4
2. Fix the sample in etanol solution (stored at –20ºC) for 30 minutes at 4ºC
3. Wash two or more times with PBS 1X
4. Place each coverslip in a glass petri dish and extract it with acetone (stored previously at –20ºC) for 3 minutes at room temperature
5. Wash two or more times with PBS 1X
6. To reduce nonspecific background staining it may be useful to pre-incubate fixed cells with PBS containing 1% BSA for 30 minutes prior to adding the first antibody staining solution (1 μg/ml Rabbit-anti-ZO-1 in PBS 1% BSA).
7. Wash two or more times with PBS 1X
8. Place the solution with the first antibody (15 μl) on the coverslip at 4ºC over night. To avoid evaporation, keep the coverslips inside a covered container during the incubation.
9. Wash two or more times with PBS 1X prior addind the second antibody staining solution (FITC-Donkey anti-Rabbit diluted 1:200 in PBS 1% BSA)
10. Place the solution with the second antibody (15 μl) on the coverslip for 1h at room temperature in dark conditions. To avoid evaporation, keep the coverslips inside a covered container during the incubation.
11. Wash two or more times with PBS 1X
12. Dry the coverslip
13. Mount the coverslip with Mowiol on a slide with the cell-side down.

PROTOCOL 2 (Obtained from Kawkitinarong et al., 2004)

1. Wash cells twice with prewarmed PBS 1X (phosphate-buffered-saline) pH 7.4
2. Fix the sample in 3.7% formaldehyde solution in PBS for 10 minutes at room temperature
3. Wash two or more times with PBS 1X
4. Place each coverslip in a glass petri dish and extract it with a solution of 0.1% Triton X-100 in PBS for 3 to 5 minutes
5. Wash two or more times with PBS 1X

6. To reduce nonspecific background staining it may be useful to pre-incubate fixed cells with Tris-Buffered-Saline-Tween 20 (TBS-T) containing 2% BSA for 30 minutes prior to adding the first antibody staining solution (1 μg/ml Rabbit-anti-ZO-1 in TBS-T 2% BSA).
7. Wash two or more times with TBS-T
8. Place the solution with the first antibody (15 μl) on the coverslip at 4ºC over night. To avoid evaporation, keep the coverslips inside a covered container during the incubation.
9. Wash two or more times with **TBS-T** prior addind the second antibody staining solution (10 μg/ml goat-anti-Rabbit ALEXA 488 diluted 1:200 in **TBS-T** 2% BSA)
10. Place the solution with the second antibody (15 μl) on the coverslip for 1h at room temperature in dark conditions. To avoid evaporation, keep the coverslips inside a covered container during the incubation.
11. Wash two or more times with **TBS-T**
12. Dry the coverslip
13. Mount the coverslip with Mowiol on a slide with the cell-side down.

TBS-T (Tris-Buffered-Saline-Tween 20).

To obtain 1 l of **10X** TBS:

- 24.2g Tris base
- 80g NaCl
- Mili-Q water

Mix to dissolve and adjust pH to 7.6 using concentrated HCl (1M)

To obtain 1 l of **1X** TBS- tween

- 100 ml 10 X TBS
- 1 ml (to obtain a final concentration of 0.1% Tween-20)
- Mili-Q water

PROTOCOL 3 (Obtained from Musch et al., 2006)

1. Wash cells twice with **K-Pipes buffer**.
2. Fix the sample with the **solution 1** for 5 minutes at room temperature.
3. Remove the **solution 1** from the sample and add the **solution 2** (pH=11) for 10 minutes at 37ºC.
4. Wash cells 3X, 3 minutes with **Rinse Buffer.**

5. Permeabilize cells with 0.1% Triton X-100 in **Rinse Buffer** for 3 to 5 minutes. (Don't go over!!).
6. Wash two or more times 3 minutes each with **Rinse Buffer.**
7. To reduce nonspecific background staining it may be useful to pre-incubate fixed cells with PBS containing 1% BSA for 1 hour prior to adding the first antibody staining solution (2.5μg/ml Rabbit-anti-ZO-1 in PBS 1% BSA).
8. Wash two or more times 3 minutes each with **Rinse Buffer.**
9. Place the solution with the first antibody (15 μl) on the coverslip at 4ºC over night. To avoid evaporation, keep the coverslips inside a covered container during the incubation.
10. Wash two or more times 3 minutes each with **Rinse Buffer** prior addind the second antibody staining solution (10μg/ml goat-anti-Rabbit ALEXA 488 diluted in PBS 1% BSA)
11. Place the solution with the second antibody (15 μl) on the coverslip for 1h at room temperature in dark conditions. To avoid evaporation, keep the coverslips inside a covered container during the incubation.
12. Wash two or more times 3 minutes each with **Rinse Buffer.**
13. Dry the coverslip
14. Mount the coverslip with Mowiol on a slide with the cell-side down.

830 mM K-Pipes (Pipes, piperazine- N, N'-bis (2-ethanesulfonic acid))

- 10 g Pipes
- 40 ml NaOH 1M

K-Pipes Buffer

To obtain 100 ml:

- 10 ml 830 mM K-Pipes (Final concentration: 80 mM)
- 22 mg $CaCl_2$ (Final concentration: 1.5 mM)
- 30.5 mg $MgCl_2$ (Final concentrstion: 1.5 mM)
- Mili-Q water

Mix to dissolve and adjust pH to 6.5 using concentrated NaOH (1M)

Solution 1

To obtain 100 ml:

- 10 ml K-Pipes buffer (Final concentration: 80 mM)
- 22 mg $CaCl_2$ (Final concentration: 1.5 mM)

- 30.5 mg $MgCl_2$ (Final concentration :1.5 mM)
- 186 mg EDTA (Final concentration : 5mM)
- 10 ml formaldehid (Final concentration: 4%)
- Mili-Q water

1 M Na-borate

To obtain 100 ml:

- 6.2 g Boric acid 1M
- Mili-Q water

Mix to dissolve and adjust pH to 8.0 using concentrated NaOH (5M)

Solution 2

To obtain 100 ml:

- 10 ml 1M Na-borate (Final concentration:100 mM)
- 10 ml formaldehid (Final concentration: 4%)
- Mili-Q water

Mix to dissolve and adjust pH to 11.0 using concentrated NaOH (5M)

Rinse buffer

- 100 ml PBS 1X
- 22 mg $CaCl_2$ (Final concentration: 1.5 mM)
- 30.5 mg $MgCl_2$ (Final concentration :1.5 mM)

Product references:

Dulbecco's phosphate buffered saline (PBS) 10X	Sigma (ref: D-1408)
Albumin from bovine serum (BSA) ≥96%	Sigma (ref: A-9418)
Formaldehyde 37% solution	Sigma (ref: F-1635)
Etanol solution 96% v/v	Scharlau (ET0003)
Mowiol	Calbiochem (ref: 475904)
Triton X-100	Sigma (ref: T-8787)
Tris base	BIO-RAD (ref: 83088B)
Tween-20	Sigma (ref: P-5927)
NaCl	Sigma (ref: S-9625)
Pipes	Sigma (ref: P-1851)

NaOH	Sigma (ref: S-7653)
$CaCl_2$	Sigma (ref: C-3881)
$MgCl_2$	Sigma (ref: M-0250)
Boric acid	Sigma (ref: B-1934)
EDTA	Sigma (ref: E-5134)

Antibodies references:

Rabbit-anti-ZO-1	Zymed (ref: 61-7300)
Donkey anti-Rabbit IgG-FITC	Santa Cruz Biotechnologies (ref: sc-2090)
Goat-anti-Rabbit ALEXA 488	Molecular Probes (ref: A-11034)

Appendix 3

List of Abbreviations

ALI	acute lung injury
ARDS	acute respiratory distress syndrome
CSK	cytoskeleton
DMSO	dimethyl sulfoxide
ECM	extracellular matrix
EDTA	ethylenediaminetetraacetic acid
ELISA	enzyme- linked immunoabsorbent assay
ERK	extracellular signal-regulated kinase
HEPES	N-(2-Hydroxyethyl)piperazine-N'-(2-ethanesulfonic acid)
HAEC	human alveolar epithelial cells
IL-1, 6, 8, 10	interleukin 1, 6, 8, 10
JNK	c-Jun N-terminal kinase
MAPK	mitogen- activated protein kinase
MEK	MAPKK, mitogen- activated protein kinase kinase
MLC	myosin light chain
(NF)- κB	nuclear transcription factor
NHBE	normal human bronchial epithelial cells
NHNE	normal human nasal epithelial cells
NS	no significant differences
OMTC	optical magnetic twisting cytometry
OSA	obstructive sleep apnea
PAR(s)	protease- activated receptor(s)
RGD	arginine- glycine- aspartic acid

SEM	standard error of the mean
TER	transepithelial electrical resistance
Thr	thrombin
TLC	total lung capacity
TNF	tumor necrosis factor
VCAM	vascular cell adhesion molecular
VILI	ventilator induced lung injury

Appendix 4

Publications and conference communications

A. PUBLICACIONS

1. Almendros I, I. Acerbi, **F. Puig**, J.M. Montserrat, D.Navajas and R. Farré. *Upper airway inflammation triggered by vibration in a rat model of snoring.* Articles in Press. Journal Sleep (September 25, 2006)

2. Trepat,X*****, **F. Puig***, N. Gavara, J. J. Fredberg, R. Farre, D. Navajas. *Effect of stretch on the structural integrity and micromechanics of human alveolar epithelial cell monolayers exposed to thrombin.* Am J Physiol Lung Cell Mol Physiol 290:1104-1110, 2006.
   *** Both authors contributed equally to this work.**

3. **Puig,F**, F. Rico, I. Almendros, J.M. Montserrat, D. Navajas, R. Farre. *Vibration enhances Interleukin-8 release in a cell model of snoring-induced airway inflammation.* SLEEP 2005;28(10):1312-1316

4. Trepat, X, M. Grabulosa, **F. Puig**, G.N. Maksym, D. Navajas and R. Farré. *Viscoelasticity of human alveolar epithelial cells subjected to stretch.* Am J Physiol Lung Cell Mol Physiol 287:L1025-L1034, 2004.

B. CONFERENCE COMMUNICATIONS

1. International conferences

1. Bonsignore, M.R, L. Chimenti, **F. Puig**, , D. Navajas, R. Farré. *Effects of repeated stretching and mild hyperosmolar exposure on IL-8 release by bronchial epithelial cells.* (Abstract sended). International Conference American Thoracic Society, San Francisco, USA, May, 2007

2. Farré, R, **F. Puig**, R. Ferrer, A. Artigas, D. Navajas. *Changes induced by activated protein C in the mechanics of alveolar epithelial cells subjected to thrombin.* (Abstract sended). International Conference American Thoracic Society, San Francisco, USA, May, 2007.

3. Farré, R, **F. Puig,** N. Gavara, R. Sunyer, D. Navajas. *Cell stiffening and contraction induced by thrombin in alveolar epithelial cells treated with dexamethasone.* (Abstract). 16th European Respiratory Society Annual Congress, Munich, Germany, September, 2-6, 2006.

4. **Puig F.**, N.Gavara, R.Sunyer, D.Navajas, R.Farré. *Dexamethasone induces stiffening of alveolar epithelial cells.* (Abstract). 5th World Congress of Biomechanics, Munich, Germany, August 31-September 4, 2006.

5. Gavara N., **Puig F.**, R.Sunyer, R.Farré, D.Navajas. *Effects of dexamethasone in contraction of alveolar epithelial cells.* (Abstract). 5th World Congress of Biomechanics, Munich, Germany, August 31-September 4, 2006.

6. Farré, R, **F. Puig**, F. Rico, M. Rotger, J.M. Montserrat, D Navajas. *Inflammation induced in bronchial epithelial cells by vibration at snoring frequencies: Role of MAP kinase pathways in the production of IL-8.* (Abstract) International Conference American Thoracic Society, San Diego, USA, May, 2005.

7. Trepat, X, **F. Puig**, N. Gavara, R. Farré, D. Navajas. *Combined effect of thrombin and stretching on the mechanical properties of alveolar epithelial cells.* (Abstract) International Conference American Thoracic Society, San Diego, USA, May, 2005.

8. Farré, R, **F. Puig**, L. Buscemi, M. Grabulosa, J. M. Montserrat, D. Navajas. *Vibration at snoring frequencies (60 Hz) induces interlukin-8 in bronchial epithelial cells in culture.* (Abstract) 14th European Respiratory Society Annual Congress, Glasgow, U.K, September, 4-8, 2004.

2. National conferences

1. **Puig F.**, R. Ferrer, D. Navajas, A. Artigas, R. Farre. *Combined effect of Activated Protein C and Thrombin on the Viscoelasticity of Human Alveolar Epithelial Cells.* (Abstract). 19th European Society of Intensive Care Medicine (ESCIM), Barcelona, Spain, September, 24-27, 2006.

2. Almendros, I. **F. Puig**, J.M. Montserrat, D. Navajas, R. Farre. *Modelo animal para el estudio de los efectos inflamatorios del ronquido en la vía aérea superor.* (Oral contribution). XXXIX Congreso Nacional SEPAR, Sevilla, Spain, June, 3-5, 2006.

3. **Puig, F**, X. Trepat, D. Biedma i R. Farré. *Efecte del lipopolisacàrid d'Escheridia coli en la rigidesa de cèl·lules epitelials alveolars (A-549) mitjançant citometria de torsió magnètica.* (Oral contribution) IV Jornades de Recerca en Enginyeria Biomèdica, (JEBC'04), Barcelona, Spain, June 8-10, 2004.

4. Trepat, X, **F. Puig**, M. Rotger i R. Farré. *Nanomanipulació de Microesferes Magnètiques per l'estudi de la Mecánica Cel·lular.* IV Jornades de Recerca en Enginyeria Biomèdica, (JEBC'04), Barcelona, Spain, June 8-10, 2004.

5. Roca-Cusachs, P, C. Mills, E. Martínez, **F. Puig**, J. Samitier, D. Navajas. *Fabrication of microneedle arrays via Focused Ion Beam technology for the study of cell adhesión.* IV Jornades de Recerca en Enginyeria Biomèdica, (JEBC'04), Barcelona, Spain, June 8-10, 2004.

6. Trepat, X, M. Grabulosa, L. Buscemi, **F. Puig**, D. Navajas, R. Farré. *Effect of stretching on the stiffness of alveolar epithelial cells.* (Abstract) 4th European Biophysics Congress. Alacant, Spain, July 5-9, 2003.